DOCTORAL THESIS

A new therapeutical approach to reduce viral persistence, immune activation, and inflammation in people with HIV-1 on antiretroviral therapy

Sílvia Bernal Santateresa

Doctoral thesis to obtain the PhD degree in Medicine and Biomedical Sciences of the Universitat de Vic - Universitat Central de Catalunya

Directors: Dr. Javier Martinez-Picado and Dr. Maria Carmen Puertas Castro

Tutor: Dr. Javier Martinez-Picado

2023

UNIVERSITAT DE VIC
UNIVERSITAT CENTRAL DE CATALUNYA
Escola de Doctorat

Sílvia Bernal Santateresa was supported by the Ph.D. fellowship of the Chair of Infectious Diseases and Immunity from the University of Vic - Central University of Catalonia and the IrsiCaixa AIDS Research Institute. The content of this thesis was partly supported by Abivax S.A. under the project “An open-label study of the safety, pharmacokinetics, and pharmacodynamics of obefazimod in HIV-1 seronegative and seropositive adults” to IrsiCaixa AIDS Research Institute.

Als meus pares i a la meva germana,

Per la seva motivació, confiança i recolzament incondicionals,

que em donen forces per aconseguir tot el que em proposi.

“If we knew what it was we were doing,

it would not be called research, would it?”

Albert Einstein

ABBREVIATIONS

AE	Adverse event
AIDS	Acquired Immune Deficiency Syndrome
Allo-HSCT	Allogeneic hematopoietic stem cell transplantation
APC	Antigen presenting cell
ART	Antiretroviral therapy
AZT	Azidothymidine
CA	Capsid
CBC	Cap binding complex
CCL2	C-C chemokine ligand 2
CCL4	C-C chemokine ligand 4
CCR5	C-C chemokine receptor 5
CCR7	C-C chemokine receptor 7
CD	Crohn's disease
CD3	Cluster of differentiation 3
CD4	Cluster of differentiation 4
CD8	Cluster of differentiation 8
CD14	Cluster of differentiation 14
CD27	Cluster of differentiation 27
CD38	Cluster of differentiation 38
CD45	Cluster of differentiation 45
CD163	Cluster of differentiation 163

CDC	Center for Disease Control
cDNA	Complementary DNA
CRP	C-reactive protein
CTLA-8	Cytotoxic T-lymphocyte-associated antigen 8
CXCL8	C-X-C chemokine ligand 8
CXCL9	C-X-C chemokine ligand 9
CXCL10	C-X-C chemokine ligand 10
CXCR4	C-X-C receptor 4
ddPCR	Droplet digital PCR
DLT	Dose limiting toxicity
DNA	Deoxyribonucleic acid
dNTP	Deoxynucleoside triphosphates
DSMB	Data safety monitoring board
DSS	Dextran sulphate sodium
DTT	Dithiothreitol
EDTA	Ethylenediaminetetraacetic
ELISA	Enzyme-linked immunosorbent assay
EMA	European Medicines Agency
Env	Envelope
FACS	Fluorescence-activated cell sorting
FDA	Food and Drug Administration

GALT	Gut-associated lymphoid tissue
G-CSF	Granulocyte colony-stimulating factor
GM-CSF	Granulocyte-macrophage colony-stimulating factor
gp41	Glycoprotein 41
gp120	Glycoprotein 120
HIV	Human Immunodeficiency Virus
HIV-1	Human Immunodeficiency Virus type 1
HIV-2	Human Immunodeficiency Virus type 2
HLA-DR	Human leukocyte antigen-DR isotype
HSCT	Hematopoietic stem cell transplantation
IFN-γ	Interferon-γ
IL-1β	Interleukin-1β
IL-2	Interleukin-2
IL-4	Interleukin-4
IL-6	Interleukin-6
IL-7	Interleukin-7
IL-8	Interleukin-8
IL-10	Interleukin-10
IL-12	Interleukin-12
IL-17α	Interleukin-17α
IL-18	Interleukin-18

IL-22	Interleukin-22
IN	Integrase
INSTI	Integrase strand transfer inhibitor
IP-10	Interferon-γ-induced protein 10
IPDA	Intact proviral DNA assay
IQR	Interquartile range
L-FABP	Liver-type fatty acid binding protein
LOD	Limit of detection
LTR	Long terminal repeat
m7G	7-methylguanosine
MA	Matrix
MCP-1	Monocyte chemoattractant protein-1
M-CSF	Macrophage colony-stimulating factor
MIG	Monokine induced by Interferon-γ
MIP-1β	Macrophage inflammatory protein-1β
miRNA	MicroRNA
miR-124	MicroRNA-124
mRNA	Messenger RNA
NC	Nucleocapsid
Nef	Negative regulating factor
NNRTI	Non-nucleoside reverse transcriptase inhibitor

NRTI	Nucleoside/nucleotide reverse transcriptase inhibitor
PBMC	Peripheral blood mononuclear cell
PCR	Polymerase chain reaction
PD-1	Programmed death receptor type 1
PI	Protease inhibitor
Pol	Polymerase
PR	Protease
PrEP	Pre-exposure prophylaxis
PWH	People with HIV
RA	Rheumatoid arthritis
Rev	Regulator of expression proteins
RNA	Ribonucleic acid
RNase	Ribonuclease
RPP30	Ribonuclease P/MRP subunit 30
RRE	Rev-responsive element
RT	Reverse transcriptase
RT-ddPCR	Reverse transcription ddPCR
RT-qPCR	Real-time quantitative PCR
SIV	Simian Immunodeficiency Virus
TAR	Transactivation responsive

Tat	Trans-activating regulatory protein
TBP	TATA-box binding protein
T_{CM}	T central memory
T_{EM}	T effector memory
T_{FH}	T follicular helper
T_{H}	T helper
T_{MM}	T migratory memory
T_{N}	T naïve
TNFa	Tumor necrosis factor alfa
T_{reg}	T regulatory
T_{RM}	T resident memory
T_{SCM}	T stem cell memory
T_{TD}	T terminally differentiated
T_{TM}	T transitional memory
$T_{\gamma\delta}$	T gamma delta
UC	Ulcerative colitis
UNAIDS	Joint United Nation Programme on HIV/AIDS
Vif	Viral infectivity factor
Vpr	Viral protein r
Vpx	Viral protein x

TABLE OF CONTENTS

SUMMARY & RESUM

The Human Immunodeficiency Virus (HIV) pandemic has been a major threat for global health since its onset in the 80's. About 85.6 million people have become infected with HIV and 40.4 million people have died from HIV-related diseases worldwide. Nowadays, nearly 39 million people are currently living with HIV and 1.3 million people are newly infected with HIV globally. Thanks to the discovery of antiretroviral therapy (ART) and global efforts for better prevention and diagnosis, the number of newly infected individuals and HIV-related deaths has declined drastically. However, ART is not able to cure HIV infection because it cannot eradicate the latent viral reservoir. Indeed, these latent proviruses are a potential source for viral rebound upon treatment interruption and thus lifelong treatment is needed for effective control of HIV infection. Hence, there remains an urgent need to investigate and implement novel therapeutic approaches that could impact the latent viral reservoir wherein it is more likely to persist and reverse the chronic immune activation and inflammation exhibited by people with HIV (PWH) despite long-term ART suppression. In this context, the aim of this thesis is to investigate a promising new therapeutical approach based on ART intensification with a novel drug, obefazimod (formerly ABX464), that has been described in previous preclinical and clinical studies to inhibit viral replication, through a unique mechanism of interfering the biogenesis of viral RNA, and to have strong anti-inflammatory effects, by the selective induction of miR-124 and subsequent attenuation of production of pro-inflammatory cytokines, and therefore it might contribute to simultaneously reduce the persistence of viral reservoirs, chronic immune activation, and inflammation in long-term ART-suppressed PWH. For that purpose, we evaluated the safety and impact of obefazimod on viral persistence, chronic immune activation, and inflammation in a non-randomized, open-label, phase II clinical study with PWH on suppressive ART.

Our results showed that obefazimod, taken up to 150 mg daily for 4 weeks, has a good safety and tolerability profile either alone or in combination with ART. Moreover, we observed that obefazimod potentially impacts viral persistence by transiently reducing viral transcription initiation and elongation, residual viraemia, and total proviral reservoir size, in a dose-dependent manner, when it is

administered in combination with ART. Furthermore, we observed that obefazimod reduces chronic immune activation and inflammation in long-term ART-suppressed PWH by reducing the surface expression of the activation-induced markers CD38, HLA-DR, and PD-1 on T cells, selectively upregulating the expression of miR-124, and reducing the expression of multiple HIV-inductive soluble inflammation biomarkers, such as G-CSF, GM-CSF, CD14, IL-1β, IL-2, IL-7, IL-10, IL-12 (p70), IL-17α (or CTLA-8), MIP-1β (or CCL4), and MCP-1 (or CCL2), and this effect is maintained up to 4 weeks after obefazimod discontinuation.

Altogether, our study showed that this novel compound, with its unique mode of action, may have important implications for new strategies aimed at sustained virological remission and immune restoration. Moreover, our results also support the search of alternative drugs that target viral transcription, processing, and/or maturation of viral transcripts with potential to eliminate or silence viral persistence and simultaneously suppress virus-induced immune activation and inflammation. Further studies should investigate intermediate doses of obefazimod and longer treatment periods than those used in the present study as they could result in a sustained impact on viral persistence, chronic immune activation, and inflammation, while limiting drug-related adverse events.

La pandèmia del virus de la immunodeficiència humana (VIH) ha estat una amenaça important per a la salut mundial des del seu inici als anys 80. Al voltant de 85.6 milions de persones han estat infectades amb el VIH i 40.4 milions han mort per malalties relacionades amb el VIH arreu del món. Actualment, prop de 39 milions viuen amb el VIH i hi ha 1.3 milions de noves infeccions arreu del món. Gràcies al descobriment de la teràpia antiretroviral (TAR) i als esforços globals per millorar la prevenció i el diagnòstic, el nombre de noves infeccions i morts relacionades amb el VIH han disminuït dràsticament. No obstant, la TAR no cura la infecció pel VIH perquè no és capaç d'erradicar el reservori latent del virus. Els provirus latents són la font principal del rebot del virus després d'aturar el tractament i, per tant, els individus amb VIH han de tractar-se durant tota la vida per a un control efectiu de la infecció. Per aquesta raó, hi ha una necessitat urgent d'investigar i implementar noves estratègies terapèutiques dirigides a eliminar o silenciar aquest reservori latent del virus i revertir l'activació immune i la inflamació cròniques que presenten les persones amb VIH malgrat estar suprimides amb la TAR durant anys. En aquest context, l'objectiu d'aquesta tesi és investigar una nova i prometedora estratègia terapèutica basada en la intensificació de la TAR amb un nou fàrmac, l'obefazimod (també anomenat ABX464), que, en anteriors estudis pre-clínics i clínics, ha demostrat inhibir la replicació viral, mitjançant un mecanisme únic d'interferència de la biogènesi del ARN viral, i tenir un potent efecte antiinflamatori, mitjançant la inducció selectiva del miR-124 i la conseqüent atenuació de la producció de citocines pro-inflamatòries, i, per tant, podria contribuir a reduir simultàniament la persistència dels reservoris virals, l'activació immune i la inflamació cròniques en persones suprimides per la TAR. Amb aquesta finalitat, es va avaluar la seguretat i l'efecte de l'obefazimod en la persistència viral, l'activació immune i la inflamació cròniques en persones amb VIH en tractament antiretroviral en un estudi clínic de fase II, obert i no aleatoritzat.

Els resultats de l'estudi van mostrar que l'obefazimod, administrat fins a dosis diàries de 150 mg durant 4 setmanes, és segur i ben tolerat, tant sol com en combinació amb la TAR; que l'obefazimod té un fort impacte en la persistència viral mitjançant la reducció transitòria de la iniciació i elongació de la transcripció viral,

la virèmia residual i la mida total del reservori proviral, de manera dosi-dependent, quan s'administra conjuntament amb la TAR; i que l'obefazimod redueix l'activació immune i la inflamació cròniques en persones amb VIH en tractament antiretroviral, mitjançant la reducció de l'expressió dels marcadors d'activació CD38, HLA-DR i PD-1 a la superfície de les cèl·lules T, de la inducció selectiva de l'expressió del miR-124 i de la reducció de l'expressió de varis biomarcadors d'inflamació solubles com ara el G-CSF, GM-CSF, CD14, IL-1β, IL-2, IL-7, IL-10, IL-12 (p70), IL-17α (o CTLA-8), MIP-1β (o CCL4) i MCP-1 (o CCL2), i que aquest efecte es manté fins a 4 setmanes després de la retirada del fàrmac.

En general, el nostre estudi va demostrar que aquest nou fàrmac, amb un mecanisme d'acció únic, pot tenir implicacions importants per a noves estratègies terapèutiques dirigides a la remissió del virus i a la restauració immunològica. A més, els nostres resultats també donen suport a la recerca de fàrmacs alternatius dirigits a inhibir la transcripció, processament i/o maduració dels transcrits virals amb potencial per eliminar o silenciar la persistència viral i alhora suprimir l'activació immune i la inflamació induïdes pel virus. En un futur, els propers estudis haurien d'investigar l'administració de dosis intermèdies de l'obefazimod i períodes de tractament més llargs que els emprats en aquest estudi, ja que podrien tenir un impacte sobre la persistència viral, l'activació immune i la inflamació cròniques sostingut en el temps, i alhora limitar els efectes adversos relacionats amb el fàrmac.

Chapter 1. INTRODUCTION

1. Human Immunodeficiency Virus

1.1. History and origin

In 1981, the U.S. Center for Disease Control (CDC) reported high rates of rare and unusual types of pneumonia (*Pneumocystis jirovecii*), aggressive cancers, such as Kaposi's sarcoma, and other opportunistic infections in young, previously healthy, gay men. All reported cases presented a depletion of $CD4^+$ T cells and signs of severe immune deficiency, so this devastating disease was named as Acquired Immune Deficiency Syndrome (AIDS)[1,2].

In 1983, Françoise Barré-Sinoussi and Luc Montagnier, at the Pasteur Institute in Paris, isolated and characterized a T-lymphotropic retrovirus in cultured T cells from an individual with AIDS-like symptoms[3]. For this discovery, they received the Nobel Prize in Medicine in 2008. In 1984, Robert Gallo, at the National Cancer Institute in Bethesda, isolated the same retrovirus from a larger group of individuals and suggested causative involvement in AIDS[4]. This T-lymphotropic retrovirus was later named Human Immunodeficiency Virus (HIV) by the International Committee on the Taxonomy of Viruses[5]. In 1986, a morphologically similar but antigenically distinct causative virus of AIDS was found in western Africa and was denominated HIV type 2 (HIV-2) to distinguish it from the original type (HIV-1)[6].

Epidemiologic and phylogenetic analyses have proved that HIV-1 and HIV-2 are closely related to Simian Immunodeficiency Virus (SIV)[7] found in Central African chimpanzees (SIVcpz)[8] and West African sooty mangabeys (SIVsm)[9], respectively. These relationships provided the first evidence that HIV-1 and HIV-2 evolved from different non-human primate species through cross-species transmissions and were introduced into the human population around 1920 to 1940 and spread from Africa through other parts of the world[10,11].

1.2. Global HIV pandemic

Since the start of the epidemic, 85.6 million people have become infected with HIV and 40.4 million people have died from HIV-related diseases. Nowadays, HIV

continues to be one of the major global health challenges, particularly in low- and middle-income countries. In 2022, the Joint United Nations Programme on HIV/AIDS (UNAIDS) estimated that nearly 39 million people were living with HIV and 1.3 million people became newly infected with HIV worldwide[12]. The African Region is the most affected area, with 25.6 million people living with HIV, and accounts for almost 60% of the global new HIV infections. In Spain, nearly 150,000 people were living with HIV and 3,900 people became infected for the first time in 2022 (Figure 1).

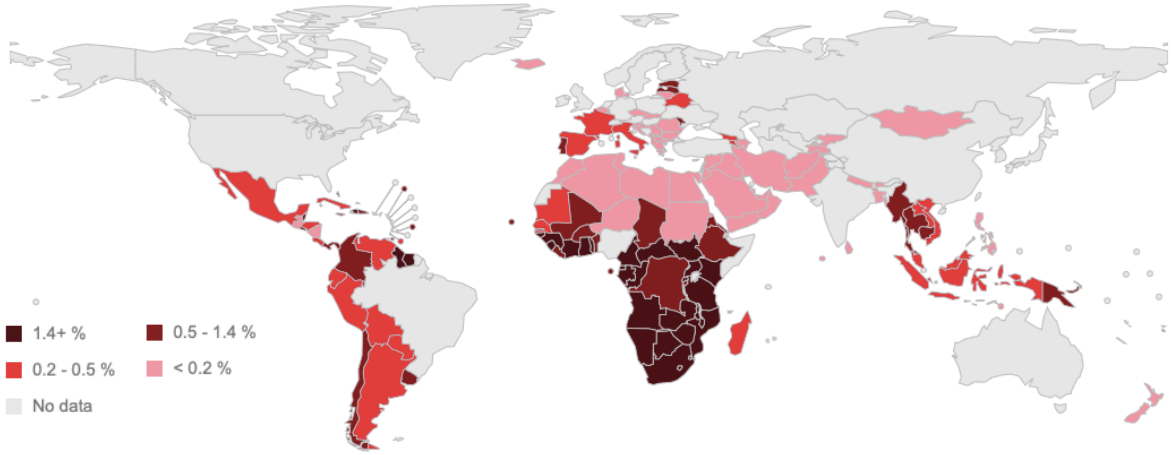

Figure 1. Prevalence of adults living with HIV worldwide in 2022. Map based on modelled HIV estimates methodology from UNAIDS[12].

Since its peak in 1996, new HIV infections have fallen globally by 59% as by the end of 2022 29.8 million people with HIV were receiving antiretroviral therapy (ART) and were virally suppressed, limiting new HIV transmissions. However, 630,000 people still died from HIV-related causes in 2022 because they did not know they were infected, did not have access to treatment or were not virally suppressed[12].

In 2022, UNAIDS estimated that 86% of people living with HIV knew their status, 76% were receiving treatment, and 71% were virally suppressed. New global strategies must be addressed to reach the ambitious 95-95-95 target by 2030, which aims at 95% of people living with HIV knowing their status, 95% receiving treatment and 95% being virally suppressed. Despite HIV infection rates have declined or stabilized in many countries across the world with increasing access to effective HIV prevention, diagnosis, and treatment, there is still no cure for HIV infection.

1.3. Groups and subtypes

HIV is grouped to the genus *Lentivirus* within the family of *Retroviridae*, subfamily *Orthoretroviridae*[13]. Based on the genetic characteristics and differences in the viral antigens, HIV is classified in two types: HIV-1 and HIV-2. HIV-1 is the most prevalent type of HIV worldwide, whereas HIV-2 is mainly restricted to West Africa. Their different distribution could be explained by the poor capacity for transmission and reduced pathogenicity of HIV-2[14].

Based on sequence homology, HIV-1 is subdivided into the groups M (main), O (outlier), N (nonmajor/nonoutlier), and P (putative). HIV-1 group M represents the majority of global infections and is subdivided into subtypes A, B, C, D, F, G, H, J, K, and several circulating recombinant forms. The most prevalent is subtype C, which predominates in Africa and India, while subtype B predominates in western Europe, America, and Australia[15].

1.4. Structure and genome

HIV particle is approximately 100 nm in diameter[16] with an outer envelope composed of a lipid bilayer membrane containing trimers of the surface glycoprotein gp120 and the transmembrane glycoprotein gp41 (Figure 2). The viral envelope covers the matrix (MA), a symmetrical outer capsid membrane which is formed by the matrix protein p17. The matrix surrounds the conical-shape capsid (CA) core, assembled from the inner capsid protein p24, and the nucleocapsid (NC) which is composed of the nucleocapsid protein p7. Within the capsid, there is enclosed the viral RNA genome bound to the NC and several viral enzymes: reverse transcriptase (RT), integrase (IN), and protease (PR)[17].

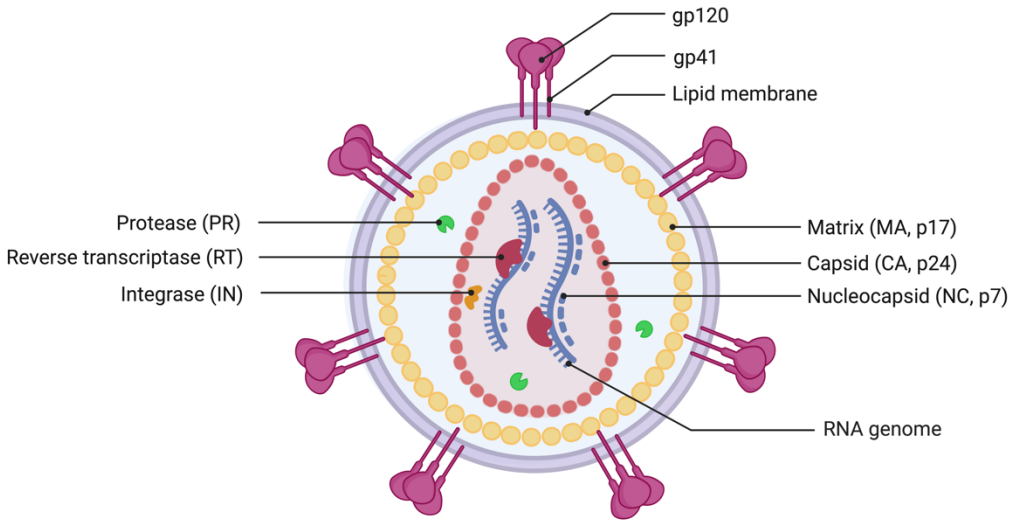

Figure 2. Structure of HIV-1. Schematic representation of the HIV-1 particle.

The viral genome consists of two identical positive, single-stranded RNA of approximately 9.8 kb in length[18] that is flanked at both ends by long terminal repeat (LTR) sequences and contains nine genes that code for proteins necessary for the assembly of new viruses (Figure 3).

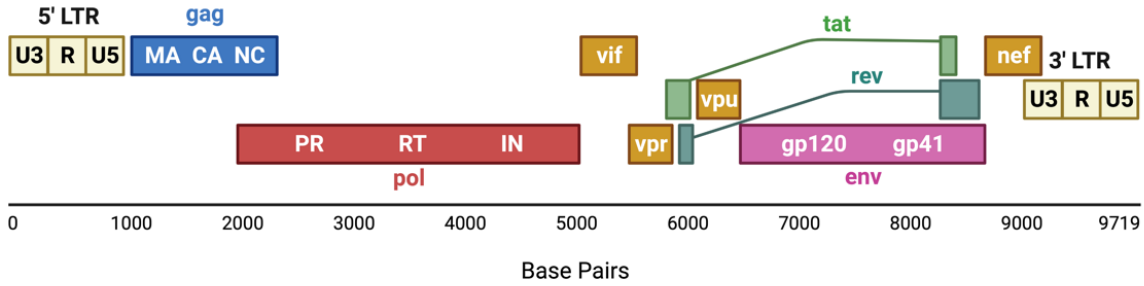

Figure 3. HIV-1 genomic organization. Schematic representation of the HIV-1 genome and their encoding proteins according to the reading frame.

The 5' LTR region codes for the promotor for transcription of the viral genes. In the direction 5' to 3' of the reading frame, the *gag* (group specific antigen) gene follows, encoding the structural proteins of the MA (p17), CA (p24), NC (p7) and a smaller, nucleic acid-stabilizing protein (p6). The *gag* reading frame is followed by the *pol* (polymerase) gene, coding for the viral enzymes: RT, IN, and PR. Adjacent to *pol*, the *env* (envelope) gene follows, encoding the two envelope glycoproteins gp120 and gp41, which enable viral fusion with target cells.

In addition to the major structural and functional proteins, the viral genome encodes for two regulatory proteins, Tat (transactivator of transcription), that modulates transcription, and Rev (regulator of expression of virion proteins), that facilitates nuclear export of non-spliced and partially spliced viral mRNA.

Ultimately, the viral genome encodes four other regulatory/accessory proteins: Nef (negative regulating factor), Vif (viral infectivity factor), Vpr (viral protein r), and Vpu (viral protein unique), whose functions are not essential for viral replication but enhance infectivity of viral particles. HIV-2 codes for Vpx (viral protein x) instead of Vpu, which is partially responsible for the reduced pathogenicity of HIV-2[19].

1.5. HIV-1 replication cycle

Viral replication at the cellular level proceeds through sequential steps that start when the virus productively engages cell surface receptors and ends when nascent virions mature into infectious viruses.

1.5.1. Viral entry: binding and fusion

In the initial step of infection of a cell, the viral surface glycoprotein gp120 binds to the CD4 receptor on the surface of the host target cell. HIV-1 preferentially infects $CD4^+$ T cells and macrophages. This binding initiates a cascade of conformational changes that allow gp120 binding the co-receptor CCR5 or CXCR4 on the cell surface and gp41 inserting into the cellular membrane and culminating in the fusion between the viral and the host cellular membranes (Figure 4, steps 1-2)[20,21].

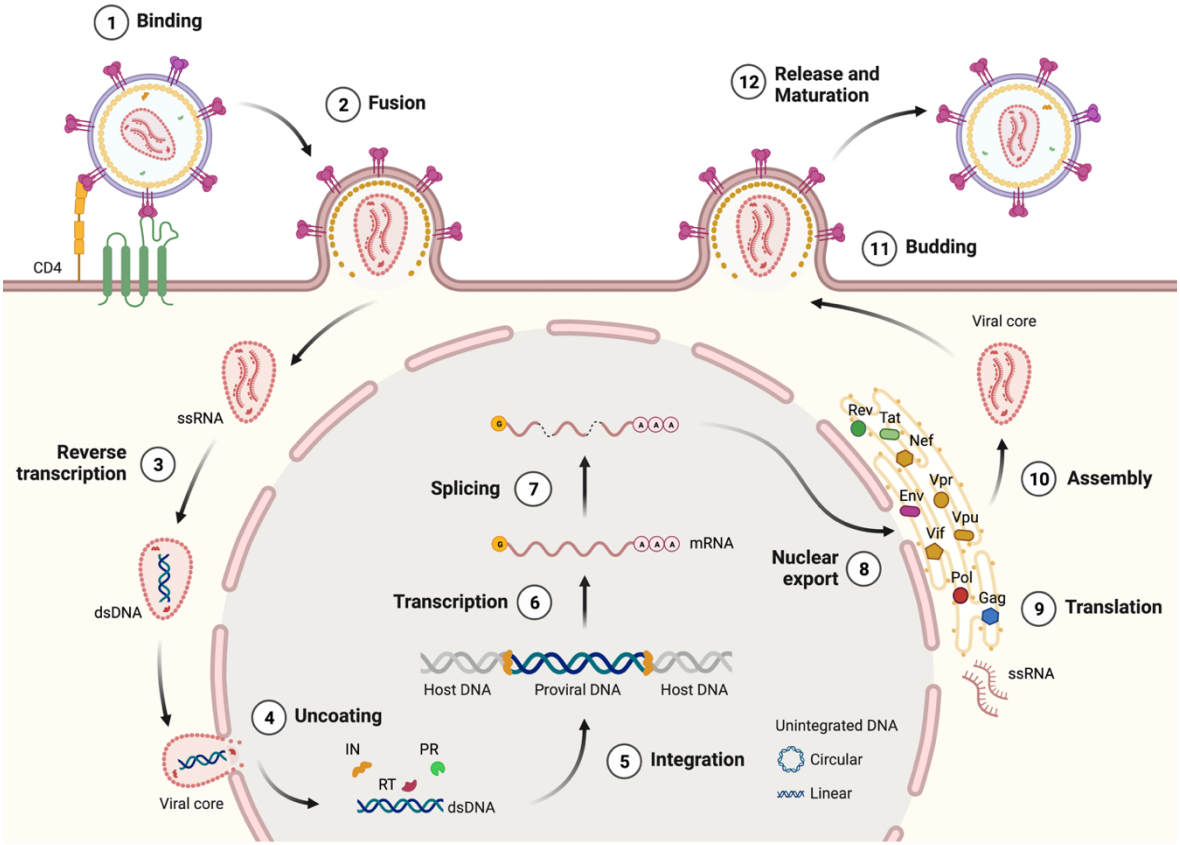

Figure 4. HIV-1 replication cycle. Schematic overview of the sequential steps in the HIV-1 replication cycle: (1) binding of the HIV-1 particle to the CD4 receptor and co-receptor CCR5 or CXCR4; (2) fusion between the viral and the host cellular membranes; (3) reverse transcription of the single-stranded RNA into double-stranded DNA (proviral DNA) and translocation into the nuclear pore; (4) uncoating of the viral capsid, and release of the proviral DNA and proteins into the cell nucleus; (5) integration of the proviral DNA into the host genome; (6) transcription of the integrated proviral DNA into viral mRNA; (7) alternative splicing of full-length (~9.8 kb) mRNA; (8) nuclear export of all protein encoding mRNAs; (9) translation of mRNAs into viral proteins; (10) translocation of viral proteins and genomic RNA to the cell membrane and assembly of new HIV-1 virions; (11) viral budding out of the cell and subsequent membrane scission; and (12) maturation into new infectious virions. Created with BioRender.com.

1.5.2. Post-entry events: uncoating to integration

Fusion of the viral and cellular membranes leads to internalization of the viral capsid into the cell cytoplasm. At the same time, a slow uncoating begins, which consists in the disassembly of the cone-shaped capsid into smaller fragments. Initially, the viral capsid was assumed to rapidly disassemble upon entry into the cytoplasm, but more recent evidence indicates that incoming capsids remain intact at least through the initial stages of reverse transcription. Conceptually, the viral

core needs to reach the nuclear pore containing a substantial amount of the assembled capsid, since it protects the viral genome against detection by innate immune sensors of the cell and is required for both nuclear import and reverse transcription[22,23].

When the intact or nearby intact capsid containing the viral genome reach the nuclear compartment of cells, reverse transcription of the RNA genome into double-stranded DNA occurs in the cell nucleus alongside uncoating. Following completion of reverse transcription, the proviral DNA is integrated into the host genome by the viral enzyme IN. Aborted integration DNA can be found as episomal linear or circular DNA. Integrated proviral DNA can be replicated, transcribed, and translated together as part of the host genome or can persist in a reversible latent state of non-productive infection[24]. Integration of the proviral DNA finalizes the establishment of a persistent infection of the cell (Figure 4, steps 3-5).

1.5.3. Viral RNA biogenesis: transcription to translation

Once the infected cell becomes activated, the integrated proviral DNA is transcribed into viral mRNA of approximately 9.8 kb in length by a variety of cellular transcription factors and RNA polymerases recruited at the 5' LTR promoter. Before full-length mRNA is ready to be exported of the nucleus, it needs to be processed by acquiring a 7-methylguanosine (m7G) cap structure at the 5' end, splicing of coding sequences, and adding a poly(A) tail at the 3' end. When the nascent mRNA is only 20-40 nucleotides long, is capped with a m7G at the 5' end by a series of enzymatic reactions. The m7G cap is recognized and attached by the cap binding complex (CBC), which plays a critical role in the stabilization, processing, nuclear export, and translation initiation of the mRNA[25].

Then, the nascent mRNA undergoes a complex series of splicing events to generate different arrangement of transcripts coding for the nine viral proteins. The splicing process relies on multiple viral regulatory sequences and a large ribonucleoprotein complex, the spliceosome. Spliced viral transcripts can be classified in single spliced and multiple spliced transcripts. The smaller, multiple spliced (~2 kb) mRNAs, coding for the regulatory proteins Tat, Rev, and Nef, are

exported from the nucleus to the cytoplasm to be translated, while unspliced (~9.8 kb) and single spliced (~4 kb) mRNAs are retained in the nucleus, restricting the expression of these sequences. Then, Tat and Rev regulatory proteins return to the nucleus, where Tat binds to the transactivation responsive (TAR) sequence, enhancing transcription initiation and elongation, and Rev binds to the Rev-responsive element (RRE) in the *env* gene, promoting nuclear export and efficient translation of the unspliced and single spliced mRNAs into viral proteins. The unspliced transcripts code for the Gag and Gag-Pol precursor polyproteins and serve as viral genome for the nascent virions, while the spliced transcripts code for the structural/accessory proteins of the new virions Env, Vif, Vpr, and Vpu required for productive viral infection. Altogether are packaged within the nascent virions (Figure 5)[26].

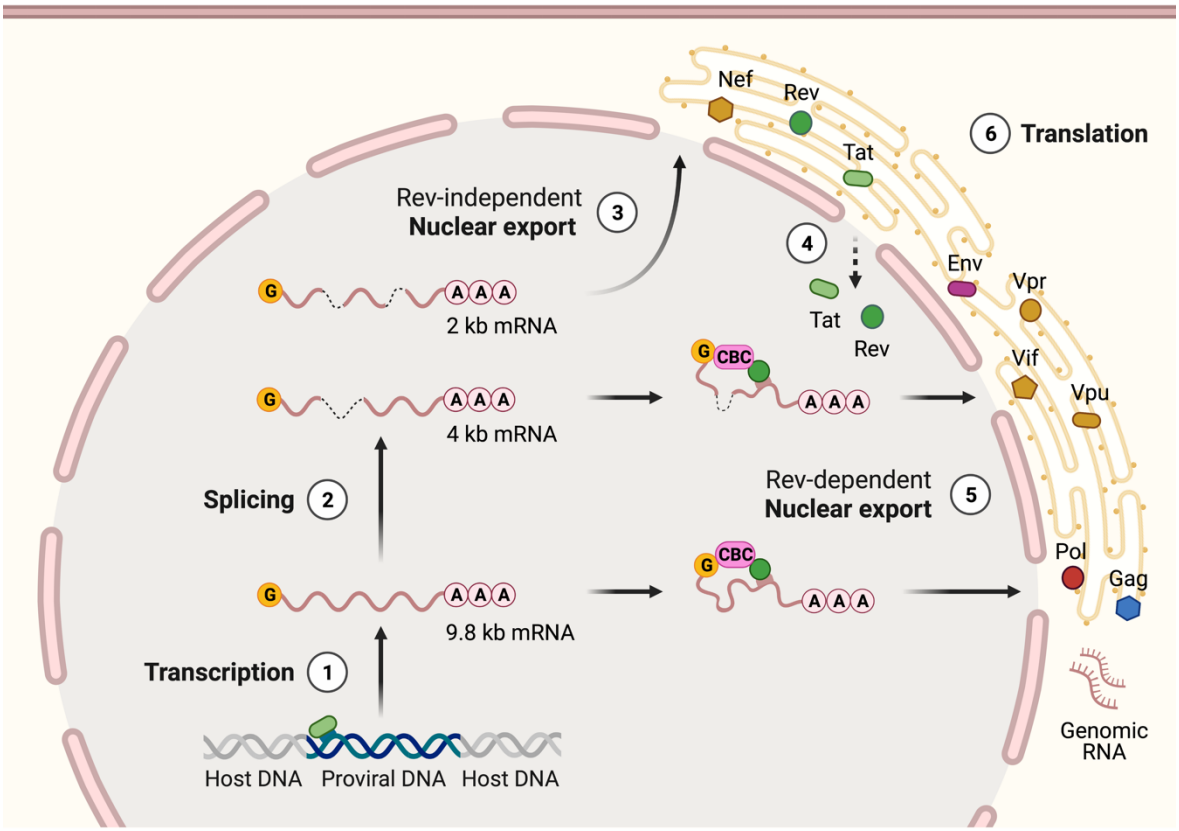

Figure 5. Viral transcription and mRNA processing. Schematic overview of the sequential mRNA processing events in the HIV-1 replication cycle: (1) transcription of the integrated proviral DNA into viral mRNA; (2) alternative splicing of full-length (~9.8 kb) mRNA into single spliced (~4 kb) and multiple spliced (~2 kb) mRNAs; (3) nuclear export of multiple spliced mRNAs coding for Tat, Rev, and Nef; (4) return of Tat and Rev regulatory proteins to the nucleus; (5) Rev-dependent nuclear export of unspliced and single spliced mRNAs; and (6) translation of mRNAs into viral proteins. G: 5' 7-methylguanosine cap structure; CBC: cap binding complex; A: 3' Poly(A) tail. Created with BioRender.com.

Of note, all protein encoding mRNAs contain a uniform 3' end consisting of 200-400 adenosine residues, the poly(A) tail, which is added by the cellular polyadenylation machinery and regulates degradation of the mRNA and their translation (Figure 4, steps 6-9)[27].

1.5.4. Viral release: assembly, budding, and proteolytic maturation

Assembly of new HIV-1 virions occurs at the plasma membrane of the host cell through the Gag precursor polypeptide and its proteolytic maturation products. The MA domain allows Gag to associate preferentially with the plasma membrane rather than intracellular membranes. Viral budding out of the cell through the plasma membrane and subsequent membrane scission, required to form the nascent viral particle, are also mediated by the Gag precursor polypeptide and cellular endosomal sorting complexes required for transport. In the final step of the viral replication cycle, the viral enzyme PR converts immature viral particles to infectious virions via the proteolysis of Gag and Gag-Pol precursor polypeptides to yield the structural components MA, CA and NC, and the PR, RT and IN enzymes, respectively (Figure 4, steps 10-12)[28].

1.6. Pathogenesis

HIV can be transmitted by the exchange of body fluids from infected people such as blood, semen, vaginal secretion, and breast milk. HIV can also be transmitted from infected mother to child during pregnancy, delivery, or breastfeeding. However, sexual transmission through the genital tract or rectal mucosa represents the highest proportion of new infections[29].

Transmission of HIV across mucosal membranes is usually established by one founder virus. The primary target of HIV is activated $CD4^+$ T cells. Nevertheless, other cells expressing the CD4 surface molecule may also be infected, including resting $CD4^+$ T cells, monocytes, macrophages, and dendritic cells. After transmission of the founder virus there is a rapid increase in viral replication. Then, the virus passes through the draining lymph nodes, disseminates to blood, and

establishes the infection into the secondary lymphoid tissues, particularly the gut-associated lymphoid tissue (GALT)[30].

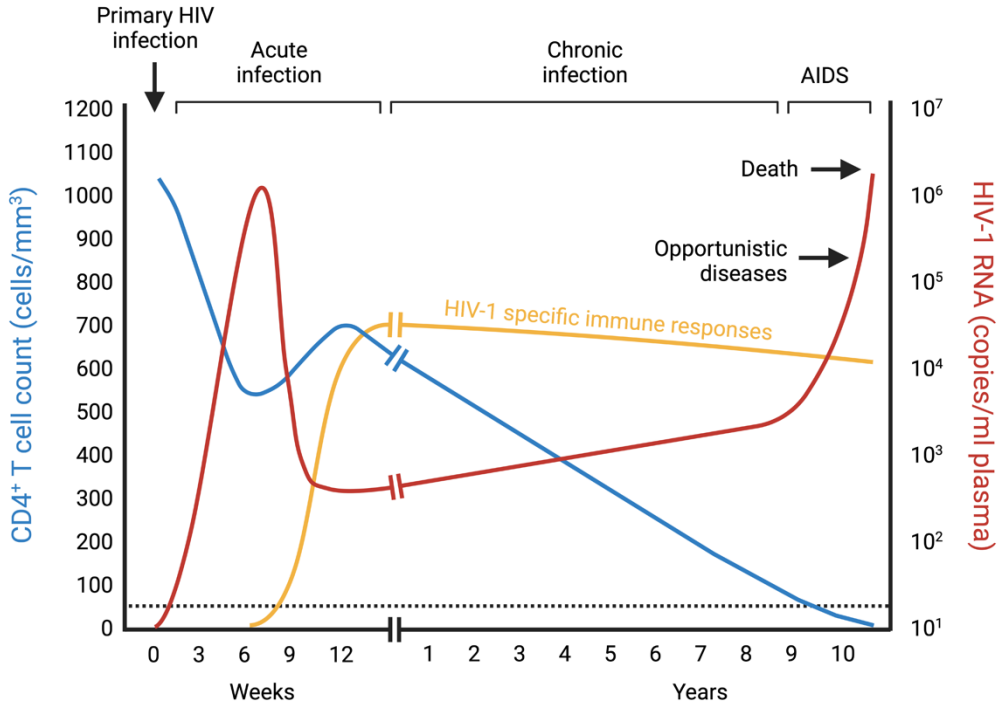

Figure 6. Natural course of HIV-1 infection. Schematic representation of the progressive decline of CD4+ T-cell count (blue line), contrasted with the increase in HIV-1 viral load (red line), and HIV-1-specific immune responses (yellow line) over time in the absence of ART. Adapted from reference [31].

The natural course of HIV – in the absence of ART – commonly includes three different stages: acute infection, chronic infection, and AIDS (Figure 6). Overall, HIV infection causes a progressive decline of CD4+ T-cell count, chronic immune activation, and subsequent exhaustion of the immune system, which is associated with the development of opportunistic infections and cancers, the progression to AIDS, and eventually the death of people with HIV (PWH)[31].

Acute infection is characterized by an initial peak in viral load (10^5-10^7 HIV RNA copies/ml plasma) and a consequent massive depletion of CD4+ T cells. During this stage, PWH may develop virus-like clinical symptoms such as fever, pharyngitis, lymphadenopathy, and rash. This phase spans up to 3 months after infection until the immune system generates HIV-specific antibodies (seroconversion) and CD8+ T-cell immune responses against HIV antigens exposed on the surface of infected

cells, which drives a reduction of plasma viraemia and increases the levels of $CD4^+$ T cells[32]. During this phase, the massive depletion of mucosal $CD4^+$ T cells, especially in the gastrointestinal tract, can result in structural changes to the gut mucosa and cause an apparent breakdown of its epithelial barrier, which leads to systemic translocation of microbial products so further increasing immune activation[33].

Acute infection is followed by chronic and generally asymptomatic phase of infection that can last up to ten years and is characterized by a progressive decline of peripheral $CD4^+$ T-cell count, partial control of viral replication, and chronic immune activation. Despite the stable viral load, the virus continues replicating and disseminating to lymphoid tissues. This persistent exposure to viral antigens is responsible for the constant stimulation of the immune system.

Once the peripheral $CD4^+$ T-cell count drops below 200 cells/mm^3 or a weakened immune system enables for the occurrence of opportunistic infections and cancers associated with HIV infection, the disease reaches the AIDS phase, which eventually can lead to death[34].

2. Antiretroviral treatment to HIV infection

2.1. Antiretroviral therapy

Antiretroviral therapy (ART) has transformed HIV infection from one of the world's deadliest infections into a manageable chronic condition. In 1987, the U.S. Food and Drug Administration (FDA) approved the first antiretroviral drug, Azidothymidine (AZT), a reverse transcriptase inhibitor[35]. Since then, significant progress has been achieved in the therapy of HIV-1 infection, especially with the introduction of protease inhibitors in 1996 and the administration of combined ART[36]. To date, more than 25 drugs that block HIV-1 replication at many steps in the virus lifecycle have been approved by the FDA and the European Medicines Agency (EMA) and are still available and/or recommended for the treatment of HIV-1 infection (Table 1)[37].

Table 1. Antiretroviral drugs currently recommended for the treatment of HIV-1 infection. Compounds are listed according to drug class, identified by generic and brand names, and sorted by approval date. Table based on information from FDA.

Generic name	Brand name	Approval date
Entry inhibitors		
Enfuvirtide	Fuzeon	March 13, 2003
Maraviroc	Selzentry	August 6, 2007
Ibalizumab-uiyk	Trogarzo	March 6, 2018
Fostemsavir	Rukobia	July 2, 2020
Nucleoside reverse transcriptase inhibitors (NRTIs)		
Zidovudine	Retrovir	March 19, 1987
Lamivudine	Epivir	November 17, 1995
Abacavir	Ziagen	December 17, 1998
Tenofovir disoproxil fumarate	Viread	October 26, 2001
Emtricitabine	Emtriva	July 2, 2003
Non-nucleoside reverse transcriptase inhibitors (NNRTIs)		
Nevirapine	Viramune	June 21, 1996
	Viramune XR	March 25, 2011
Efavirenz	Sustiva	September 17, 1998
Etravirine	Intelence	January 18, 2008
Rilpivirine	Edurant	May 20, 2011
Doravirine	Pifeltro	August 30, 2018
Integrase strand transfer inhibitors (INSTIs)		
Raltegravir	Isentress	October 12, 2007
	Isentress HD	May 26, 2017
Dolutegravir	Tivicay	August 12, 2013
	Tivicay PD	June 12, 2020
Cabotegravir	Vocabria	January 22, 2021

Generic name	Brand name	Approval date
Protease inhibitors (PIs)		
Saquinavir	Invirase	December 6, 1995
Ritonavir*	Norvir	March 1, 1996
Atazanavir	Reyataz	June 20, 2003
Fosamprenavir	Lexiva	October 20, 2003
Tipranavir	Aptivus	June 22, 2005
Darunavir	Prezista	June 23, 2006
Capsid inhibitors		
Lenacapavir	Sunlenca	December 22, 2022
Pharmacokinetic enhancers		
Cobicistat	Tybost	September 24, 2014

*Ritonavir is a PI, although it is generally used as a pharmacokinetic enhancer.

These antiretroviral drugs are classified in five major classes based on the steps of the HIV-1 replication cycle they target (Figure 7):

- **Entry inhibitors**: two different kinds of inhibitors block the entry of the virus into target cell by thwarting either the interaction between the viral envelope glycoprotein gp120 and the CCR5 co-receptor or the fusion between the viral envelope glycoprotein gp41 and the cellular membrane.
- **Nucleoside/nucleotide reverse transcriptase inhibitors (NRTIs)** and **non-nucleoside reverse transcriptase inhibitors (NNRTIs)**: target the reverse transcription step that converts the viral RNA genome into proviral DNA.
- **Integrase strand transfer inhibitors (INSTIs)**: block integrase enzyme activity that is required to insert proviral DNA into the host genome.
- **Protease inhibitors (PIs)**: inhibit protease enzyme activity that is critical for the proteolytical maturation of viral particles that bud out from infected cells.

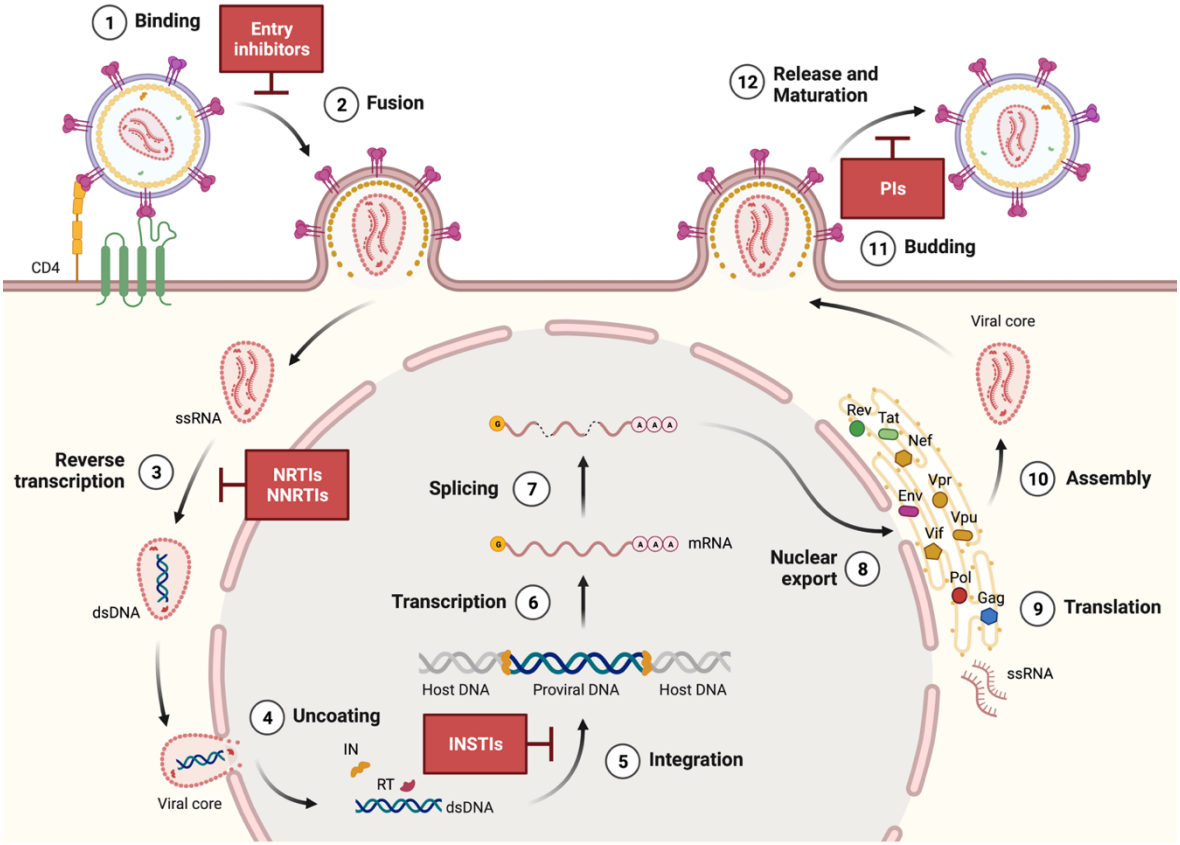

Figure 7. HIV-1 replication cycle showing the sites of action of different classes of antiretroviral drugs. Schematic overview of the five major classes of antiretroviral drugs and the steps of the HIV-1 replication cycle they target: entry inhibitors; nucleoside/nucleotide reverse transcriptase inhibitors (NRTIs) and non-nucleoside reverse transcriptase inhibitors (NNRTIs); integrase strand transfer inhibitors (INSTIs); and protease inhibitors (PIs). Created with BioRender.com.

Standard ART regimens generally combine at least two antiretroviral drugs directed against at least two distinct targets. Typically, two NRTIs combined with either a NNRTI, a PI, or an INSTI (Table 2)[38]. The combinatorial approach significantly increases efficacy and reduces the probability of the virus developing drug resistance.

Table 2. Combination medicines for the treatment of HIV-1 infection. Different combinatorial medicines are listed according to the generic names of the drugs used in fixed-dose combination formulations, identified by brand names, and sorted by approval date. Table based on information from FDA.

Generic name	Brand name	Approval date
Lamivudine and Zidovudine	Combivir	September 27, 1997
Lopinavir and Ritonavir	Kaletra	September 15, 2000

Generic name	Brand name	Approval date
Abacavir, Lamivudine, and Zidovudine	Trizivir	November 14, 2000
Abacavir and Lamivudine	Epzicom	August 2, 2004
Emtricitabine and Tenofovir disoproxil fumarate	Truvada	August 2, 2004
Efavirenz, Emtricitabine, and Tenofovir disoproxil fumarate	Atripla	July 12, 2006
Emtricitabine, Rilpivirine, and Tenofovir disoproxil fumarate	Complera	August 10, 2011
Elvitegravir, Cobicistat, Emtricitabine, and Tenofovir disoproxil fumarate	Stribild	August 27, 2012
Abacavir, Dolutegravir, and Lamivudine	Triumeq	August 22, 2014
	Triumeq PD	March 30, 2022
Atazanavir and Cobicistat	Evotaz	January 29, 2015
Elvitegravir, Cobicistat, Emtricitabine, and Tenofovir alafenamide	Genvoya	November 5, 2015
Darunavir and Cobicistat	Prezcobix	January 29, 2015
Emtricitabine and Tenofovir alafenamide	Descovy	April 4, 2016
Emtricitabine, Rilpivirine, and Tenofovir alafenamide	Odefsey	March 1, 2016
Dolutegravir and Rilpivirine	Juluca	November 21, 2017
Bictegravir, Emtricitabine, and Tenofovir alafenamide	Biktarvy	February 7, 2018
Lamivudine and Tenofovir disoproxil fumarate	Cimduo	February 28, 2018
Doravirine, Lamivudine, and Tenofovir disoproxil fumarate	Delstrigo	August 30, 2018
Efavirenz, Lamivudine, and Tenofovir disoproxil fumarate	Symfi	March 22, 2018
	Symfi Lo	February 5, 2018
Darunavir, Cobicistat, Emtricitabine, and Tenofovir alafenamide	Symtuza	July 17, 2018
Lamivudine and Tenofovir disoproxil fumarate	Temixys	November 16, 2018
Dolutegravir and Lamivudine	Dovato	April 8, 2019
Cabotegrabir and Rilpivirine	Cabenuva	January 22, 2021

In 2022, 29.8 million people were accessing ART, which represents 76% of all people living with HIV[12]. ART suppresses viral replication and reduces viral load to concentrations below the lower limit of detection (LOD) of standard assays used for clinical monitoring (<50 HIV-1 RNA copies/ml plasma) resulting in a significant reconstitution of the immune system as measured by an increase in circulating $CD4^+$ T cells (Figure 8)[39]. Thus, starting ART early after infection and strict adherence to daily therapy improve prognosis of HIV-1 infection and prevent the risk of viral transmission. In addition, antiretroviral drugs are highly effective as pre-exposure prophylaxis (PrEP) for preventing HIV-1 infection in people who are at risk of being exposed to HIV-1 through sex or injection drug use. Truvada and Descovy are the two combination regimens approved by the FDA for use as PrEP. However, if PrEP is not taken as prescribed it may not block the virus.

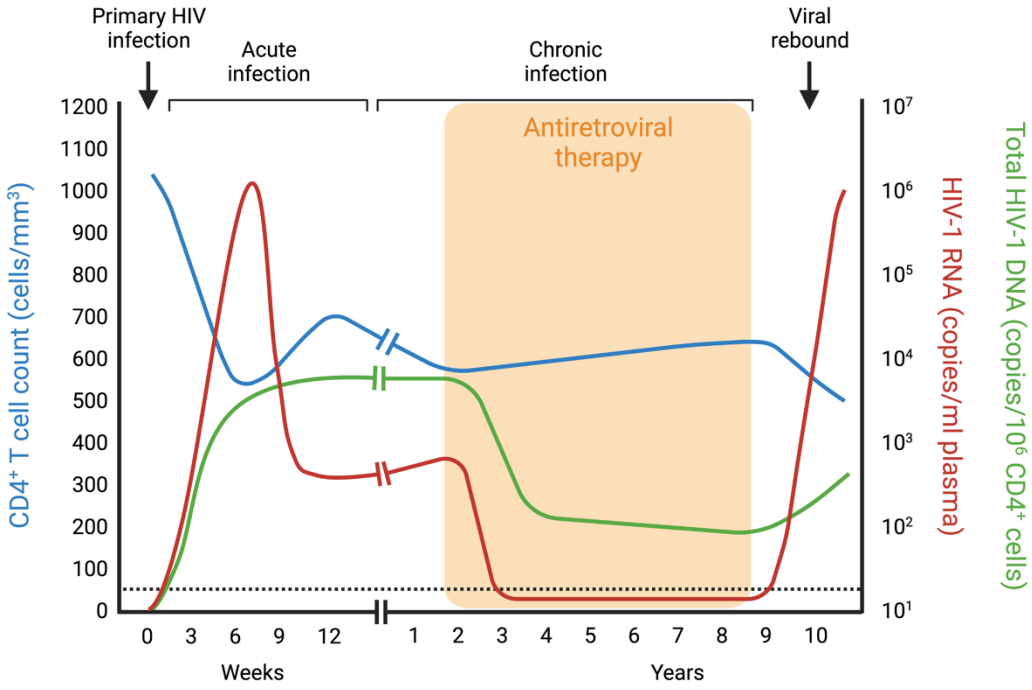

Figure 8. Natural course of HIV-1 infection and changes after ART. Schematic representation of the progressive restoration of $CD4^+$ T-cell count (blue line), contrasted with the suppression of HIV-1 viral load (red line) and reduction of proviral HIV-1 DNA (green line) over time in the presence of ART. Dot line represents the LOD of the viral load by standard clinical assays (50 HIV-1 RNA copies/ml plasma). Adapted from reference [40].

Although ART is very successful in the control of viral replication and has demonstrated significant reduction of morbidity and mortality, it is unable to cure HIV-1 infection because it cannot target proviral DNA already integrated in a

quiescent state into host genomes[41]. If treatment is interrupted, these cells may be a source for viral rebound and subsequent drop of CD4+ T-cell count (Figure 8)[42]. Hence, lifelong treatment is needed for effective control of HIV-1 infection. However, the economic costs of providing ART to all PWH for life might be unsustainable on the long-term. Moreover, extended use of ART exposes people to toxic effects of drugs, complex drug-drug interactions (polypharmacy), and development of drug resistance, particularly for those individuals who are unable to fully adhere to treatment[43].

2.2. Viral persistence in treated HIV-1 infection

In the past years, it has been extensively demonstrated that HIV-1 persists in individuals receiving suppressive ART integrated into the genome of long-lived latently infected cells as part of what is known as the latent reservoir. This latent reservoir can be induced to produce virions at any given time and, in the absence of ART, it might reignite infection, thus representing the main barrier for curing HIV-1 infection[44]. In this context, latency is defined as integration of proviral DNA into the host genome in the absence of virus expression.

2.2.1. Cellular reservoirs for HIV-1

In 1995, it was first described the role of resting CD4+ T cells as a reservoir for HIV-1[41] and they are still regarded as the largest reservoir and the primary barrier to a cure. CD4+ T cells are the preferred target for HIV-1 as they express high amounts of CD4, which is the primary receptor required for HIV-1 binding. Several different CD4+ T-cell subsets can be identified according to their differentiation and memory status. The earliest differentiation stage and the precursors of memory cells are the naïve CD4+ T cells (T_N). The memory CD4+ T cells are the major source of latent HIV-1 DNA and can be classified based on their differentiation and memory status into T stem cell memory (T_{SCM}), central memory (T_{CM}), transitional memory (T_{TM}), effector memory (T_{EM}), and terminally differentiated (T_{TD}) cells (Figure 9)[45].

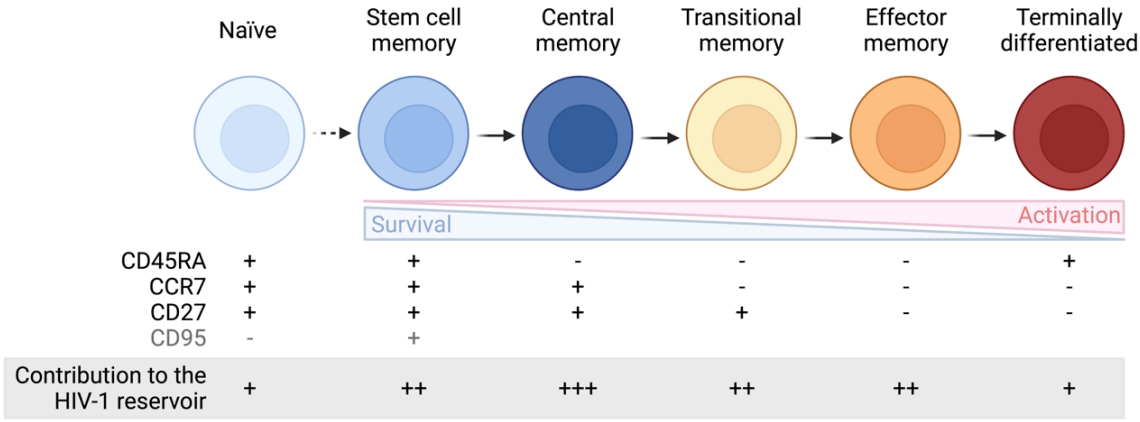

Figure 9. Contribution of CD4+ T-cell subsets to the HIV-1 reservoir in treated HIV-1 infection. Schematic representation of CD4+ T-cell subsets, classified according to their differentiation and memory status. Cell-surface markers can be used to identify each individual subset. The relative contribution of each subset to the HIV-1 reservoir is indicated. Adapted from reference [46].

Overall, T_{CM} followed by T_{EM} and T_{TM} subsets consistently contain the highest level of integrated HIV-1 DNA and due to their relatively large size, high homeostatic proliferation ability, and long-life span, are considered the major cellular reservoirs for HIV-1[45]. T_{SCM} subset represents also a significant long-term reservoir for HIV-1 due to their extreme stability over time and homeostatic self-renewal maintenance, although this cell subset is relatively small in size[47]. T_N and T_{TD} subsets only minimally contribute to latent HIV-1 reservoir in most individuals.

In addition to the resting memory cell subsets described above, other CD4+ T cells such as T helper (T_H), follicular helper (T_{FH}), regulatory (T_{reg}), migratory memory (T_{MM}), tissue resident memory (T_{RM}), and γδ ($T_{\gamma\delta}$) cells have been demonstrated to harbor integrated HIV-1 DNA in individuals on suppressive ART[48]. Furthermore, other cell types may also contribute to the viral reservoir such as myeloid cells, including monocytes, macrophages, and dendritic cells, as well as microglial cells and astrocytes in the central nervous system[47].

2.2.2. Establishment and maintenance of the HIV-1 reservoir

The HIV-1 reservoir is established within the first days following HIV-1 infection[49], so early treatment initiation can limit but not totally prevent the seeding of the latent reservoir[50,51]. The HIV-1 reservoir is established in a small but extremely

stable pool of resting memory CD4+ T cells by both infection of activated CD4+ T cells which revert to a resting state as memory cells, or by direct infection of resting memory CD4+ T cells[52]. Activated CD4+ T cells generally die within a few days from cytopathic effects of the virus or cytolytic effector mechanisms of the immune system, but some infected cells survive long enough to revert to a resting state as memory cells, thereby establishing a stable latent reservoir of resting memory CD4+ T cells (Figure 10).

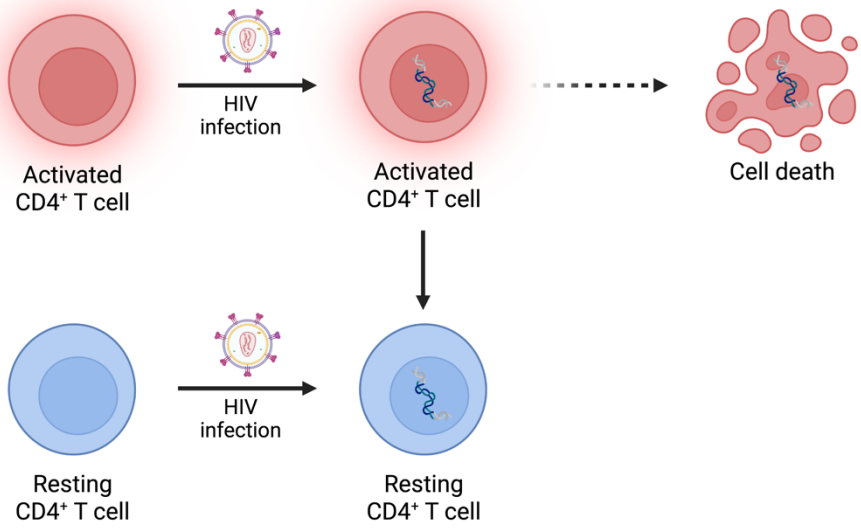

Figure 10. Establishment of the HIV-1 reservoir in resting memory CD4+ T cells. Schematic representation of the establishment of the HIV-1 reservoir, via survival of activated infected CD4+ T cells which revert to a resting state or, less frequently, by direct infection of resting memory CD4+ T cells.

The stability of the memory CD4+ T-cell reservoir over time is naturally maintained by T-cell survival and clonal expansion, providing viral reservoir with the ability to expand in the absence of viral replication. First, the stability of the latent reservoir reflects the basic biology of memory CD4+ T cells and the long-term survival of these cells. Thus, these long-lived memory CD4+ T cells are an ideal long-term viral reservoir and ensure the persistence of virus in this cell population for years. Second, the size of the HIV-1 reservoir is maintained by clonal expansion of memory CD4+ T cells with integrated viral genome, due to both homeostatic and antigenic driven proliferation[48]. Homeostatic proliferative renewal is mediated by cytokines such as IL-7[53] in response to a decline in the number of CD4+ T cells.

Antigenic driven proliferation occurs when the T-cell receptor of a memory CD4⁺ T cell is stimulated by a specific antigen that drives clonal expansion (Figure 11).

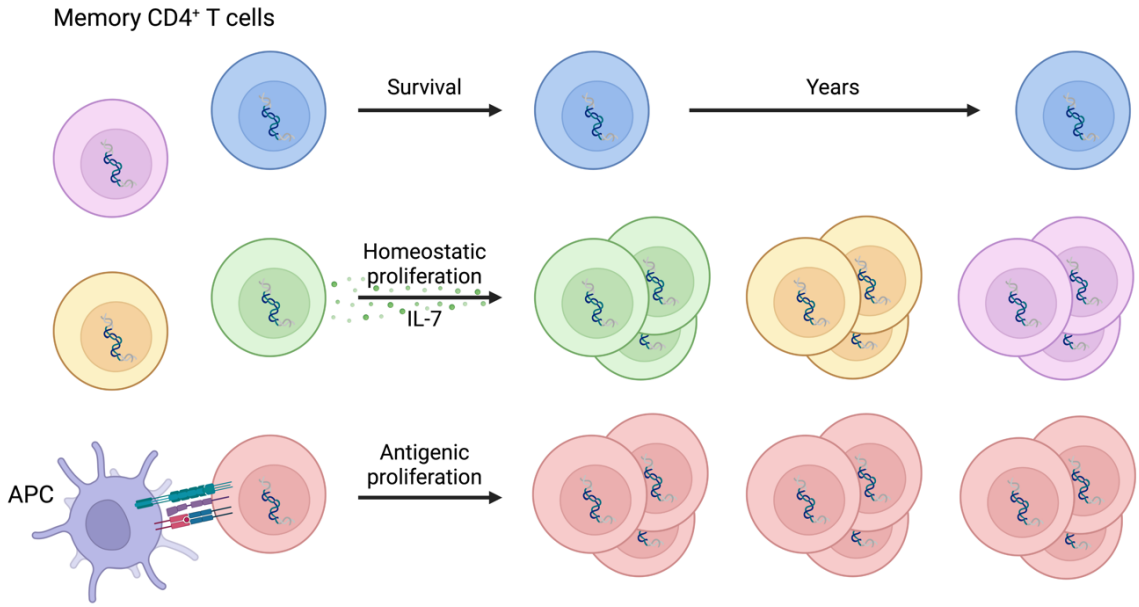

Figure 11. Mechanisms that contribute to the maintenance of the HIV-1 reservoir. Schematic representation of the maintenance of the resting memory CD4⁺ T-cell reservoir, by cell survival and both homeostatic and antigenic driven proliferation. Each cell color represents a different clone of resting memory CD4⁺ T cells with integrated viral genome. APC: Antigen presenting cell.

2.2.3. Anatomical reservoirs for HIV-1

All cell types that harbor integrated HIV-1 DNA and comprise viral reservoirs described above, persist with different contributions in a variety of tissues and organs including lymphoid tissues, central nervous system, liver, lungs, skin, adipose tissue, and genital and urinary tracts[54]. Peripheral blood is the most accessible source of these latently infected cells and therefore the best studied and understood reservoir. However, only 2% of lymphocytes are found in circulation while 98% reside in lymphoid tissues[55], which suggests that the number of latently infected CD4⁺ T lymphocytes may be higher in tissues than in circulation, indicating that the HIV-1 reservoir in peripheral blood is just a small and unrepresentative portion of the total body reservoir.

Lymphoid tissues, which comprise the bone marrow, thymus, lymph nodes, spleen, and gut-associated lymphoid tissue (GALT), are not only the primary sites

for viral replication and CD4+ T-cell destruction, but also major sites of viral persistence during ART[56]. GALT is considered the largest lymphoid tissue in the body, and it is estimated to comprise the largest proportion (83-95%) of the total HIV-1 reservoir, mainly formed by memory CD4+ T cells from the peripheral blood and macrophages that migrate into GALT[57].

Anatomical reservoirs may serve as both pharmacologic and immunologic privileged sites for HIV-1 that can theoretically prevent effective drug penetration and immune recognition. Therefore, infected cells in these sanctuaries could be a source of persistent viral production, thus contributing to viral reservoir replenishment and maintenance in the setting of combination therapy.

2.2.4. Residual viraemia in treated HIV-1 infection

ART is fully effective at blocking HIV-1 replication. However, it has no effect on the cells that are already infected, nor can prevent viral expression from integrated HIV-1 genomes. Because of this, most PWH on ART for prolonged periods of time show residual viraemia in peripheral blood (Figure 12)[58].

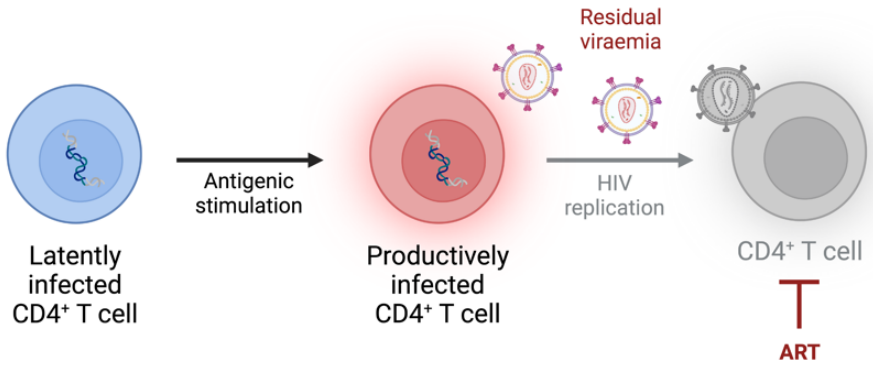

Figure 12. Residual viraemia in HIV-1 treated infection. Schematic representation of the continued viral production and subsequent residual viraemia during ART.

This residual viraemia may originate from reactivation of virus in a small proportion of latently infected cells that are undergoing stimulation. Indeed, residual viraemia may also be attributed to the high frequency of activated CD4+ T cells and persistent inflammation observed within GALT since CD4+ T-cell activation is crucial for *de novo* infection and is associated with higher concentration of virus-expressing cells and a progressive loss of the efficacy of viral suppression[59]. Thus, there likely

exists a bi-directional association between residual viraemia in suppressed individuals and the size of viral reservoir since residual viraemia may in turn contribute to the continuous replenishment of the viral reservoir by inducing antigenic driven proliferation of infected cells and even the initiation of new infection cycles within lymphoid tissues and immune sanctuaries with poor penetration of antiretroviral drugs[46].

2.2.5. Chronic immune activation in treated HIV-1 infection

The mechanisms driving chronic immune activation, and by extension general inflammation, during suppressive ART are multifactorial and either directly or indirectly related to the persistence of the virus. Continuous exposure of the immune system to HIV-1 antigens and, eventually, to microbial-derived products translocated to the bloodstream after gut epithelial disruption leads to phenotypic and functional hyperactivation of the innate and adaptive immune systems. This immune activation significantly decreases with administration of suppressive ART, although several pathways of immune activation and inflammation remain abnormal during suppressive ART.

Immune activation is evidenced by elevated markers of activation, such as CD38 or HLA-DR[60], and/or exhaustion, such as PD-1[61], on the surface of T cells. T-cell activation, as measured with the expression of CD38 and HLA-DR on $CD4^+$ and $CD8^+$ T cells, is a recognized predictor of the adverse prognosis during ART suppression[62]. High levels of pro-inflammatory cytokines and chemokines in both plasma and lymph nodes, are also observed in ART-suppressed individuals.

The main cause of immune activation during HIV-1 infection is viral antigenic stimulation (Figure 13). During primary infection, HIV-1 induces strong T-cell responses, in particular $CD8^+$ T cells, which can persist after ART suppression due to viral production coming from eventual reactivation of latently infected cells. Moreover, immune activation may be directly induced by viral gene products in ART-treated individuals in the absence of infectious viral particles. Most integrated viral genomes are defective, incapable of producing infectious virus but capable of transcribing non-coding viral mRNAs and translating viral proteins that may

contribute to elevated levels of immune activation in virally suppressed individuals[63]. A vicious cycle is therefore established, during which constant antigenic exposure promotes chronic immune activation as well as chronic immune activation promotes continuous viral expression from integrated genomes[64].

HIV-1 also causes immune activation and inflammation through indirect mechanisms (Figure 13). The epithelial disruption in the GALT mucosa driven by local infection and inflammation leads to increased plasma concentration of microbial products such as lipopolysaccharides. These microbial products are highly likely to result in a profound T-cell activation, through the production of pro-inflammatory cytokines, including interleukins, interferons, and chemokines, and the establishment of a systemic pro-inflammatory state[65]. ART appears to restore this damage only to a minimal extent. However, the resulting, chronic exposure to microbial-derived products is thought to be partly responsible for the chronic immune activation and inflammation seen even in PWH on ART with adequate $CD4^+$ T-cell restoration[66]. In addition to HIV-1, antigen-mediated immune activation can also be induced by other persistent viruses, especially cytomegalovirus and Epstein-Barr virus[67]. This HIV-1-related immune dysfunction may facilitate the reactivation and replication of these persistent viruses.

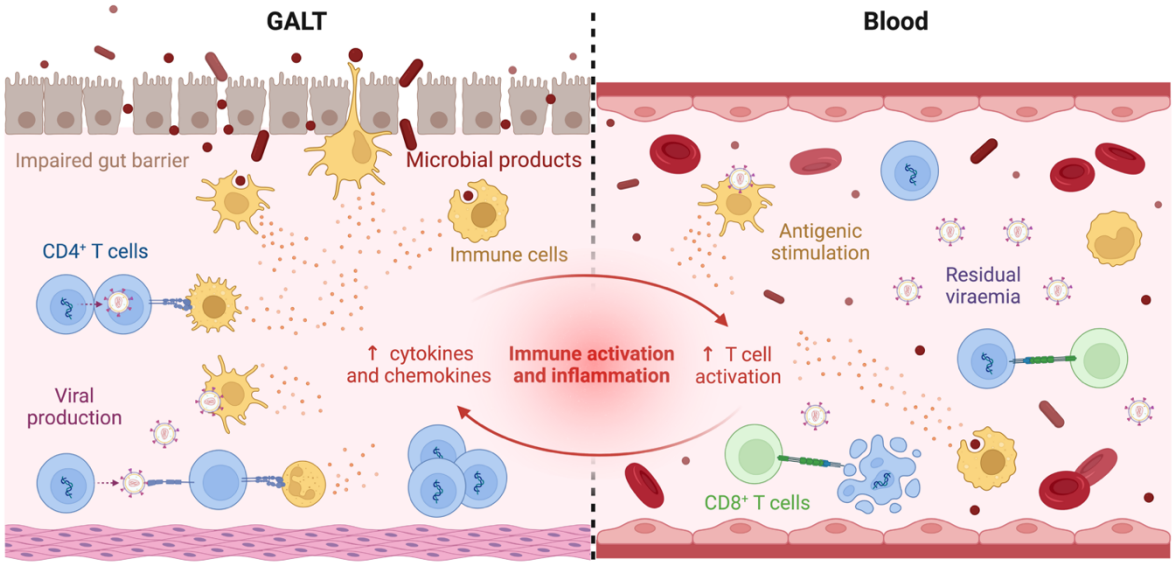

Figure 13. Mechanisms that contribute to chronic immune activation and inflammation in treated HIV-1 infection. Schematic representation of the continuous exposure of the immune system to HIV-1 antigens and, eventually, to microbial-derived products translocated to the bloodstream after gut epithelial disruption that leads to phenotypic and functional hyperactivation of the innate and adaptive immune systems. Created with BioRender.com.

The state of chronic immune activation and inflammation despite ART, has detrimental effects on the immune system. Immune activation causes notable T-cell turnover, senescence, and apoptosis, which represent a massive load for the immune system in order to maintain homeostasis. Over time, this may gradually result in an irreversible exhaustion of its regenerative capacities and the development of immunosenescence. In addition, the elevated production of pro-inflammatory cytokines and chemokines leads to systemic activation and the establishment of a pro-inflammatory state[68]. This process of chronic immune activation and inflammation may be, at least in part, responsible for the increased morbidity and comorbidities observed in PWH.

3. Novel therapeutic approaches towards a functional cure

As previously stated, ART remains the most successful therapy against HIV infection to date. However, current ART regimens are not curative, due to the persistence of latent viral reservoirs that cannot be eradicated by ART nor the immune system. In this context, multiple therapeutic approaches have been explored to target the latent viral reservoirs including intensification of treatment, latency reversal or latency silencing. These last two require either inducing latently infected cells to produce HIV-1 expression to expose these virus-producing cells for immune clearance (known as “shock-and-kill” strategy) or further silencing HIV-1 expression for prolonged drug-free remission (known as “block-and-lock” strategy)[69]. Nevertheless, none have effectively reduced the size of the latent reservoir *in vivo*. In addition, supplementary immunomodulatory therapies, cell and gene therapies, or therapeutic vaccines are being investigated although they have not yet led to an apparent and durable improvement of the immune function and/or complete clearance of HIV-1.

In this setting, allogeneic hematopoietic stem cell transplantation (allo-HSCT) with cells that harbor a homozygous CCR5Δ32 mutation, which is a genotype resulting in a mutated, non-functional CCR5 receptor that renders immune cells resistant to most HIV-1 strains, contributed to the only five documented cases of

ART-free HIV-1 remission or cure worldwide[70–75]. However, due to the very high risk of this medical intervention, this strategy is not feasible and cannot be applied outside the context of severe hematological malignancies and thus is limited to a small group of PWH. The international IciStem consortium, co-led by our team, has been extensively following PWH who undergo allo-HSCT for hematological malignancies, in order to investigate its potential for HIV cure, and has successfully contributed to the second and third reported cases of persistent HIV-1 remission after an allo-HSCT with CCR5Δ32 cells[72–74].

Considering the above, there remains a critical need to investigate and implement novel therapeutic approaches based on new molecular mechanisms of action that target viral persistence. The goal of these novel approaches is not only to achieve fully suppression of viral replication but also to improve drug penetration and reduce toxicity. Moreover, these strategies could also revert the long-term clinical consequences of chronic immune activation and inflammation driven directly or indirectly by the persistence of HIV-1 by adding another drug to conventional ART regimens in order to enhance the decay of the latent HIV-1 reservoir.

Different studies of ART intensification using different already approved antiviral drugs, such as Raltegravir, Maraviroc, Abacavir, or Darunavir/Ritonavir, have failed to demonstrate a significant reduction in the size of the viral reservoir or residual plasma viraemia[68,76]. A possible reason for these findings would be the failure to inhibit viral replication at sites with suboptimal efficacy of these drugs. However, it provides insight into the importance of the long half-life and clonal expansion of infected cells to maintain the reservoir, relative to other mechanisms of HIV-1 persistence on ART, such as new infection events. In addition, several studies of ART intensification using drugs addressed to enhance HIV-specific immune responses, such as statins and immunomodulators, have not shown any effects on clinical outcomes[77].

We have focused on this direction, suggesting ART intensification with a new drug, obefazimod, based on a promising two-fold approach: (1) targeting an alternative, post-integration step of the viral replication cycle and thus providing a

new tool to impact the HIV-1 persistence, while simultaneously (2) helps reducing chronic immune activation and inflammation exhibited by long-term ART-suppressed individuals[78].

3.1. Intensification of antiretroviral therapy with obefazimod

Few efforts have been aimed at the development and optimization of novel therapeutic candidates addressed to disrupt the mechanisms regulating viral RNA biogenesis, with the objective of minimizing viral persistence during ART by silencing transcriptionally active reservoirs. In this context, we explore obefazimod as a promising candidate to study its *in vivo* effects during treatment intensification due to its potential in inhibiting viral replication, through a unique mechanism of action based on interfering the biogenesis of the viral RNA, in addition to its widely described anti-inflammatory potential. This molecule might contribute to impact the persistence of viral reservoirs and chronic immune activation in long-term ART-suppressed individuals.

Obefazimod (formerly ABX464) is a first-in-class, small molecule (Figure 14) developed by Abivax, a biotechnology company that optimizes and develops drug candidates for the treatment of viral infections, chronic inflammatory diseases, and cancer.

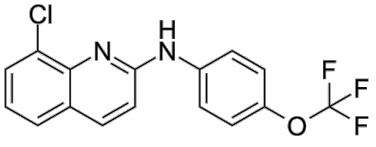

Figure 14. Obefazimod chemical structure. Schematic representation of the chemical structure of 8-chloro-*N*-[4-(trifluoromethoxy)phenyl]quinoline-2-amine (obefazimod).

Obefazimod has been described to bind to the CBC, a key complex that recruits several factors at the m7G cap structure of the nascent mRNA transcript and mediates RNA biogenesis events[25] (see section 1.5.3). By directly binding to the CBC, obefazimod targets the interaction of Rev with the CBC and prevents Rev-mediated nuclear export of viral mRNA, and therefore is capable to alter the viral expression in the HIV-1 reservoirs[79]. As described above, the Rev viral protein interacts with the RRE, located within the *env* sequence, facilitating the translocation of unspliced and single spliced mRNA from the cell nucleus to the cytoplasm

required for production of structural proteins (Gag, Pol, and Env) and generation of genomic RNA of the new virions (Figure 15). This Rev's essential role in viral replication enhances the attractiveness of Rev as a therapeutic target. Even though a variety of approaches targeting Rev function have been developed to inhibit viral replication *in vitro*[80–88], obefazimod is the first clinically available therapy based on this mechanism of action. On the other hand, obefazimod is unlikely to induce virus resistance since it targets a cellular, rather than a viral component.

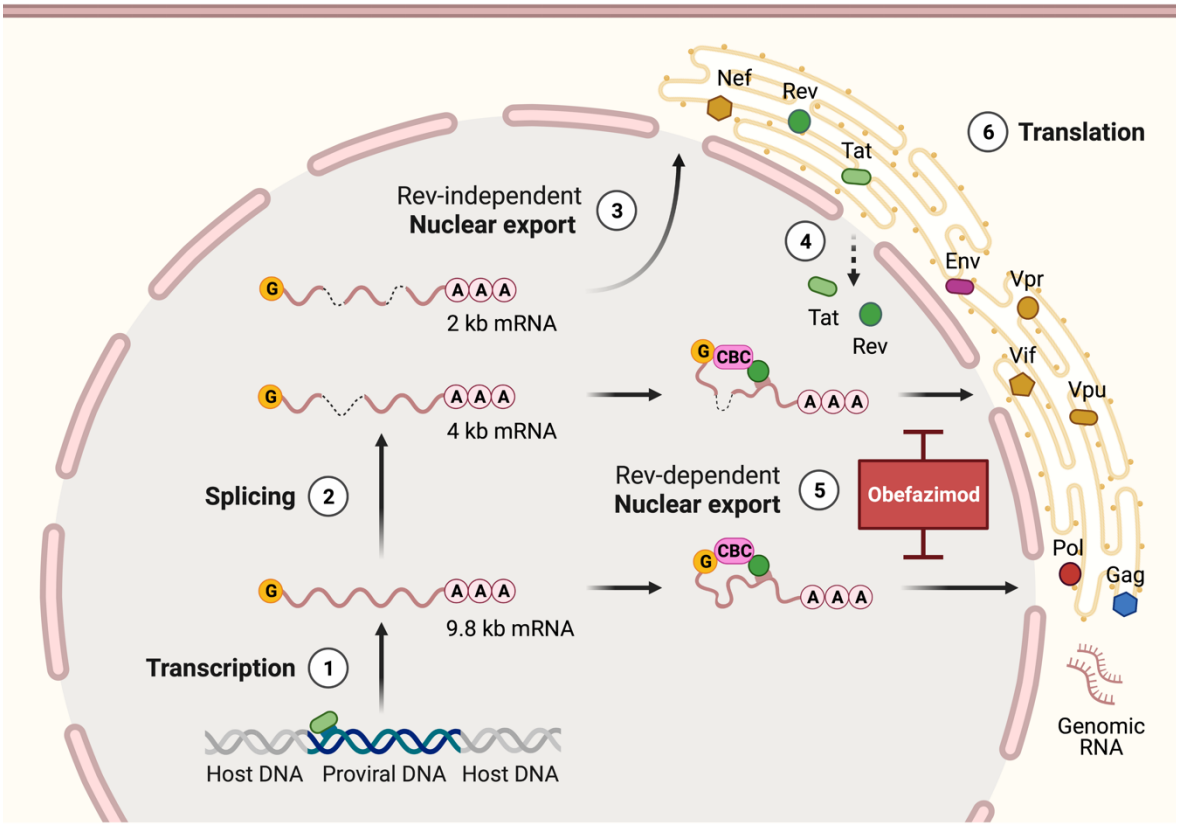

Figure 15. HIV-1 replication cycle showing the site of action of obefazimod. Schematic overview of obefazimod and the step of the HIV-1 replication cycle it targets. G: 5' 7-methylguanosine cap structure; CBC: cap binding complex; A: 3' poly(A) tail. Created with BioRender.com.

Obefazimod has previously been shown to be highly effective at inhibiting replication of different HIV subtypes in human peripheral blood mononuclear cells (PBMCs) and macrophages *in vitro*. Oral treatment with obefazimod also substantially reduced viral replication in two humanized mouse models infected with HIV-1, and this was followed by delayed viral rebound, for at least two months, after treatment interruption as compared to ART[79]. Obefazimod was therefore proposed

as the first antiviral drug able to reduce and control viral replication sustainably after treatment discontinuation. Furthermore, obefazimod demonstrated safety, tolerability, and potential reduction of viral replication in previous clinical studies:

- A first-in-human phase I study (ClinicalTrials.gov registration no. NCT02792686) conducted in 2014 in 24 healthy, HIV-negative individuals demonstrated that single ascending oral doses of 50, 100, 150 and 200 mg of obefazimod for 45 days is safe, well tolerated, and rapidly and substantially metabolized into its main metabolite obefazimod-N-glucuronide[89], which is as efficient as the parent drug in inhibiting viral replication in primary macrophages *in vitro*[79]. The most frequent drug-related adverse events (AEs) were headache, nausea, and vomiting. However, all AEs were either mild or moderate, no life-threatening AE occurred, and no AE led to premature discontinuation.

- An open-label, randomized, phase I study (ClinicalTrials.gov registration no. NCT02731885) conducted from 2014 to 2015 in 48 HIV-negative individuals confirmed the safety and good tolerability profile of the drug after single and repeated (four consecutive) oral doses of 50 mg of obefazimod over 10 days under both fed and fasted conditions[90].

- A randomized, double-blind, placebo-controlled, phase II study (ClinicalTrials.gov registration no. NCT02452242) conducted from 2015 to 2016 in 50 treatment-naïve PWH already confirmed obefazimod is safe and well tolerated when given orally as monotherapy at ascending oral doses up to 150 mg once a day. In addition, obefazimod reduced viral load especially at the highest dose (150 mg once a day for 2 weeks), confirming a dose-dependent efficacy of the drug[91].

- A randomized, double-blind, placebo-controlled, phase IIa study (ClinicalTrials.gov registration no. NCT02735863) conducted from 2016 to 2017 in 22 PWH confirmed the good safety and tolerability of obefazimod when used in combination with ART, consisting of a boosted HIV-1 protease inhibitor-based regimen (darunavir/ritonavir or darunavir/cobicistat), once a day at two oral doses of 50 mg (n=6) and 150 mg (n=16) for 4 weeks. In addition, obefazimod

potentially reduced the HIV-1 reservoir size in terms of decrease in total HIV-1 DNA copy number in PBMCs (-40 copies/10^6 PBMCs at the 150 mg dose)[92].

Overall, by binding directly to the CBC, obefazimod inhibits viral replication through a unique mechanism of action based on interfering the Rev-mediated nuclear export of viral RNA. However, the binding of obefazimod to the CBC not only interferes the biogenesis of HIV-1 RNA but also modulates the biogenesis of cellular RNA, such as the endogenous small non-coding microRNA-124 (miR-124). Obefazimod selectively enables a quick release of miR-124 through splicing of its long non-coding RNA precursor (lncRNA 0599-205) from which miR-124 is derived by splicing[93]. Indeed, obefazimod has demonstrated strong anti-inflammatory effects by the selective induction of miR-124 both *in vitro* and *in vivo* clinical studies, including PWH[93]. miR-124 functions as a negative regulator of inflammation by attenuating the production of pro-inflammatory cytokines to help maintain homeostasis and is reported to be a critical modulator of immunological and inflammatory responses dysregulated in inflammatory disorders[94]. Hence, the anti-inflammatory effect of obefazimod is potentially relevant for the intended use in treating chronic immune activation and inflammation that persist in PWH despite long-term ART.

Obefazimod strongly attenuated intestinal inflammation in mice exposed to dextran sulphate sodium (DSS), a key animal model for inflammatory bowel disease, and demonstrated long-term protection against the lethal effects of prolonged DSS-exposure after drug interruption by triggering the production of IL-22, a cytokine involved in the intestinal tissue repair process, in activated macrophages. Consistently, obefazimod reduced by several-fold the production of the pro-inflammatory cytokines IL-6 and TNFα and the chemokine MCP-1 in obefazimod-treated mice[95]. Moreover, obefazimod drastically reduced the incidence of arthritis in a collagen-induced arthritis mouse model[96], and demonstrated safety, and strong anti-inflammatory effects in previous clinical studies:

- A randomized, double-blind, placebo-controlled, phase IIa proof-of-concept study (ClinicalTrials.gov identifier: NCT03093259) conducted from 2017 to 2019

in 32 individuals with moderate to severe ulcerative colitis (UC) demonstrated obefazimod is safe and profoundly decreased inflammation and induced clinical, biological, and endoscopic remission while upregulating miR-124 when administered at 50 mg daily oral dose for 8 weeks. In addition, an open-label long-term extension phase (ClinicalTrials.gov identifier: NCT03368118) in 22 individuals who completed the previous study and were eligible to continue showed a sustained remission and brought additional participants into remission when given as maintenance therapy at 50 mg daily oral dose for 52 weeks[97].

- A randomized, double-blind, placebo-controlled, phase IIb clinical study (ClinicalTrials.gov identifier: NCT04023396) conducted from 2020 to date in 190 individuals with moderate to severe active UC supported the efficacy and safety of obefazimod when given at ascending oral daily doses of 25 mg (*n*=63), 50 mg (*n*=63), and 100 mg (*n*=64) for 16 weeks. The main AEs were headache and nausea, consistent with all clinical studies, with higher rates in the higher dosage group, indicating that some AEs could be dose dependent. Furthermore, an open-label extension phase after completion of the randomized study confirmed a new or sustained efficacy and brought additional participants into remission when given as maintenance therapy at 50 mg daily oral dose for 48 weeks. A 96-week long-term extension is ongoing[98].

- A randomized, double-blind, placebo-controlled, phase IIa proof-of-concept study (ClinicalTrials.gov identifier: NCT03813199) conducted from 2019 to date in 60 individuals with moderate to severe active rheumatoid arthritis (RA) showed good safety and tolerability, and promising efficacy of obefazimod when used in combination with methotrexate once a day at two oral doses of 50 mg (*n*=6) and 100 mg (*n*=16) for 12 weeks. Nevertheless, mild-to-moderate gastrointestinal AEs led to a high drop-out rate of participants in the 100 mg dose. An open-label extension phase (ClinicalTrials.gov identifier: NCT04049448) in 40 participants receiving 50 mg daily oral dose of obefazimod as maintenance therapy for 52 weeks is ongoing[99].

Obefazimod, with its unique mode of action, is currently in three pivotal phase III clinical studies (ClinicalTrials.gov identifier: NCT05507203, NCT05507216, and NCT05535946) to evaluate efficacy and safety of 25 and 50 mg oral daily doses in inducing clinical remission in more than 1,200 individuals with moderate-to-severe active UC. Moreover, based on the promising efficacy results obtained with obefazimod in UC and the clinical similarities of Crohn's disease (CD) and UC, Abivax has been encouraged by several key opinion leaders to initiate a pivotal phase IIb/III clinical study for the treatment of CD. Thus, the specific dual ability of obefazimod to impact both viral persistence and inflammation might transform the treatment of both HIV infection and multiple inflammatory diseases.

Chapter 2. HYPOTHESIS AND OBJECTIVES

The persistence of HIV-1 in latent reservoirs despite antiretroviral therapy (ART) is the major barrier to cure HIV-1 infection. These latent reservoirs are capable of producing virus upon appropriate activation conditions and contribute to chronic immune activation, and by extension inflammation, in people with HIV (PWH) receiving standard ART regimens for prolonged periods of time. Thus, there remains a critical need to investigate and implement novel therapeutic approaches based on new mechanisms of action that target viral persistence and could also revert the long-term clinical consequences of chronic immune activation and inflammation. In this context, we suggest ART intensification with a new drug, obefazimod (formerly ABX464), due to its specific dual ability in inhibiting viral production through a unique mechanism of action based on interfering the biogenesis of viral RNA and reducing inflammation.

Hence, the **hypothesis** of this thesis is that treatment with obefazimod may reduce HIV-1 persistence, chronic immune activation, and inflammation in PWH on suppressive ART.

The **objective** of this thesis is to evaluate in a non-randomized, open-label, phase II clinical study:

1. The safety and tolerability of obefazimod in both PWH on suppressive ART and HIV-negative individuals.
2. The impact of obefazimod on total size and productivity of viral reservoir in PWH on suppressive ART.
3. The impact of obefazimod on chronic immune activation and inflammation in PWH on suppressive ART.

Chapter 3. MATERIALS AND METHODS

1. Study design

1.1. Participants

We performed a non-randomized, open-label, phase II clinical study to evaluate the safety and otherwise virological and immunological efficacy of obefazimod (formerly ABX464) administered once daily at two doses of 50 mg and 150 mg in combination with antiretroviral therapy (ART) in people with HIV (PWH)[78].

All participants were recruited from the Germans Trias i Pujol University Hospital (Barcelona, Spain) from March 2017 to December 2018. Eligible participants were cisgender male aged 18-65 years with adequate hematological and biochemical laboratory parameters (hemoglobin >9.0 g/dl; absolute neutrophil count ≥750 cells/mm^3; absolute platelets count ≥100,000 cells/mm^3; total serum creatinine ≤1.3 x upper limit of normal; creatinine clearance >50 ml/min by the Cockcroft-Gault equation; serum lipase ≤2.0 x upper limit of normal; total serum bilirubin <1.5 x upper limit of normal; alkaline phosphatase, aspartate aminotransferase, and alanine aminotransferase <1.5 x upper limit of normal). Participants with HIV required to be on an integrase inhibitor-based regimen (dolutegravir or raltegravir combined with either tenofovir and emtricitabine or abacabir and lamivudine) for at least 12 months prior to enrollment, with undetectable plasma viral load (≤50 HIV-1 RNA copies/ml) during the 6 months prior to screening, with a maximum of 2 blips of ≤1000 copies during this period. In addition, they were required to have CD4$^+$ T-cell count with at least 600 cells/mm^3 at screening and above 250 cells/mm^3 since diagnosis. The main exclusion criteria were diagnosis of acute or chronic infectious disease, immunodeficiency, or autoimmune disease other than HIV infection, or any other clinically relevant medical problem determined by physical examination and/or laboratory screening and/or medical history. All study participants fulfilled all inclusion criteria and provided signed informed consent.

The study protocol (ABX464-005) was approved by the Hospital ethics committee (AC-16-047-CEIM), and the Spanish Agency of Medicines and Medical

Products (EudraCT: 2016-002797-12). The study was done and reported in accordance with the study protocol. ClinicalTrials.gov identifier: NCT02990325.

1.2. Procedures

Thirty-six participants were allocated to treatment with either 50 mg or 150 mg daily oral doses of obefazimod. Eleven PWH received 150 mg of obefazimod for 4 weeks ($HIV^{150mg/4w}$ group), thirteen PWH received 50 mg of obefazimod for 12 weeks ($HIV^{50mg/12w}$ group), and a control group of twelve HIV-negative individuals received 50 mg of obefazimod for 4 weeks ($HN^{50mg/4w}$ group).

The original fixed dose (50 mg) of the study drug was selected based on the safety data generated with this dose in previous clinical studies[89–92]. However, obefazimod demonstrated a dose-dependent antiviral efficacy of the drug and based on this finding it was decided to treat the second group of participants with a highest dose (150 mg). Moreover, obefazimod demonstrated a sustained, long-term, and possibly greater anti-inflammatory efficacy of the drug in individuals with moderate-to-severe ulcerative colitis (UC) or rheumatoid arthritis (RA) treated for 52 weeks and based on this finding it was decided to extend the treatment duration of the first group of participants to 12 weeks.

The study had a 21-day screening period. During this period, participants were assessed for study eligibility, demographics, medical history, and concomitant medications. Eligible participants were treated for 4 or 12 weeks followed by a 4-week post-treatment follow-up. During the treatment phase, obefazimod at 50 mg or 150 mg was administered either alone or in addition to participants background ART, orally once a day in a fed condition. At week 4 or 12 the treatment phase was terminated with obefazimod discontinuation. Samples were drawn for total and intact HIV-1 DNA, cell-associated HIV-1 RNA, residual viraemia, immunophenotype, and several inflammatory biomarkers monitorization at baseline, after the treatment phase (at week 4 or 12, depending on the treatment group), and the first 4 weeks of follow-up after obefazimod discontinuation (Figure 16).

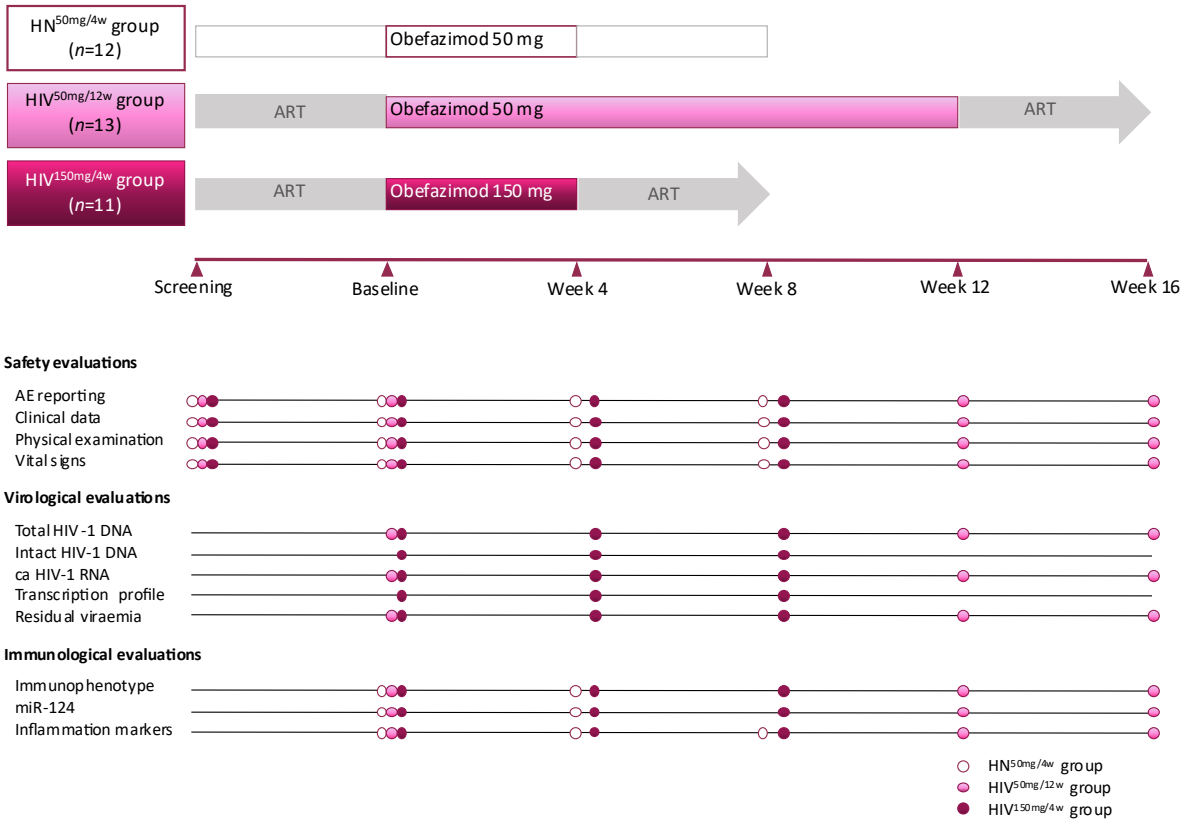

Figure 16. Study design. Diagram of obefazimod administration and schedule of safety, virological, and immunological evaluations carried out for each timepoint.

The group of participants that underwent 150 mg were enrolled in a second phase of the study, on the basis of a dose relationship antiviral efficacy of the drug. As indicated in Figure 16, additional virological parameters were evaluated in the HIV$^{150mg/4w}$ group, including intact HIV-1 DNA and viral transcription profile.

1.3. Sample collection

Blood and GALT samples were collected at baseline (BL), end of intervention (EoI), and 4 weeks after drug discontinuation (EoI+4w) from each eligible participant at the timepoints shown in the schedule of study events (Figure 16).

Fresh blood samples were collected in EDTA tubes and processed in order to separate the cell fraction from the blood plasma. Peripheral blood mononuclear cells (PBMCs) were immediately isolated from the cell fraction by density gradient centrifugation at 390 *g* for 30 min using LymphoPrep™ (Axis-Shield PoC AS), which is a high-density solution that contains sodium diatrizoate and polysaccharide, that

has been widely used to form density gradients for isolating mononuclear cells from human blood with minimal damage. Four million of freshly isolated PBMCs were used for the immunophenotyping. The remaining PBMCs were cryopreserved in liquid nitrogen until use for $CD4^+$ T-cells purification whereas plasma samples were stored at -80ºC until use for the quantification of residual viraemia and soluble inflammation biomarkers. Total $CD4^+$ T cells were then purified from thawed PBMCs by negative immunomagnetic selection using the $CD4^+$ T-cell isolation kit (Miltenyi Biotech), which is based on cell labeling with biotin-conjugated antibodies and magnetic microparticles coated with anti-biotin antibodies, and subsequent automated magnetic cell separation using the autoMACS Pro Separator (Miltenyi Biotech), following the manufacturer's instructions. Purified $CD4^+$ T cells were preserved differently according to their subsequent use. On the one hand, 2-4x10^6 $CD4^+$ T cells were resuspended in lysis buffer at a concentration of 5x10^4 cells/μl and stored at -80ºC until quantification of total and intact HIV-1 DNA. Lysis buffer consisted of 10 mM Tris-HCl (pH=9.0), 0.1% Triton x-100 (Sigma) and 400 μg/ml Proteinase K (Ambion). Cell lysates were incubated at 55°C for 15-20 hours, followed by a 5-minute inactivation of proteinase at 95°C. On the other hand, another 2-4x10^6 $CD4^+$ T cells were preserved in RNAlater solution (Ambion) and stored at -80ºC until RNA extraction for quantification of cell-associated HIV-1 RNA.

Rectal biopsies (2.7 mm diameter) were collected at 15 cm from the anal margin during flexible sigmoidoscopy. Immediately after collection, up to twenty mucosal biopsies were placed in complete medium (RPMI 1640 with 10% fetal bovine serum; both from Gibco) supplemented with antibiotics (500 μg/ml piperacillin/tazobactam; Fresenius Kabi) and antifungal (1.25 μg/ml amphotericin B; Gibco) and processed in order to purify the leukocyte population as follows. Samples were processed within 1 hour after collection to minimize leukocyte loss and/or contamination. Intraepithelial and lamina propria cell suspensions were obtained using a dithiothreitol/ethylenediaminetetraacetic (DTT/EDTA)-based treatment for epithelial layer removal followed by non-enzymatic disruption of the tissue[100]. The mixed cell suspension was stained with the CD45 (clone 2D1) antibody conjugated with APC-Cyanine7 and sorted by fluorescence-activated cell sorting (FACS) using the BD

FACSAria II sorter. Freshly sorted $CD45^+$ cells, assumed as leukocytes from the epithelium and lamina propria, were used for immunophenotyping. Rectal biopsies were also preserved in RNAlater solution (Ambion) and stored at -80°C until use for the quantification of the anti-inflammatory miR-124.

2. Safety

2.1. Safety and tolerability

Safety and tolerability were evaluated in all participants based on number and grade of adverse events (AEs), individual values for clinical data (including signs and symptoms, laboratory toxicities, and clinical events), physical examinations, and vital signs at each timepoint as described in Figure 16.

Any untoward medical occurrence (*i.e.* clinically significant laboratory abnormality, new finding in routine physical examinations, and/or change in vital signs) temporally associated with the administration of obefazimod, whether or not considered related to the investigational product, was considered an AE. The severity of AEs was assessed according to the 'Division of AIDS toxicity table for severe adult and pediatric adverse events'. Dose limiting toxicity (DLT) was defined as a grade 3 or higher AE. The causal relationship between the study treatment and the occurrence of each AE was considered by the Data Safety Monitoring Board (DSMB). Alternative causes, such as natural history of the underlying diseases, concomitant medications, other risk factors, and the temporal relationship of the event to the investigational drug, were considered. If more than two DLTs had occurred during the treatment period, the enrolment of additional participants would have been stopped. Moreover, in case of a grade 4, life-threatening AE, enrolment, and treatment of ongoing participants had to be immediately discontinued. In both cases, enrolment had only to be resumed upon the decision of the sponsor if the DSMB could conclude that the causality of the event was unrelated or unlikely to be related to the study treatment.

3. Viral persistence

3.1. Total HIV-1 DNA

To assess the size of the proviral reservoir of individuals on suppressive ART, peripheral CD4+ T cells were used to measure total HIV-1 DNA by droplet digital polymerase chain reaction (ddPCR; Bio-Rad). ddPCR was used because it enables absolute quantification, highest precision, and sensitivity than conventional quantitative PCR at low abundance targets, and it is relatively less dependent on PCR efficiency, which may be reduced by sequence mismatches or inhibitors. ddPCR is based on the fractioning of the sample, in this case DNA, into up to 20,000 droplets where the target sequence amplification by PCR occurs independently within each droplet, and consequent analysis of the proportion of positive droplets to give precise, absolute quantification of target sequence in the sample (Figure 17).

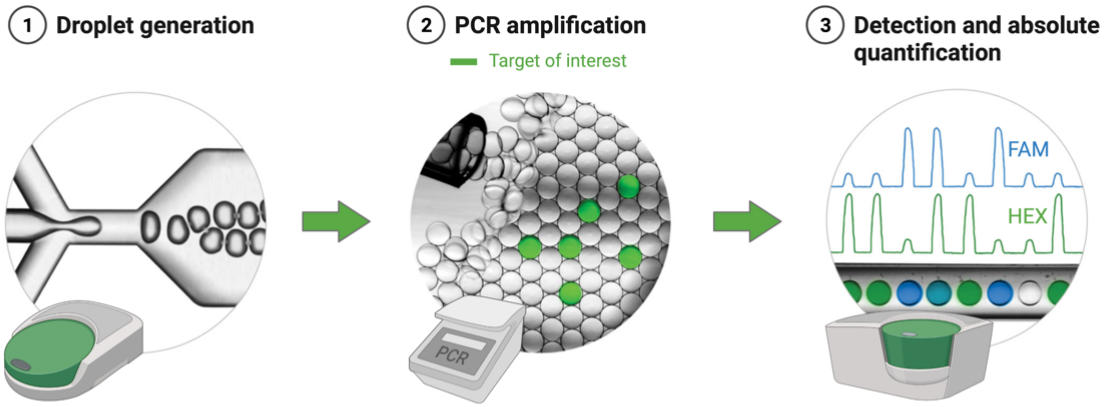

Figure 17. Application of ddPCR. Schematic overview of ddPCR workflow. Adapted from www.bio-rad.com.

Lysed CD4+ T cells (2-4x10^6 cells) were used to measure total HIV-1 DNA by ddPCR using two different primer/probe sets annealing to the 5' LTR and *gag* conserved regions of the viral genome in order to avoid potential primer mismatches in viral sequences (Figure 18 and Table 3). All samples were assessed in parallel using both primer/probe sets to ensure reliable absolute quantification, and 5' LTR or *gag* primer/probe set was selected depending on the efficiency of detection in each participant[100].

ddPCR was performed using the QX100 Droplet Digital PCR System (Bio-Rad) and each reaction consisted of 2 μl of lysed $CD4^+$ T cells (equivalent to 100,000 cells) mixed with 10 μl of 2x ddPCR Supermix for Residual DNA Quantification (Bio-Rad), 18 μM of primers, and 5 μM of ZEN/Iowa Black FQ double-quenched probe labelled in FAM or HEX (Integrated DNA Technologies) in a total volume of 20 μl. This reaction mix was loaded into a droplet generator cartridge (Bio-Rad) along with 70 μl of droplet generation oil. The cartridge was placed in the QX100 Droplet Generator (Bio-Rad), where the reaction mix was partitioned into up to 20,000 nanoliter-sized droplets. Droplets were transferred to a 96-well plate, which was subsequently sealed using the PX1 PCR plate sealer (Bio-Rad). DNA was amplified using a C100 Touch thermal cycler (Bio-Rad) with the following cycling conditions: initial denaturation at 95ºC for 10 min, 40 cycles of 30 s at 94ºC and 57ºC for 60 s, and a final droplet curation step of 10 min at 98°C. Following amplification, droplets were read immediately by the QX100 droplet reader (Bio-Rad) and analyzed using the QuantaSoft v.1.6 software (Bio-Rad) in the absolute quantification mode.

Samples were tested in duplicate. PBMCs from HIV-negative donors were assayed in each plate and used as negative controls to set the positive/negative threshold for ddPCR analysis. The ribonuclease P/MRP subunit p30 (*RPP30*) housekeeping gene was quantified in parallel to normalize target DNA copies by cell input.

3.1.1. Intact HIV-1 DNA

To distinguish the intact HIV-1 DNA from the vast excess of defective HIV-1 DNA, additional samples of $CD4^+$ T cells from the group of participants that underwent 150 mg of obefazimod for 4 weeks were used to measure intact, 5' defective, and 3' defective HIV-1 DNA using the intact proviral DNA assay (IPDA) by ddPCR[101]. Standard assays based on PCR to detect proviral DNA use short genomic amplicons in conserved regions and do not distinguish intact and defective proviruses. However, only 2.4% of proviruses are intact and the remaining 97.6% have fatal defects including deletions and/or G→A hypermutations, which alter start codons and/or introduce stop codons in most open-reading frames.

Peripheral CD4+ T cells (2-4x10^6 cells) were used to extract genomic DNA on the basis of differential solubility using TRI Reagent (Molecular Research Center Inc.) following the manufacturer's instructions. DNA concentration and purity were assessed using spectrophotometry (NanoDrop 1000). Genomic DNA extracts were used for the quantification of intact, 5′ deleted, and 3′ deleted and/or hypermutated HIV-1 DNA by ddPCR using two strategically placed amplicons in the packaging signal (Ψ) and *env* regions and hypermutation discrimination probes that can jointly identify more than 90% of defective proviruses (Table 3). Positive amplification at the packaging signal (Ψ), which is a frequent site of small deletions and is included in many large deletions in the proviral genome, discriminates 3' defective proviruses, with the defect attributable to either hypermutation or deletion. Positive amplification at the RRE sequence within the *env* region discriminates 5' defective proviruses, with the defect attributable to deletion. Positive amplification at both regions is indicative of intact full-length provirus (Figure 18).

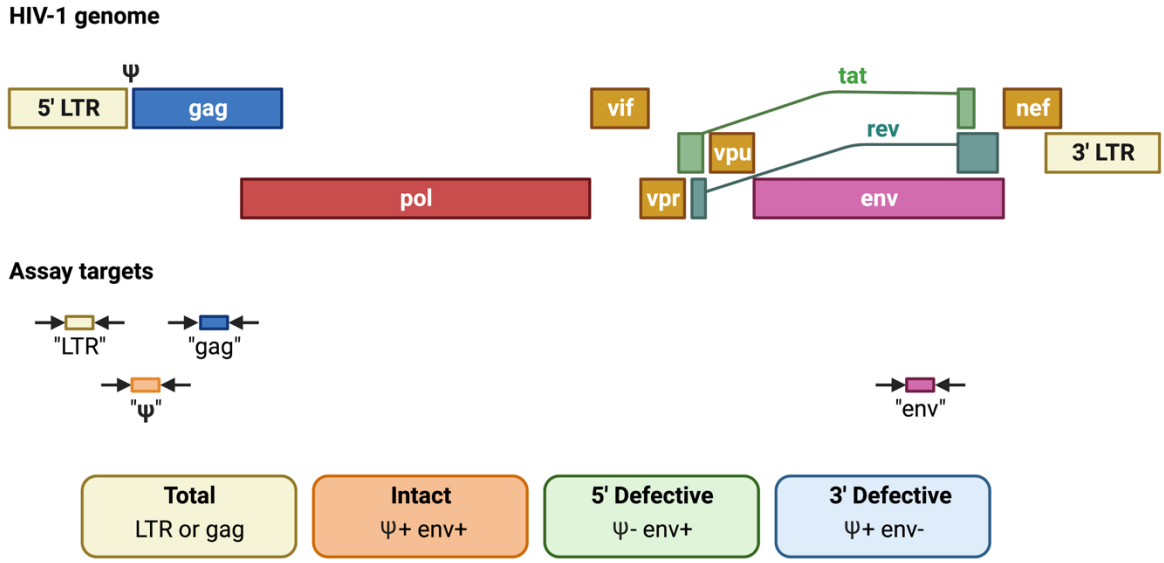

Figure 18. Distinguishing total, intact, and defective HIV-1 DNA. Schematic overview of the sequence regions detected by IPDA assay used to characterize total, intact, 5' defective, and 3' defective proviruses. Ψ: packaging signal.

ddPCR was also performed using the QX100 Droplet Digital PCR System (Bio-Rad) with the following cycling conditions: initial denaturation at 95ºC for 10 min, 45 cycles of 30 s at 94ºC and 59ºC for 60 s, and a final droplet curation step of 10 min at 98°C. An important aspect for the quantification of intact HIV-1 DNA was

correction for DNA shearing between amplicons. This was done accurately using separate amplification of two amplicons in the *RPP30* housekeeping gene spaced at exactly the same distance as the Ψ and *env* amplicons on each sample. This provided a measure of input cell number and DNA integrity.

3.2. Cell-associated HIV-1 RNA

To assess the transcriptional activity of the viral reservoir of individuals on suppressive ART, peripheral $CD4^+$ T cells were used to measure cell-associated HIV-1 RNA by one-step reverse transcription ddPCR (RT-ddPCR; Bio-Rad). Cellular RNA was extracted from $CD4^+$ T cells preserved in RNAlater solution (2-4x10^6 cells) using RNeasy Mini kit (Qiagen) following the manufacturer's instructions, including the use of polyacryl carrier (20 ng). RNA concentration and purity were assessed using spectrophotometry (NanoDrop 1000). Cellular RNA extracts were used to measure cell-associated HIV-1 RNA by one-step RT-ddPCR using the 5' LTR or *gag* primer/probe set, depending on the efficiency of detection in each participant.

One-step RT-ddPCR was performed using the QX100 Droplet Digital PCR System (Bio-Rad) and each reaction consisted of 8 μl of RNA (equivalent to 200 ng of RNA) mixed with 10 μl of 2x One-Step RT-ddPCR Advanced Kit for Probes Mastermix (Bio-Rad), 18 μM of primers, 5 μM of ZEN/Iowa Black FQ double-quenched probe labelled in FAM or HEX (Integrated DNA Technologies), 300 nM of DTT, and 2 μl of RT enzyme in a total volume of 20 μl. This reaction mix was loaded into the Bio-Rad droplet generator cartridge and the droplets were generated as previously described for total HIV-1 DNA. Droplets were transferred to a 96-well plate, which was subsequently sealed using the PX1 PCR plate sealer (Bio-Rad). RNA was retrotranscribed and amplified using the C100 Touch thermal cycler (Bio-Rad) with the following cycling conditions: reverse transcription at 50ºC for 60 min, enzyme activation at 95ºC for 10 min, 40 cycles of 30 s at 95ºC and 61ºC for 60 s, and a final droplet curation step of 10 min at 98°C. Following amplification, droplets were read immediately by the QX100 droplet reader (Bio-Rad) and analyzed using the QuantaSoft v.1.6 software (Bio-Rad) in the absolute quantification mode.

Samples were tested in duplicate. PBMCs from HIV-negative donors were assayed in each plate and used as negative controls to set the positive/negative threshold for one-step RT-ddPCR analysis, as for total HIV-1 DNA. The TATA-box binding protein (*TBP*) housekeeping gene was quantified in parallel to normalize target RNA copies.

3.2.1. HIV-1 RNA transcription profiling

To investigate specific blocks to different stages of HIV-1 RNA transcription, additional samples of $CD4^+$ T cells from the group of participants that underwent 150 mg of obefazimod for 4 weeks, were used to simultaneously quantify the expression of different cell-associated HIV-1 RNA transcripts. Read-through, initiated (TAR), 5' elongated (R-U5/*gag*), unspliced (*pol*), polyadenylated (PolyA), and multiple spliced (*tat/rev*) viral transcripts were quantified by two-steps RT-ddPCR[102]. Because HIV-1 transcription normally begins with the transcription of the TAR loop (in the R sequence of 5' LTR region) and all HIV-1 transcripts contain TAR (full-length transcripts, twice), the level of TAR-containing transcripts serves as a measure of HIV-1 transcriptional initiation. Transcriptional interference should result in read-through transcripts that begin upstream of the normal HIV-1 transcription initiation site (in the U3 sequence of 5' LTR region). Longer, processive transcripts can be detected using targets for downstream sequences, *i.e.* R-U5/*gag* or *pol*, that measure the degree of transcriptional elongation beyond the 5' LTR sequence region. Moreover, *pol* sequence region is present only in unspliced transcripts. Polyadenylated (in the U3-PolyA sequence of 3' LTR region) transcripts suggest completion of HIV-1 transcription, which facilitate nuclear export, RNA stability and translation. Finally, multiple spliced transcripts can be detected by an amplicon that spans the boundary between *tat* and *rev* sequences and may indicate the relative ability to overcome blocks to initiation, elongation, and splicing, which are three of the main proposed mechanisms of latency (Figure 19).

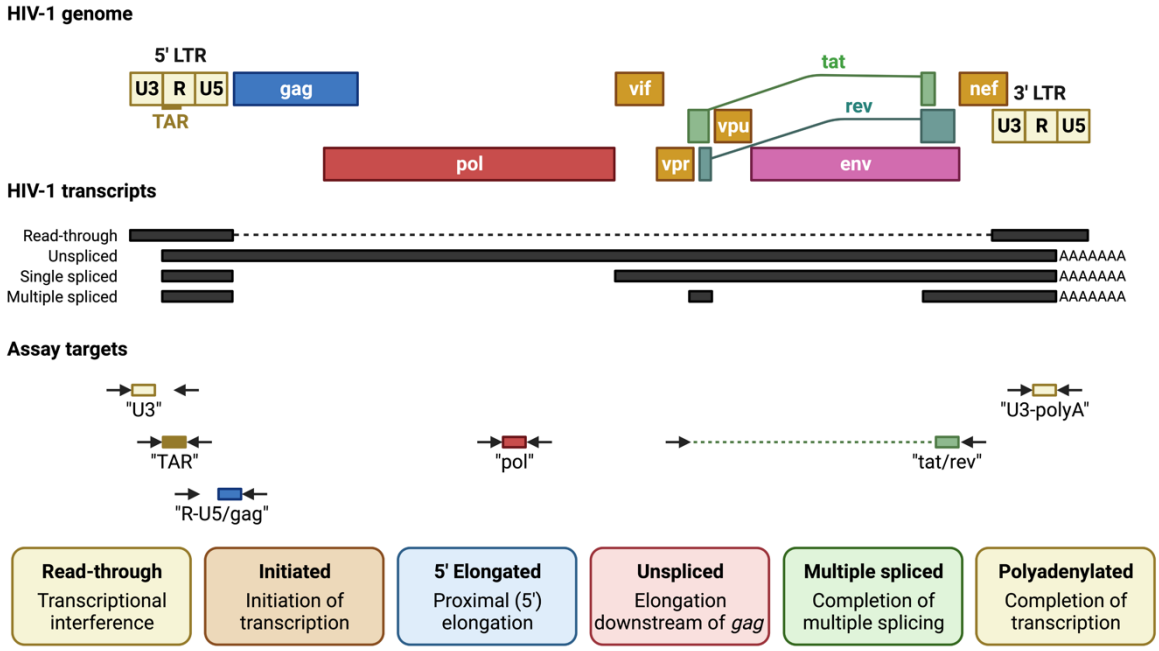

Figure 19. HIV-1 RNA transcription profiling. Schematic overview of the sequence regions detected by different assays used to characterize HIV-1 RNA transcription profile.

Peripheral CD4⁺ T cells (2-4x10^6 cells) were used to extract cellular RNA using TRI Reagent (Molecular Research Center Inc.) following the manufacturer's instructions. RNA concentration and purity were assessed using ultraviolet spectrophotometry (NanoDrop 1000). Cellular RNA extracts were used in a common RT reaction to generate complementary DNA (cDNA) for the ddPCR assays. Except the TAR assay, which requires previous polyadenylation for efficient RT of transcripts containing the TAR loop, likely due to its short length and a tight hairpin structure that hinders primer binding. Hence, one aliquot of cellular RNA was used in a polyadenylation-RT reaction to generate cDNA for the TAR assay, whereas another aliquot was used in a separate RT reaction to generate cDNA for the other transcripts assays.

Polyadenylation reaction for the TAR assay consisted in 0.5 μg of RNA mixed with 1.5 μl of 10× SuperScript III buffer (Invitrogen), 1.5 μl of 50 mM $MgCl_2$, 0.5 μl of 10 mM adenosine 5'-triphosphate (Epicentre), 1 μl of PolyA polymerase (4 U/μl; Epicentre), and 0.25 μl of RNAseOUT (40 U/μl; Invitrogen) in a total volume of 10 μl. Polyadenylation reaction was performed in a conventional thermal cycler at 37°C

for 45 min. Subsequently, the remaining RT reagents were added in a total volume of 15 μl containing 0.75 μl of random hexamers (50 ng/μl; Invitrogen), 0.75 μl of 50 μM oligo dT15, 0.75 μl of 10 mM dNTPs and 0.5 μl of SuperScript III RT (200 U/μl; Invitrogen). Common RT reactions for all assays (except the TAR assay) consisted of 5 μg of RNA mixed with 6 μl of 10× SuperScript III buffer (Invitrogen), 6 μl of 50 mM $MgCl_2$, 3.5 μl of random hexamers (50 ng/μl; Invitrogen), 3.5 μl of 50 μM oligo dT15, 3.5 μl of 10 mM deoxynucleoside triphosphates (dNTPs), 1.5 μl of RNAseOUT (40 U/μl; Invitrogen), and 3.5 μl of SuperScript III RT (200 U/μl; Invitrogen) in a total volume of 60 μl. A combination of random hexamers and poly-dT was used to avoid bias toward RT of the 5' end as can be seen with random hexamers, the 3' end as can be seen with poly-dT, or any one gene as occurs with gene-specific primers. RT reactions were performed in a conventional thermal cycler at 25°C for 10 min, 50°C for 50 min, followed by an inactivation step at 85°C for 5 min. Control RT reactions were established using RNA but no RT enzyme and RNA extracted from HIV-negative donor PBMCs were used as negative controls. For best comparison of different transcripts, same cDNA was used in subsequent ddPCR assays for read-through, R-U5-*gag*, *pol*, PolyA, and *tat/rev* sequence regions.

Expression of read-through, initiated (TAR), 5' elongated (R-U5/*gag*), unspliced (*pol*), polyadenylated (PolyA), and multiple spliced (*tat/rev*) HIV-1 transcripts were simultaneously quantified by ddPCR using the primer/probe sets listed in Table 3. ddPCR was performed using the QX100 Droplet Digital PCR System (Bio-Rad) and each reaction consisted of 500 ng of cDNA fragmented using a QIAshredder column (Qiagen) mixed with 10 μl of ddPCR Probe Supermix (no deoxyuridine triphosphate), 0.9 of μM primers, and 0.25 μM of ZEN/Iowa Black FQ double-quenched probe labelled in FAM (Thermo Fisher Scientific) in a total volume of 20 μl. This reaction mix was loaded into the Bio-Rad droplet generator cartridge and the droplets were generated as previously described for total HIV-1 DNA. Droplets were transferred to a 96-well plate, which was subsequently sealed using the PX1™ PCR plate sealer (Bio-Rad). cDNA was amplified using a 7900 thermal cycler (Life Technologies) with the following cycling conditions: initial denaturation at 95ºC for

10 min, 45 cycles of 30 s at 95ºC and 59ºC for 60 s, and a final droplet cure step of 10 min at 98°C. Following amplification, droplets were read immediately by the QX100™ droplet reader (Bio-Rad) and analyzed using the QuantaSoft v.1.6 software (Bio-Rad) in the absolute quantification mode. Samples were tested in duplicate. cDNA from HIV-negative donors were assayed in each plate and used as negative controls to set the positive/negative threshold for ddPCR analysis. The *TBP* housekeeping gene was quantified in parallel to normalize target copies by cell input. Given the changes in HIV-1 DNA, each transcript was also normalized to copies per provirus (HIV-1 RNA/HIV-1 DNA ratio).

Table 3. Primers and probes. Primers and probes used for total HIV-1 DNA and cell-associated HIV-1 RNA quantification.

Target	Name	Sequence (5'→3')	Function
5' LTR	LTR-U5 integrated	GTTCGGGCGCCACTGCTAG	Forward
	LTR-R integrated	TTAAGCCTCAATAAAGCTTGCC	Reverse
	New integrated-2 probe	CCAGAGTCACACAACAGACGGGCA	Probe
gag	HIV_F (SCA)	CATGTTTTCAGCATTATCAGAAGGA	Forward
	HIV_R (SCA)	TGCTTGATGTCCCCCCACT	Reverse
	HIV Probe (SCA)	CCACCCCACAAGATTTAAACACCATGCTAA	Probe
Ψ	Ψ F	CAGGACTCGGCTTGCTGAAG	Forward
	Ψ R	GCACCCATCTCTCTCCTTCTAGC	Reverse
	Ψ Probe	TTTTGGCGTACTCACCAGT	Probe
env	Env F	AGTGGTGCAGAGAGAAAAAAGAGC	Forward
	Env R	GTCTGGCCTGTACCGTCAGC	Reverse
	Env intact probe	CCTTGGGTTCTTGGGA	Probe
	Env hypermut	CCTTAGGTTCTTAGGAGC	Probe
Rth	Freadth-2	GCCCTCAGATGCTRCATATAA	Forward
	Rreadth-1	AGAGTCACACAACAGACGG	Reverse
	Preadth-1	TGCCTGTACTGGGTCTCTCTGGTTAG	Probe

Target	Name	Sequence (5'à3')	Function
TAR	TAR-F7	GTCTCTCTGGTTAGACCAG	Forward
	TAR-R6	TGGGTTCCCTAGYTAGCC	Reverse
	TAR-P3	AGCCTGGGAGCTC	Probe
R-U5/*gag*	Kumar F	GCCTCAATAAAGCTTGCCTTGA	Forward
	Kumar R	GGGCGCCACTGCTAGAGA	Reverse
	Kumar P	CCAGAGTCACACAACAGACGGGCACA	Probe
pol	Pol mf299	GCACTTTAAATTTTCCCATTAGTCCTA	Forward
	Pol mf1	CAAATTTCTACTAATGCTTTTATTTTTTC	Reverse
	Pol P	AAGCCAGGAATGGATGGCC	Probe
PolyA	Freadth-2	GCCCTCAGATGCTRCATATAA	Forward
	5T25	TTTTTTTTTTTTTTTTTTTTTTTTTTGAAG	Reverse
	Preadth-1	TGCCTGTACTGGGTCTCTCTGGTTAG	Probe
tat/rev	mf1	CTTAGGCATCTCCTATGGCAGGAA	Forward
	mf83	GGATCTGTCTCTGTCTCTCTCTCCACC	Reverse
	Mf226mod	ACCCGACAGGCC	Probe
RPP30	RPP30-F	GATTTGGACCTGCGAGCG	Forward
	RPP30-R	GCGGCTGTCTCCACAAGT	Reverse
	RPP30-Probe	CTGACCTGAAGGCTCT	Probe
TBP	TBP-S	TTCGGAGAGTTCTGGGATTGTA	Forward
	TBP-AS	TGGACTGTTCTTCACTCTTGGC	Reverse
	TBP-Probe	CCGTGGTTCGTGGCTCTCTTATCCTCA	Probe

3.3. Residual viraemia

To evaluate the persistent viral production of individuals on suppressive ART, residual viraemia was measured using an ultrasensitive viral load test that can detect down to one single copy of HIV-1 RNA per ml of plasma (LOD was 0.55 HIV-

1 RNA copies/ml) whereas the detection limit of standard methodologies is 20-50 copies of HIV-1 RNA per ml of plasma.

Plasma samples (9 ml) were concentrated by ultracentrifugation at 170,000 *g* at 4°C for 30 min prior to HIV-1 RNA extraction and quantification using the m2000 RealTime System device (Abbott Molecular) and laboratory-defined applications software from the instrument[103]. HIV-1 RNA copies in the low range were determined using an in-house calibration curve set (range 10^1-10^3 copies/ml), which had previously been validated using a pre-quantified standard HIV-1 RNA control from the World Health Organization. Plasma samples from HIV-negative donors were used as negative controls.

4. Immune responses

4.1. Immunophenotype

To evaluate the immune activation state in all participants, distribution and activation of T-cell subsets were measured within PBMCs and sorted leukocytes from the rectal biopsies using flow cytometry. Freshly isolated PBMCs ($4x10^6$ cells) and rectal leukocytes (10^5-10^6 cells) were incubated for 30 min at 4ºC with the following antibodies: CD3 (clone SK7) conjugated with PerCP, CD4 (clone RPA-T4) conjugated with BV605, CD8 (clone SK1) conjugated with BV510, CD45RA (clone HI100) conjugated with AlexaFluor647, CCR7 (clone G043H7) conjugated with PE-Dazzle594, CD27 (clone M-T271) conjugated with FITC, HLA-DR (clone L243) conjugated with PE-Cyanine7, CD38 (clone HB7) conjugated with PE, and PD-1 (clone EH12.2H7) conjugated with BV421. Samples were acquired with forward scatter threshold set at 5,000 to exclude debris using a BD FACS Aria II (Beckton Dickinson) flow cytometer. 'Fluorescence minus one' controls were used to set the positivity threshold. Flow cytometry data were analyzed using the FlowJo software (v.10.6.1).

T cells ($CD4^+$ and $CD8^+$) were initially identified according to morphological parameters and CD3 expression. $CD4^+$ T cells were identified as $CD3^+$ cells following the exclusion of $CD8^+$ cells, which included those cells with downregulated CD4 expression because of HIV-1 infection. Specific $CD4^+$ T-cell subsets were identified based on the expression of CD45RA, CCR7, and CD27 as follows: T naïve (T_N; $CD45RA^+CCR7^+CD27^+$), T central memory (T_{CM}; $CD45RA^-CCR7^+CD27^+$), T transitional memory (T_{TM}; $CD45RA^-CCR7^-CD27^+$), T effector memory (T_{EM}; $CD45RA^-CCR7^-CD27^-$), and T effector memory re-expressing CD45RA (T_{EMRA}; $CD45RA^+CCR7^-CD27^-$). Expression of activation-induced markers (CD38, HLA-DR and PD-1) was also measured on $CD4^+$ and $CD8^+$ T cells from both peripheral blood and rectal biopsies using the cell percentage expressing the markers. Gating strategy is detailed in Figure 20.

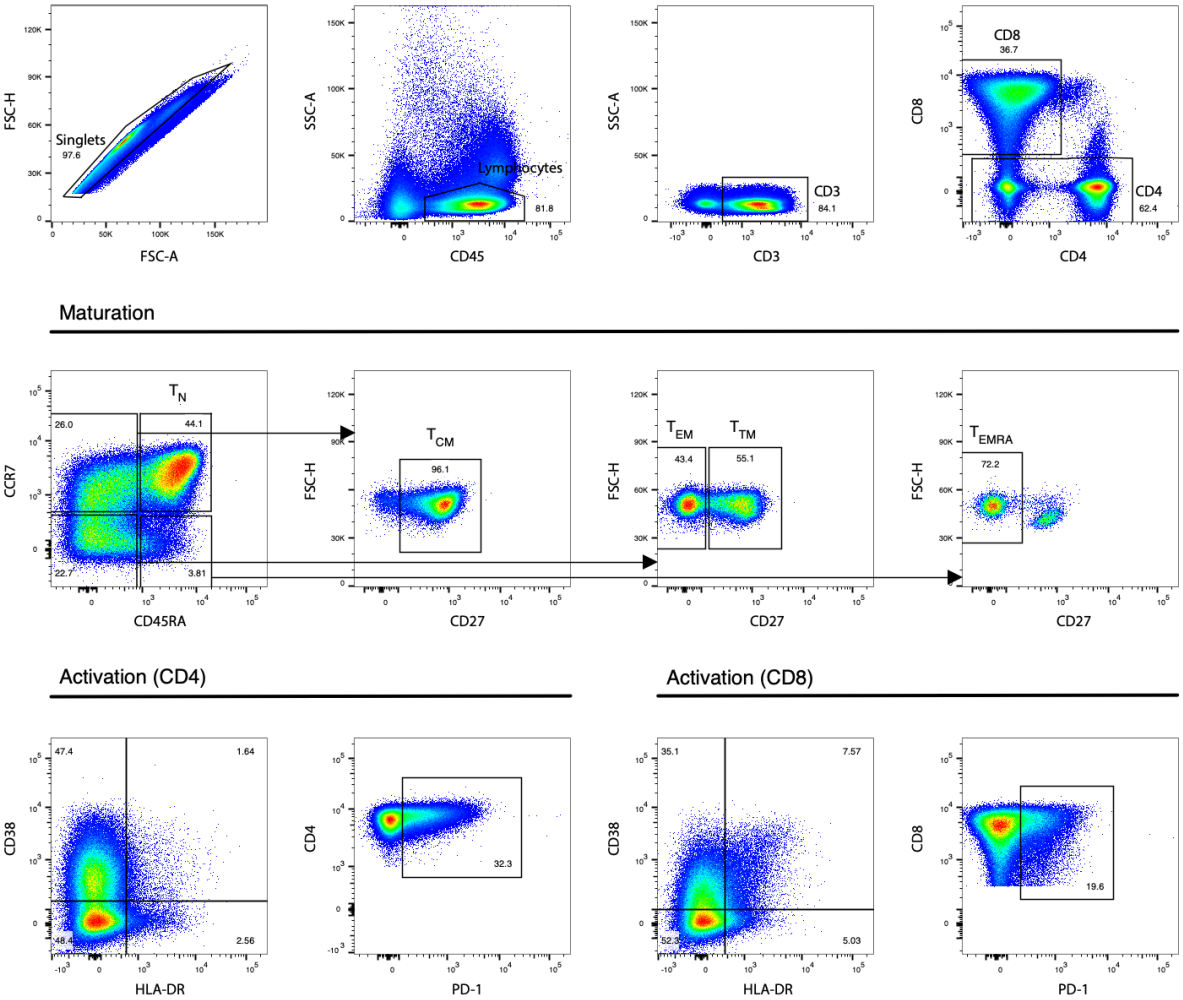

Figure 20. Flow cytometry gating strategy for T-cell analysis. Schematic diagram of the flow cytometry gating strategy to identify $CD4^+$ and $CD8^+$ T cells, maturation, activation, and exhaustion, as previously described.

4.2. Inflammation biomarkers

To evaluate the intestinal and systemic inflammation state in all participants, the anti-inflammatory miR-124 expression was measured in rectal tissue and otherwise concentration of several soluble inflammation biomarkers was measured in plasma samples.

Thawed rectal biopsies were disrupted and homogenized using TissueLyser LT (Qiagen) and miRNA was extracted using miRNeasy kit (Qiagen), following the manufacturer's instructions. miRNA concentration and purity were assessed using ultraviolet spectrophotometry (NanoDrop 1000). miRNA extracts (70 ng) were reverse transcribed using a TaqMan Advanced miRNA cDNA synthesis kit (Applied Biosystems) to generate cDNA for the real-time quantitative PCR (RT-qPCR) assay. To improve detection of low-expressing miR-124 samples, cDNA was pre-amplified using the Universal miR-Amp primers (Applied Biosystems), which uniformly increased the amount of cDNA for each sample, maintaining the relative differential expression. Pre-amplified cDNA was used to measure miR-124 by RT-qPCR and each reaction consisted in 2.5 μl of cDNA mixed with 2x TaqMan Fast Advanced Master Mix and specific 20x TaqMan Advanced miRNA assay (Applied Biosystems) in a total volume of 10 μl[93]. RT-qPCR was performed using the LightCycler 480 Instrument II (Roche Diagnostics) with the following cycling conditions: enzyme activation at 95ºC for 20 s, 45 cycles of 3 s for denaturation and 30 s for annealing and extension with fluorescence measurement at each cycle. Five replicates were tested per sample. The endogenous miR-16 housekeeping gene was quantified in parallel for expression data normalization.

Moreover, the concentration of 26 soluble inflammation biomarkers was measured in cryopreserved plasma samples using a bead-based multiplex immunoassay using the Luminex technology or conventional enzyme-linked immunosorbent assay (ELISA). The concentrations of 17 pro-inflammatory or homeostatic cytokines/chemokines: G-CSF, GM-CSF, IFNγ, IL-1β, IL-2, IL-4, IL-6, IL-7, IL-8 (or CXCL8), IL-10, IL-12 (p40), IL-12 (p70), IL-17a (or CTLA-8), IP-10 (or CXCL10), MCP-1 (or CCL2), MIP-1β (or CCL4), and TNFα, were simultaneously

detected and quantified using a custom magnetic bead panel HCYTOMAG-60K-17 (Merck Millipore) following manufacturer's instructions. Measurements were performed using a Luminex® 200™ instrument system (Luminex Corp). The concentrations of the following 8 soluble biomarkers: CD14, CD163, IL-18, IL-18 binding protein, IL-22, M-CSF, MIG (CXCL9) (R&D Systems), and L-FABP (LifeSpam Biosciences), were measured using commercial ELISA (R&D Systems) according to manufacturer's instructions. The concentration of C-reactive protein (CRP) was measured by the nephelometric analyzer BN II System (Siemens Healthineers) following manufacturer's instructions. Data were analyzed using a standard curve for each soluble marker.

5. Data analysis

5.1. Statistical analysis

Continuous variables were described using medians and the interquartile range (IQR, defined by the 25th and 75th percentiles), whereas categorical factors were reported as percentages over available data. Longitudinal comparisons between timepoints for the expression of total and intact HIV-1 DNA, cell-associated HIV-1 RNA, residual viraemia, immunophenotype, and inflammation biomarkers were performed using the Wilcoxon signed rank test. Comparisons between groups in each timepoint for the immunophenotype and inflammation biomarkers were performed using Mann-Whitney U test. Statistical significance was set at 5% for all the tests. The statistical analyses were performed using R (v3.6) and GraphPad Prism software (v9.0.0).

Chapter 4. RESULTS

1. Study design

1.1. Baseline characteristics and participant disposition

To evaluate the safety and impact of obefazimod on viral persistence, chronic immune activation, and inflammation in long-term ART-suppressed individuals, a total of 36 eligible participants were enrolled into the study. Participants were prospectively and sequentially allocated into three groups as follows: 12 HIV-negative volunteers were assigned to 50 mg dose orally once daily for 4 weeks ($HN^{50mg/4w}$ group), 13 ART-suppressed PWH to obefazimod 50 mg dose for 12 weeks ($HIV^{50mg/12w}$ group), and 11 ART-suppressed PWH to 150 mg dose for 4 weeks ($HIV^{150mg/4w}$ group). Thirty-three participants completed the study according to the study protocol and their dose regimen: 12 from the $HN^{50mg/4w}$ group, 12 from the $HIV^{50mg/12w}$ group, and 9 from the $HIV^{150mg/4w}$ group. Three participants withdrew early from the study (one from the $HIV^{50mg/12w}$ group and two from the $HIV^{150mg/4w}$ group). The reason for withdrawal was AE. Participant disposition is summarized in Figure 21.

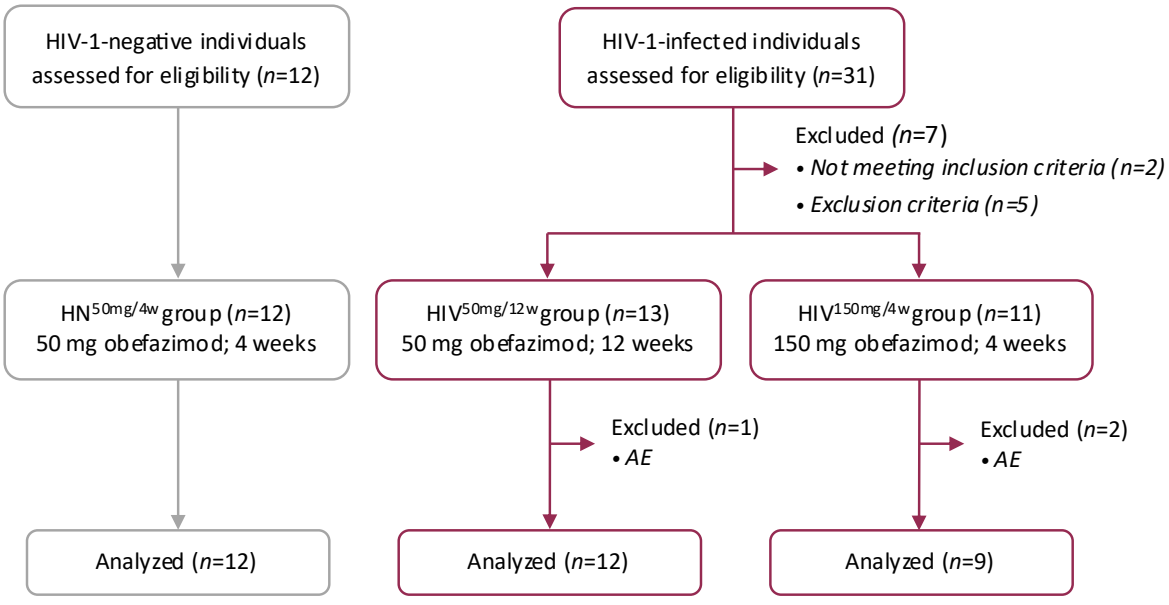

Figure 21. Study participant disposition. Consort flow diagram of the study participants. *n*: number of participants.

Baseline demographic and clinical characteristics were similar among the three groups, with a minor exception for age (Table 4). All study participants were Caucasian cisgender men with a median age of 44 years. There were no clinically significant differences between HIV^{+} groups except for the time in viral suppression by ART, which was longer in the HIV$^{150mg/4w}$ group than in the HIV$^{50mg/12w}$ group (p=0.02).

Table 4. Baseline demographic and clinical characteristics of the study population.
n: number of participants; IQR: interquartile range.

	HN$^{50mg/4w}$ (*n*=12)	HIV$^{50mg/12w}$ (*n*=13)	HIV$^{150mg/4w}$ (*n*=11)	*p*-values between HIV^{+} groups
Age				
Years, *median (IQR)*	38 (26-46)	41 (34-49)	51 (43-53)	*0.06*
Gender				
Male, *n (%)*	12 (100)	13 (100)	11 (100)	*1.0*
Ethnicity				
Caucasian, *n (%)*	12 (100)	13 (100)	11 (100)	*1.0*
CD4^{+} T-cell count				
Cells/mm^3, *median (IQR)*		1035 (694-1173)	906 (781-1439)	*0.9*
Percentage, *median (IQR)*		39 (34-44)	37 (33-45)	*0.5*
CD8^{+} T-cell count				
Cells/mm^3, *median (IQR)*		753 (554-870)	773 (647-966)	*0.4*
Percentage, *median (IQR)*		1.3 (0.9-1.6)	1.1 (0.9-1.5)	*0.6*
HIV-1 viral load				
HIV-1 RNA copies/ml		<50	<50	*1.0*
Nadir CD4^{+} T cells				
Cells/mm^3, *median (IQR)*		475 (354-655)	443 (335-729)	*0.9*
Zenit viral load				
HIV-1 RNA copies/ml, *median (IQR) log$_{10}$*		4.5 (0.4-8.0)	2.7 (0.7-4.6)	*0.7*

ART			
Months from diagnose to ART, *median (IQR)*	4 (1-38)	11 (2-77)	*0.4*
Years on ART, *median (IQR)*	5 (4-9)	11 (7-23)	***0.02***
Integrase inhibitor-based ART			
Dolutegravir, *n (%)*	10 (77)	9 (82)	
Raltegravir, *n (%)*	3 (23)	2 (18)	

2. Safety of obefazimod

2.1. Safety and tolerability

A total of 19 participants out of 36 (53%) reported AEs during obefazimod administration: 3 HIV-negative participants out of 12 (25%) who received 50 mg of obefazimod for 4 weeks, 7 participants out of 13 (54%) who received 50 mg for 12 weeks, and 9 participants out of 11 (82%) who received 150 mg for 4 weeks (Table 5). However, none of the AEs were severe (grade 3 or above), life-threatening, or disabling, and all symptoms and biochemical abnormalities normalized upon drug withdrawal. The most frequently reported AEs consist of nervous system disorders (headache) (15 participants; 42%), followed by gastrointestinal disorders (abdominal pain, nausea, and diarrhea) (14 participants; 39%), and musculoskeletal pain (back pain and myalgia) (7 participants; 19%) of mild or moderate intensity. The episodes of headache were generally of mild intensity and commonly appeared in the very first hours after drug administration although also occurred later during the course of treatment. AEs were broadly of a relatively short duration, and most of them resolved spontaneously or with symptomatic treatments. No AE persisted or had sequelae at the end of the study. Nonetheless, these events led to the investigational drug discontinuation in three participants (one from the $HIV^{50mg/12w}$ group and two from the $HIV^{150mg/4w}$ group). Overall, the incidence of AEs was numerically higher in the 150 mg dose group than in 50 mg dose group. This pattern indicated a dose relationship in the occurrence of AEs.

Table 5. Summary of AEs, by system organ class, and number and percentage of participants experiencing AEs by group. The denominator for each percentage is the number of participants within the column. *n*: number of participants.

System organ class	HN$^{50mg/4w}$ (*n*=12) *n* (%)	HIV$^{50mg/12w}$ (*n*=13) *n* (%)	HIV$^{150mg/4w}$ (*n*=11) *n* (%)	Total (*n*=36) *n* (%)
Any AE	**3 (25)**	**7 (54)**	**9 (82)**	**19 (53)**
Blood and lymphatic disorders	**0 (0)**	**0 (0)**	**1 (9)**	**1 (3)**
Thrombocytopenia	0	0	1	1
Gastrointestinal disorders	**2 (17)**	**6 (46)**	**6 (55)**	**14 (39)**
Abdominal pain	0	2	2	4
Abdominal pain upper	1	1	1	3
Constipation	0	0	1	1
Diarrhea	0	2	1	3
Dyspepsia	1	0	0	1
Flatulence	0	1	0	1
Nausea	0	0	4	4
General disorders	**0 (0)**	**3 (23)**	**3 (27)**	**6 (17)**
Asthenia	0	0	1	1
Chest pain	0	0	1	1
Feeling abnormal	0	1	0	1
Malaise	0	1	1	2
Thirst	0	1	0	1
Metabolism and nutrition disorders	**0 (0)**	**0 (0)**	**1 (9)**	**1 (3)**
Hyperamylasaemia	0	0	1	1
Hyperlipasaemia	0	0	1	1
Musculoskeletal and connective tissue disorders	**0 (0)**	**1 (8)**	**6 (55)**	**7 (19)**
Arthralgia	0	0	1	1
Back pain	0	1	4	5

Muscle spasms	0	0	1	1
Myalgia	0	0	4	4
Nervous system disorders	**2 (17)**	**5 (39)**	**8 (73)**	**15 (42)**
Headache	2	4	8	14
Migraine	0	1	0	1
Psychiatric disorders	**0 (0)**	**0 (0)**	**2 (18)**	**2 (6)**
Insomnia	0	0	1	1
Nightmare	0	0	1	1
Skin and subcutaneous tissue disorders	**0 (0)**	**0 (0)**	**2 (18)**	**2 (6)**
Folliculitis	0	0	1	1
Rash erythematous	0	0	1	1

No changes or clinically significant abnormalities were observed throughout the study duration in either clinical laboratory data, physical examinations, and vital sign parameters. Indeed, no significant changes were observed for standard viral load and counts of $CD4^+$ and $CD8^+$ T cells in either group at any timepoint, suggesting that obefazimod does not disrupt clinical control of HIV-1 infection and therefore does not negatively interact with ART (Figure 22). Hence, up to 150 mg, obefazimod was safe and well tolerated either alone or in combination with ART.

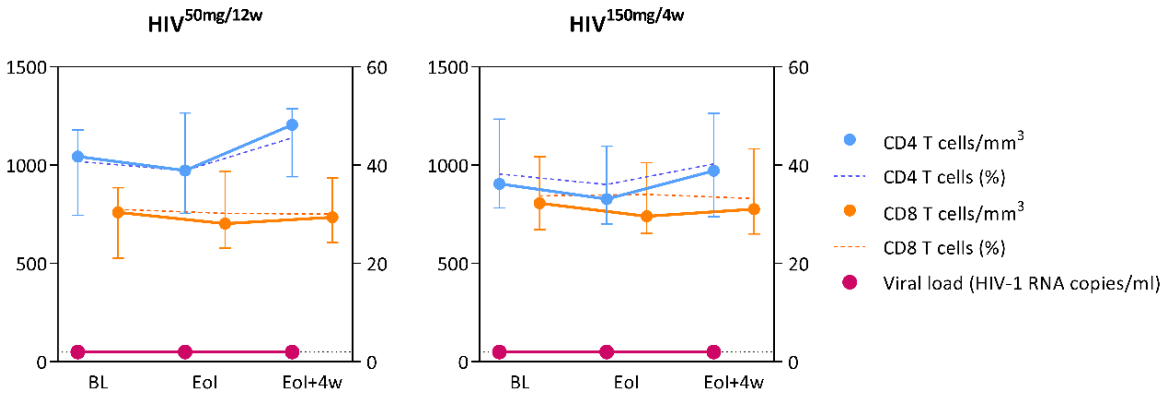

Figure 22. Clinical control of HIV-1 infection throughout obefazimod intervention and subsequent discontinuation. Median changes in viral load, $CD4^+$, and $CD8^+$ T-cell counts of each timepoint in the two groups of PWH undergoing ART. Undetectable viral load was defined as less than 50 HIV-1 RNA copies/ml (broken line). BL: baseline; EoI: end of intervention; EoI+4w: 4 weeks after end of intervention.

3. Effect of obefazimod on viral persistence

3.1. Effect of obefazimod on viral reservoir size

The impact of obefazimod on the size of proviral reservoir was evaluated by measuring total HIV-1 DNA in circulating $CD4^+$ T cells, which constitute most of the latent reservoir in peripheral blood. Total HIV-1 DNA was detectable in all participants with a median of 212 (IQR, 91-605) copies per million $CD4^+$ T cells. Longitudinal analysis confirmed a potential impact of obefazimod on latent reservoir with a statistically significant reduction of total HIV-1 DNA after intervention, only at the 150 mg dose (median fold-change=0.6, p=0.008) (Figure 23a-b). Indeed, the proportion of individuals who decreased total HIV-1 DNA after obefazimod treatment was higher at the 150 mg dose in comparison to the 50 mg dose (88.9% *vs*. 50%, respectively) (Figure 23c-d). However, this was a transient effect as total HIV-1 DNA increased, returning to basal levels, after drug discontinuation (Figure 23e-h). These results demonstrate that obefazimod reduces total proviral reservoir in a dose-dependent manner, potentially impacting viral persistence, when it is administered in combination with ART. Hence, obefazimod may act as an ART intensifier or improve ART effect.

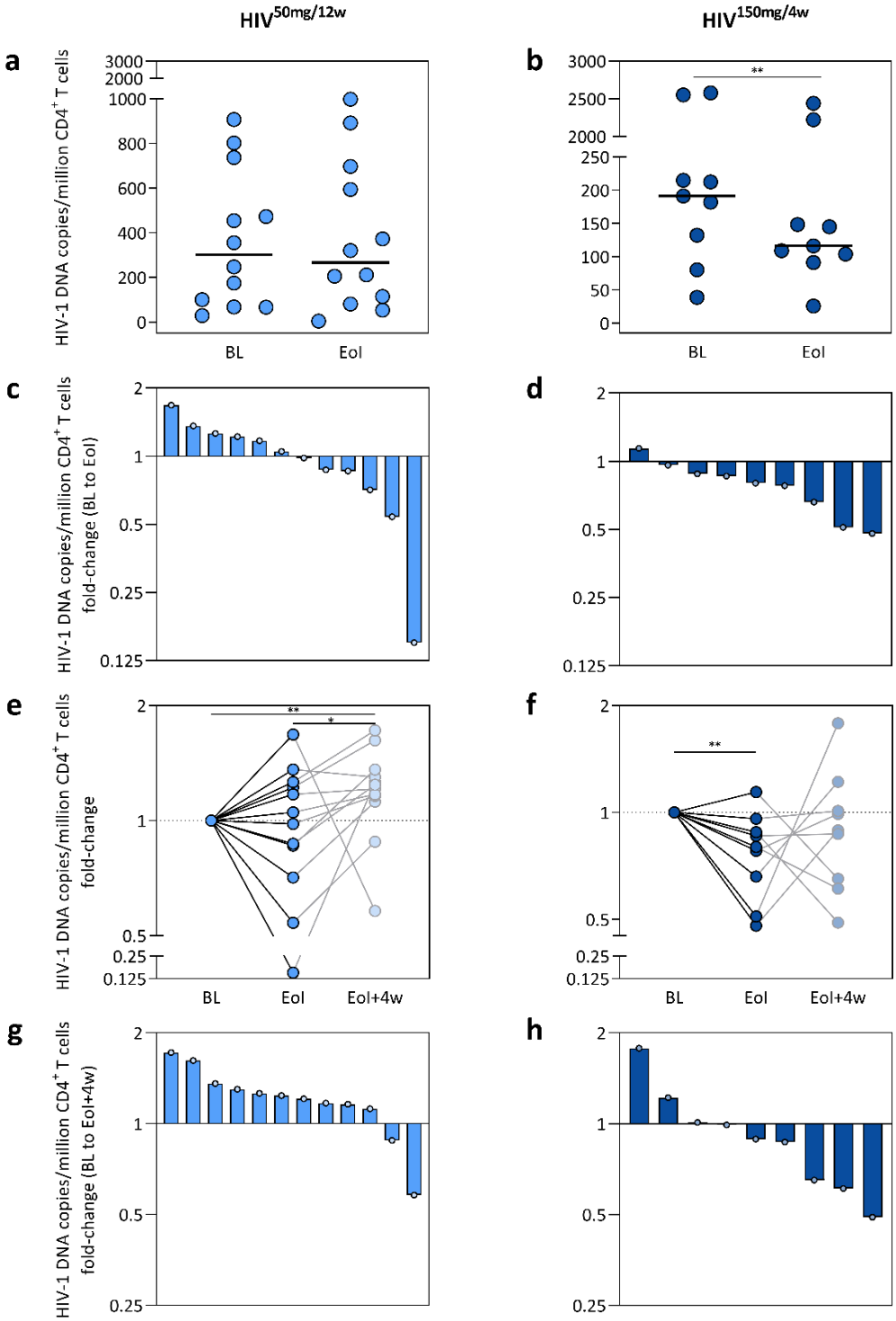

Figure 23. Effect of obefazimod on total HIV-1 DNA throughout intervention and subsequent discontinuation. (**a-b**) Changes in total HIV-1 DNA from peripheral CD4+ T cells throughout intervention in each group. (**c-d**) Waterfall charts represent the increase/decrease from baseline to end of intervention in each group. (**e-f**) Fold-changes in total HIV-1 DNA from peripheral CD4+ T cells from baseline to 4 weeks after discontinuation in each group. (**g-h**) Waterfall charts represent the increase/decrease from baseline to 4 weeks after discontinuation in each group. Black lines in a-b represent medians. Asterisks denote significant differences between time points detected using the Wilcoxon signed rank test (* $p \leq 0.05$; ** $p \leq 0.01$). BL: baseline; EoI: end of intervention; EoI+4w: 4 weeks after end of intervention.

3.1.1. Effect of obefazimod on intact viral reservoir

As total HIV-1 DNA indistinctly measures both intact and defective proviruses, the impact of obefazimod on the size of intact proviral reservoir was evaluated by measuring intact and defective proviruses, harboring deletions and/or hypermutations, in peripheral CD4+ T cells from the group of participants that underwent 150 mg of obefazimod for 4 weeks. Intact, 5' defective, and 3' defective HIV-1 DNA were detectable in all participants with a median of 16.4 (IQR, 5-66), 90.9 (IQR, 43-551), and 50.8 (IQR, 20-475) copies per million CD4+ T cells, respectively. Intact proviruses were greatly outnumbered by defective proviruses, which confirm the proviral landscape is dominated by the vast excess of defective proviruses. This small subset of proviruses has the potential to cause viral rebound, which emphasizes the importance of direct measurement of intact proviruses. Longitudinal analysis showed intact and 5' defective HIV-1 DNA trend to decrease (median fold-change=0.8, *p*=n.s. for both), while no such trend was observed for 3' defective HIV-1 DNA. However, similar to total, intact HIV-1 DNA significantly increased after drug discontinuation (median fold-change=1.4, *p*=0.008), and a trend was observed toward smaller increase in 5' defective HIV-1 DNA (median fold-change=1.4, *p*=n.s.) (Figure 24).

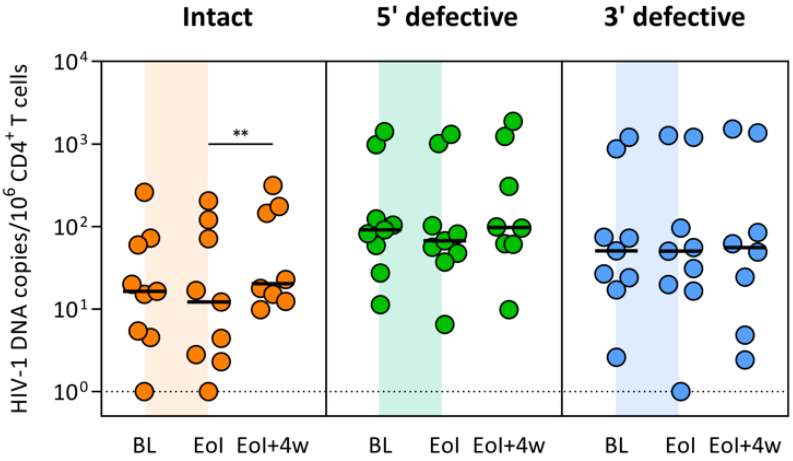

Figure 24. Effect of obefazimod on intact HIV-1 DNA throughout intervention and subsequent discontinuation. Changes in intact, 5' defective, and 3' defective HIV-1 DNA of each timepoint in individuals from the HIV$^{150mg/4w}$ group. LOD was defined as 1 HIV-1 DNA copy/10^6 CD4+ T cells (broken line). Each color represents a different assay. Black lines represent medians. Asterisks denote significant differences between timepoints detected using the Wilcoxon signed rank test (** $p \leq 0.01$). BL: baseline; EoI: end of intervention; EoI+4w: 4 weeks after end of intervention.

Since we observed differences in the increase of total and intact HIV-1 DNA after obefazimod discontinuation, we sought to determine whether the correlation between total and intact was affected by obefazimod. Total and intact HIV-1 DNA correlated strongly at baseline (r=0.72, p=0.04) and end of intervention (r=0.95, p=0.0004), whereas 4 weeks after drug discontinuation the Spearman's Rho correlation coefficient was lower and the p-value was no longer statistically significant (r=0.57, p=0.2) (Figure 25). Altogether, these results suggest that while obefazimod tended to decrease total and intact HIV-1 DNA, the intact HIV-1 DNA tended to increase more after drug discontinuation.

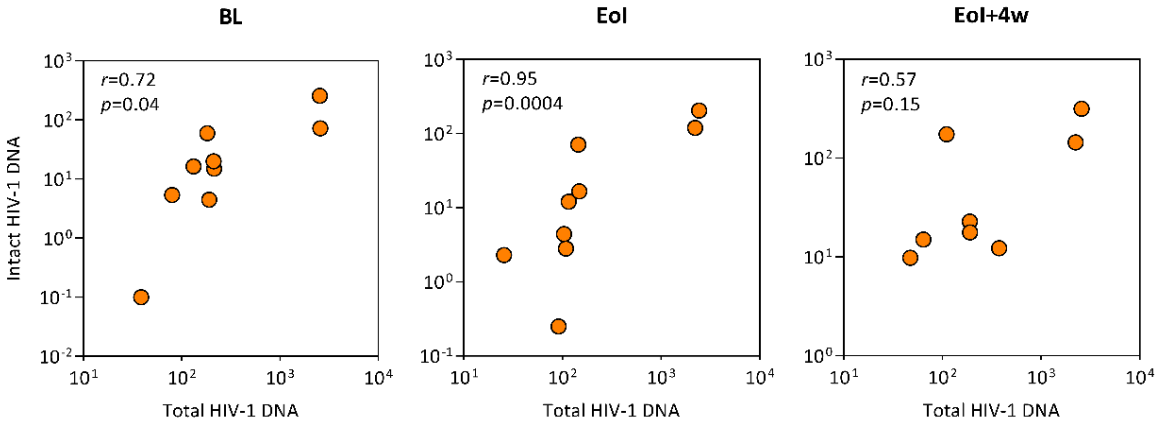

Figure 25. Correlation between total and intact HIV-1 DNA. Spearman's correlations between total and intact HIV-1 DNA of each timepoint in individuals from the HIV$^{150mg/4w}$ group. BL: baseline; EoI: end of intervention; EoI+4w: 4 weeks after end of intervention.

3.2. Effect of obefazimod on viral transcription

The impact of obefazimod on the transcriptional activity of the viral reservoir was evaluated by measuring cell-associated HIV-1 RNA in peripheral CD4$^+$ T cells. Cell-associated HIV-1 RNA was detectable in all participants with a median of 3 (IQR, 0.4-8) HIV-1 RNA copies per 10^3 *TBP* RNA copies. Longitudinal analysis showed no consistent effect of obefazimod on viral transcription during the treatment period (Figure 26a-d). These data suggest that obefazimod did not seem to affect overall viral transcription. Contrary to what was expected, 4 weeks after drug discontinuation, cell-associated HIV-1 RNA significantly increased at the 150 mg dose (median fold-change=2.1, p=0.02) and the 50 mg dose (median fold-change=1.2, p=0.02) (Figure 26e-f). Indeed, the number of individuals who

increased cell-associated HIV-1 RNA after discontinuation was higher at the 150 mg dose in comparison to the 50 mg dose (100% *vs.* 75%, respectively) (Figure 26g-h). These results suggest that obefazimod discontinuation might contribute to increase viral transcription.

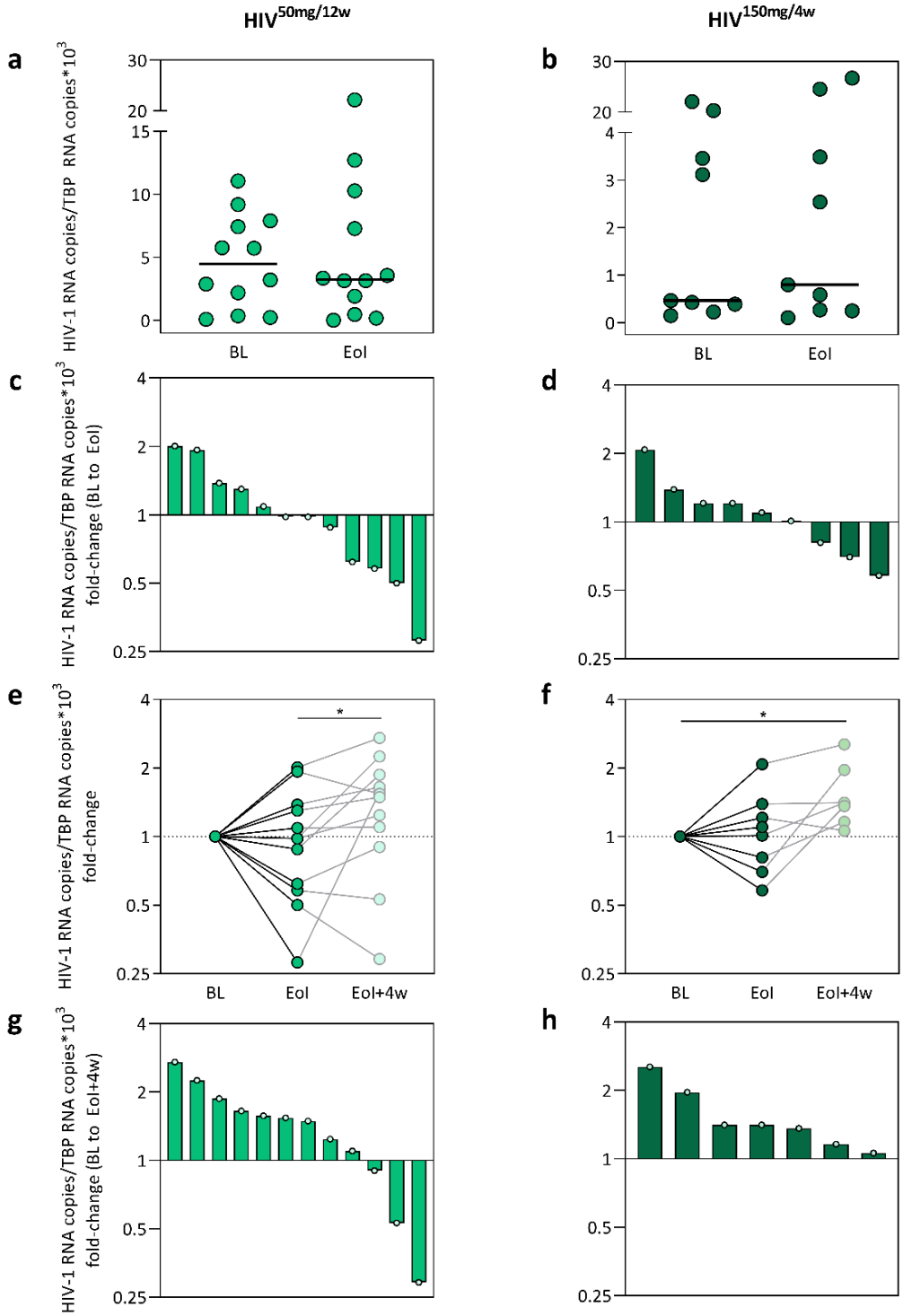

Figure 26. Effect of obefazimod on cell-associated HIV-1 RNA throughout intervention and subsequent discontinuation. (**a-b**) Changes in cell-associated HIV-1

RNA from peripheral CD4+ T cells throughout intervention in each group. (**c-d**) Waterfall charts represent the increase/decrease from baseline to end of intervention in each group. (**e-f**) Fold-changes in cell-associated HIV-1 RNA from peripheral CD4+ T cells from baseline to 4 weeks after discontinuation in each group. (**g-h**) Waterfall charts represent the increase/decrease from baseline to 4 weeks after discontinuation in each group. Data from two individuals in the HIV$^{150mg/4w}$ group were excluded from the analysis due to technical problems at timepoint EoI+4w. Black lines in a-b represent medians. Asterisks denote significant differences between time points detected using the Wilcoxon signed rank test (* $p \leq 0.05$). BL: baseline; EoI: end of intervention; EoI+4w: 4 weeks after end of intervention.

3.2.1. Effect of obefazimod on viral transcription profile

The mechanism and the degree of inhibition of obefazimod on HIV-1 RNA transcription and its potential contribution to the maintenance of latency was further evaluated by simultaneously quantifying different viral transcripts that define different steps of viral RNA production and maturation, including read-through, initiated (TAR), 5' elongated (R-U5/*gag*), unspliced (*pol*), polyadenylated (PolyA), and multiple spliced (*tat/rev*) transcripts, in peripheral CD4+ T cells from the group of participants that underwent 150 mg of obefazimod for 4 weeks. Each viral transcript was expressed as copies per million CD4+ T cells and also per provirus (HIV-1 RNA/HIV-1 DNA ratio), given the changes in HIV-1 DNA. Read-through transcripts were detected in all participants, suggesting transcriptional interference, albeit at very low levels (248-fold lower than total transcripts). Initiated (TAR) transcripts were 10-fold higher than elongated transcripts, indicating abundant transcriptional initiation but a substantial block to elongation; 5' elongated (R-U5/*gag*) transcripts were 13-fold higher than polyadenylated transcripts, suggesting another block to completion of transcription; and polyadenylated (PolyA) transcripts were 13-fold higher than multiple spliced (*tat/rev*) transcripts, suggesting a block to multiple splicing. Longitudinal analysis confirmed the impact of obefazimod on HIV-1 RNA transcription with a statistically significant reduction of initiated transcripts per provirus (median fold-change=0.5, p=0.004) and a trend toward a decrease in 5' elongated transcripts per provirus (median fold-change=0.5, p=0.07), while no significant changes were observed in unspliced, polyadenylated, nor multiple spliced HIV transcripts (Figure 27a). The very low baseline levels of multiple spliced (*tat/rev*) transcripts and the high proportion of undetectable samples might have interfered to detect changes in these transcripts. A similar pattern of transcripts and

blocks was observed when measures were normalized by cell count (Figure 27b). These data demonstrate that obefazimod decreases HIV-1 RNA transcription initiation and may also decrease viral transcripts elongation when it is administered in combination with ART. Hence, obefazimod may act directly or indirectly as a latency promoting agent. However, levels of all transcripts also increase after obefazimod discontinuation. The greatest increase was observed in 5' elongated transcripts per million CD4+ T cells (median fold-change=1.4, p=0.04) (Figure 27b). These results suggest that obefazimod discontinuation might contribute to increase viral transcription.

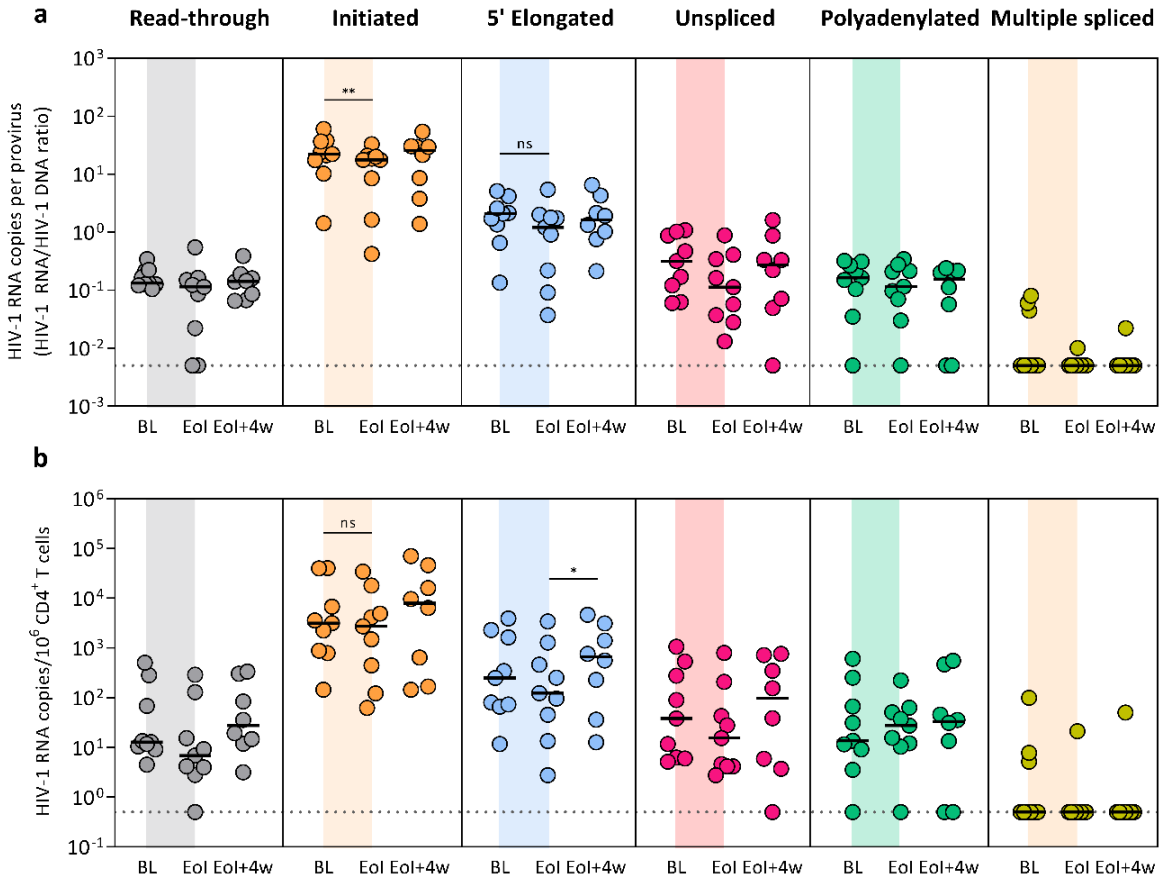

Figure 27. Effect of obefazimod on HIV-1 RNA transcription throughout intervention and subsequent discontinuation. (**a**) Changes of each transcript per provirus (HIV-1 RNA/HIV-1 DNA ratio) of each timepoint in individuals from the HIV$^{150mg/4w}$ group. LOD was defined as 0.005 HIV-1 RNA copies per provirus (broken line). (**b**) Changes of each transcript per million CD4+ T cells of each timepoint in individuals from the HIV$^{150mg/4w}$ group. LOD was defined as 0.5 HIV-1 RNA copies/10^6 CD4+ T cells (broken line). Each color represents a different assay. Black lines represent medians. Asterisks denote significant differences between timepoints detected using the Wilcoxon signed rank test (* $p \leq 0.05$; ** $p \leq 0.01$). BL: baseline; EoI: end of intervention; EoI+4w: 4 weeks after end of intervention.

3.3. Effect of obefazimod on residual viraemia

To assess residual viraemia in plasma of ART-suppressed individuals, as it is a marker of viral reservoir persistence, viral load was measured in plasma samples, in addition to routine measurement by PCR at the investigational site laboratory.

To evaluate whether changes on viral transcription might have a perceptible impact on viral production, as it is a marker of viral reservoir persistence, residual viraemia was measured in plasma samples by an ultrasensitive method (LOD=0.55 HIV-1 RNA copies/ml). Residual viraemia was detectable in 10 (47.6%) individuals (6 in the HIV$^{50mg/12w}$ group and 4 in the HIV$^{150mg/4w}$ group), despite years of undetectable viraemia before study entry. Longitudinal analysis confirmed a substantial reduction of ultrasensitive viral load in all (100%) individuals who showed detectable residual viraemia at baseline at the 150 mg dose in comparison to the ones at the 50 mg dose (56%) (Figure 28a-d). Of note, this effect was not maintained after drug discontinuation (Figure 28e-h). The very low levels of plasma HIV-1 RNA at baseline and high proportion of undetectable samples might have interfered to detect significant changes. However, even though these data are not statistically significant, they parallel the dynamics of HIV- 1 DNA in peripheral CD4^{+} T cells.

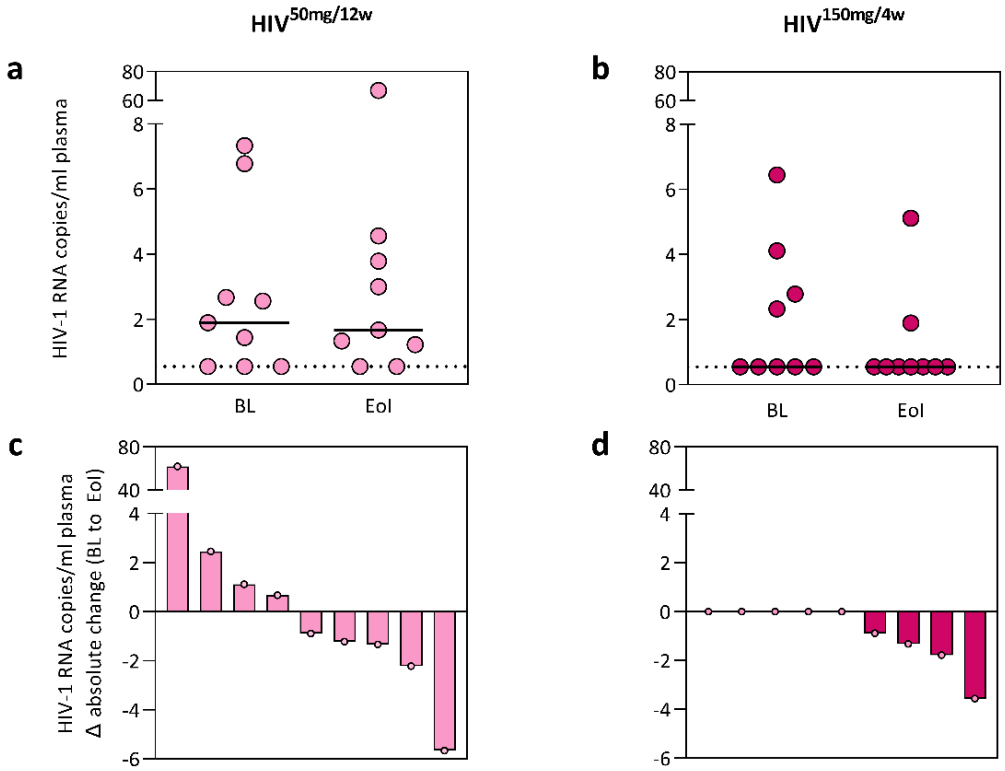

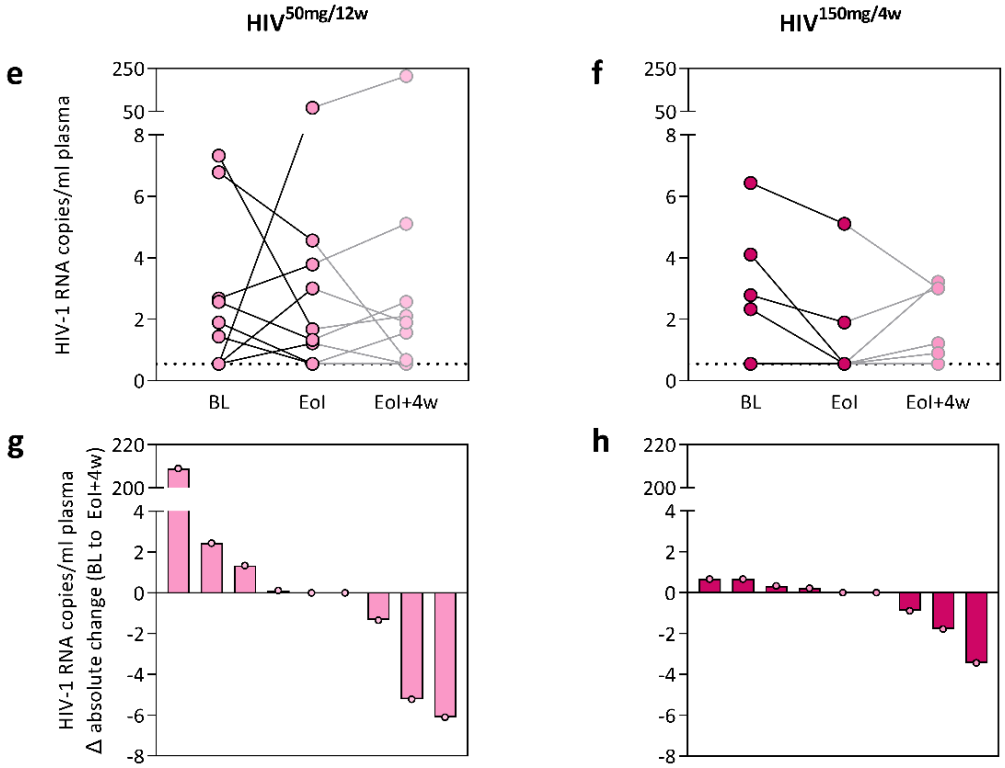

Figure 28. Effect of obefazimod on residual viraemia throughout intervention and subsequent discontinuation. (**a-d**) Changes in ultrasensitive plasma viral load throughout intervention in each group. (**e-f**) Changes in ultrasensitive plasma viral load from baseline to 4 weeks after discontinuation in each group. Upper panels represent absolute values of each timepoint in each group. Lower panels represent waterfall charts to show the increase/decrease of each timepoint in each group. Data from three individuals in the HIV$^{50mg/12w}$ group were excluded from the analysis due to technical problems. LOD was defined as 0.55 HIV-1 RNA copies/ml (broken line). Black lines in a-b represent medians. BL: baseline; EoI: end of intervention; EoI+4w: 4 weeks after end of intervention.

Overall, these data reinforce that obefazimod potentially impacts viral persistence by transiently reducing viral transcription initiation and elongation, residual viraemia, and total proviral reservoir size, in a dose-dependent manner, when it is administered in combination with ART.

4. Immune responses to obefazimod

4.1. Effect of obefazimod on immune activation

The impact of obefazimod on chronic immune activation exhibited by PWH during suppressive ART was evaluated by assessing the phenotypic distribution and

activation of T-cell subsets within PBMCs and sorted leukocytes from rectal biopsies. No significant longitudinal changes were observed in the frequency of CD4+ and CD8+ T cells nor the CD4/CD8 ratio in either group (Figure 22). In peripheral CD4+ T cells, no significant changes were observed in the frequency of any maturation subset after initiation of obefazimod in either group (Figure 29). Furthermore, no intergroup differences were observed for any maturation subset, except for a lower percentage of T_N cells at baseline in the $HIV^{150mg/4w}$ group in comparison to the $HIV^{50mg/12w}$ group (p=0.04) and a higher percentage of T_{TM} cells after obefazimod intervention in the $HIV^{150mg/4w}$ group in comparison to the $HN^{50mg/4w}$ and $HIV^{50mg/12w}$ groups (p=0.002 and p=0.004, respectively) (Figure 29 and Table 6). Overall, these results suggest there is no redistribution of cellular CD4+ T-cell subsets.

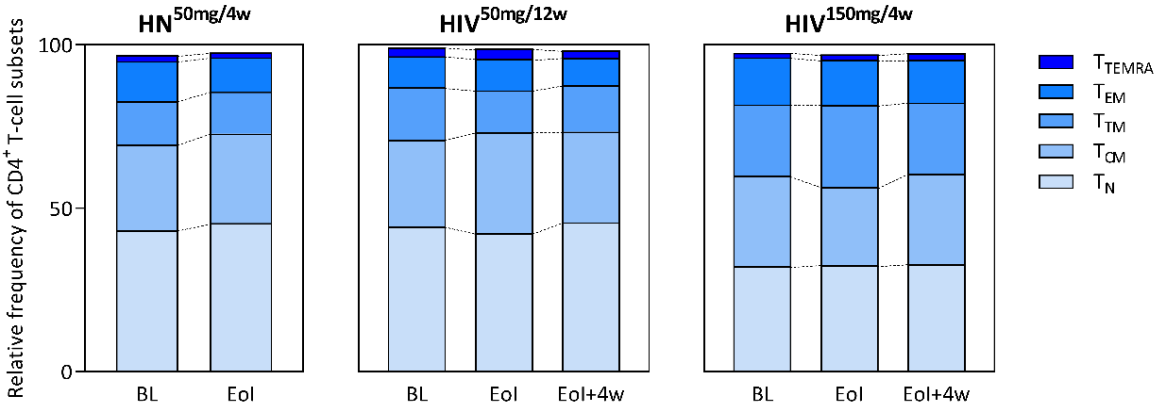

Figure 29. Effect of obefazimod on the frequency of CD4+ T-cell subsets throughout intervention and subsequent discontinuation. Relative frequency of each maturation subset among peripheral CD4+ T cells of each timepoint in each group. Bars represent medians of each subset. BL: baseline; EoI: end of intervention; EoI+4w: 4 weeks after end of intervention.

The baseline expression of the activation-induced markers CD38, HLA-DR and PD-1 in CD4+ and CD8+ T cells from peripheral blood and rectal biopsies was similar between groups except for higher percentage of PD-1+ in rectal CD4+ T cells in the $HIV^{150mg/4w}$ group in comparison to the group of HIV-negative participants (p=0.04) (Table 6). Longitudinal analysis demonstrated a potential impact of obefazimod on immune activation with a statistically significant reduction of T-cell activation in both peripheral blood and GALT. In peripheral blood, the percentage of PD-1+ in both

CD8⁺ and CD4⁺ T cells significantly decreased over time in the HIV$^{50mg/12w}$ group (p=0.007 and p=0.02, respectively). Moreover, activated CD38⁺HLA-DR⁺ in CD4⁺ T cells significantly decreased throughout intervention in the HIV$^{50mg/12w}$ group (p=0.04). Same trend was observed in the HIV$^{150mg/4w}$ group when CD38, HLA-DR and PD-1 expression was analyzed in CD4⁺ and CD8⁺ T cells (Figure 30a-d and Table 7). The fact that the reduction of T-cell activation in peripheral blood is only significant when obefazimod is given for at least 12 weeks, suggests a lasting effect of obefazimod at reducing immune activation in PWH on suppressive ART. Of note, these results were reinforced by the findings in GALT, as the percentage of activated CD38⁺HLA-DR⁺ in both CD4⁺ and CD8⁺ T cells from rectal biopsies significantly decreased over time in the HIV$^{150mg/4w}$ group (p=0.008 and p=0.02, respectively). However, obefazimod transiently increased the percentages of activated CD38⁺HLA-DR⁺ in rectal CD8⁺ T cells in the HIV$^{50mg/12w}$ group throughout intervention (p=0.03) (Figure 30e-h and Table 8). No significant changes were observed for the expression of activation-induced markers in T cells from either peripheral blood or rectal biopsies in the HIV-negative group over time, except for a higher percentage of PD-1⁺ in rectal CD4⁺ T cells after intervention (p=0.01) (Table 6). Altogether, these results suggest that obefazimod may reduce chronic immune activation in PWH.

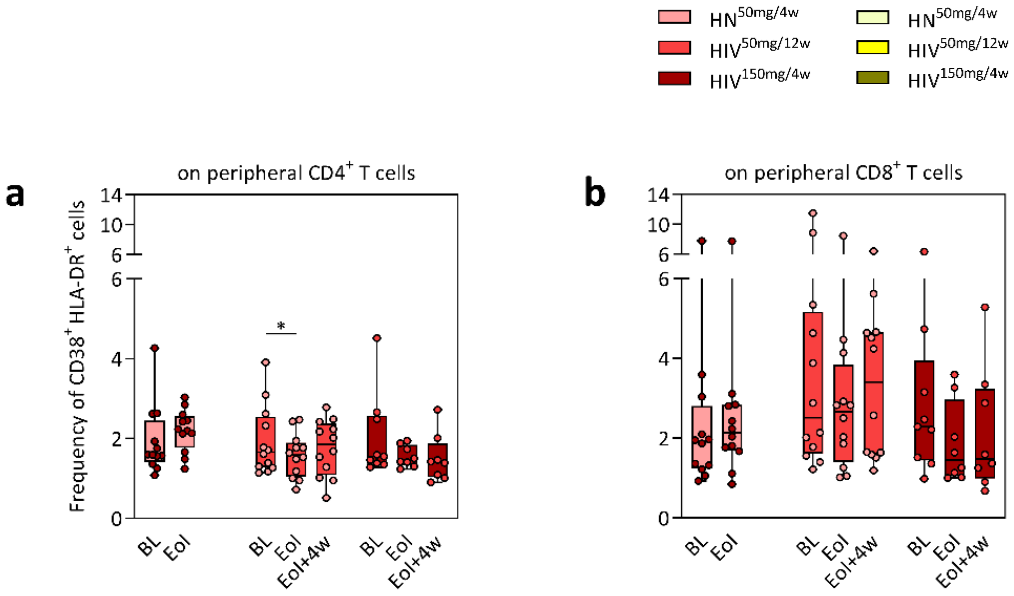

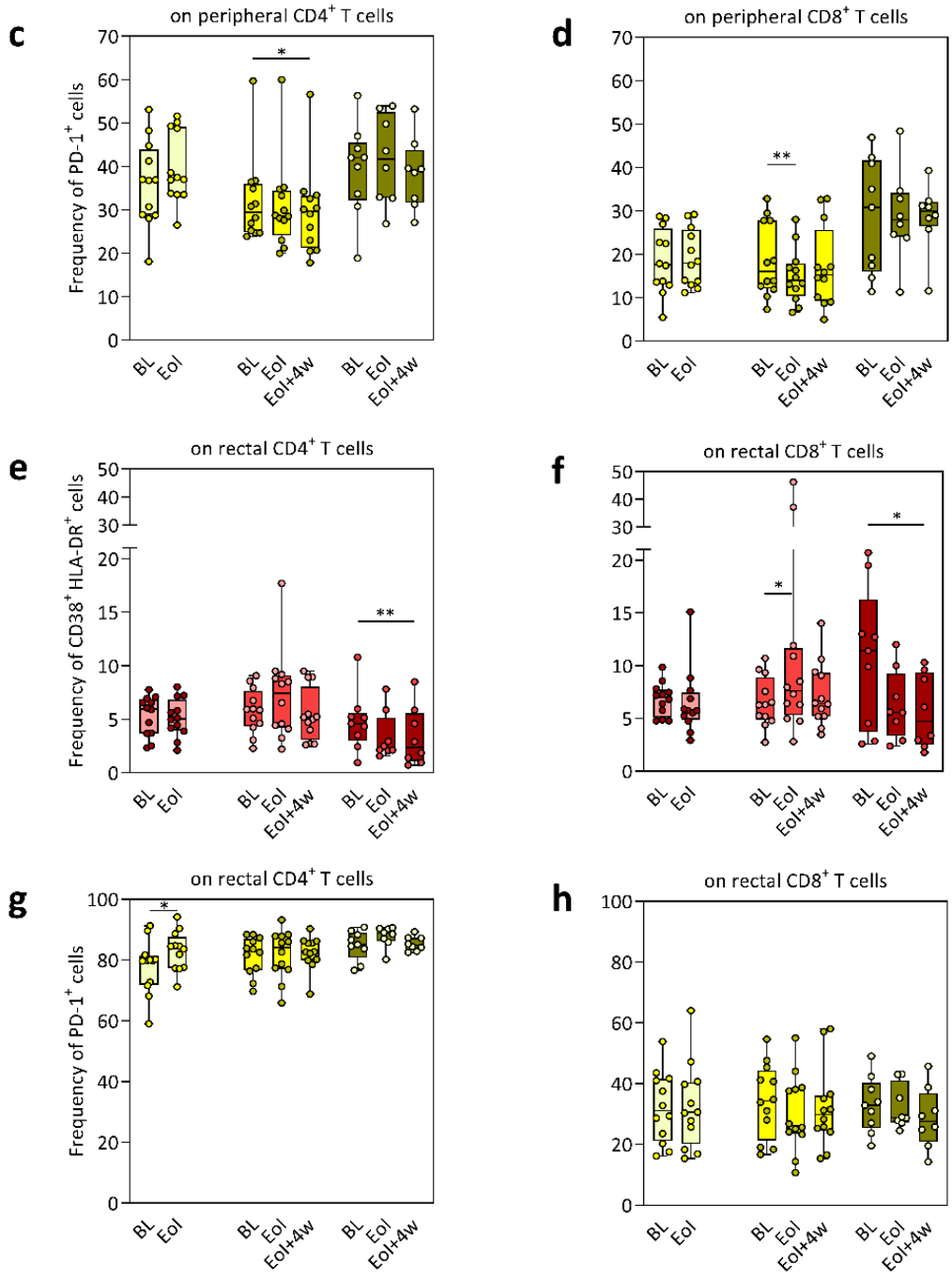

Figure 30. Effect of obefazimod on T-cell activation throughout intervention and subsequent discontinuation. (**a-b**) Frequency of CD38+HLA-DR+ in both CD4+ and CD8+ T cells from peripheral blood of each timepoint in each group. (**c-d**) Frequency of PD-1+ in both CD4+ and CD8+ T cells from peripheral blood of each timepoint in each group. (**e-f**) Frequency of CD38+HLA-DR+ in both CD4+ and CD8+ T cells from GALT of each timepoint in each group. (**g-h**) Frequency of PD-1+ in both CD4+ and CD8+ T cells from GALT of each timepoint in each group. Median and IQR are represented. Asterisks denote significant differences between timepoints detected using the Wilcoxon signed rank test (* $p \leq 0.05$; ** $p \leq 0.01$). BL: baseline; EoI: end of intervention; EoI+4w: 4 weeks after end of intervention.

Table 6. Effect of obefazimod on distribution of T-cell subsets throughout intervention and subsequent discontinuation. *p*-values between timepoints in each group were determined using Wilcoxon signed rank test. *p*-values between groups were determined using Mann-Whitney U test. *n*: number of participants; IQR: interquartile range; BL: baseline; EoI: end of intervention; EoI+4w: 4 weeks after end of intervention.

				p-values between groups at baseline		
	$HN^{50mg/4w}$ (*n*=12)	**$HIV^{50mg/12w}$ (*n*=13)**	**$HIV^{150mg/4w}$ (*n*=11)**	***$HIV^{50mg/12w}$ vs $HIV^{150mg/4w}$***	***$HN^{50mg/4w}$ vs $HIV^{50mg/12w}$***	***$HN^{50mg/4w}$ vs $HIV^{150mg/4w}$***
Peripheral $CD4^+$ T-cell percentages, *median [IQR]*						
$CD4^+CD45RA^+CCR7^+$ (T_N) at BL	40.1 [35.2 - 54.6]	48.5 [37.8 - 52.9]	34.2 [30.7 - 40.8]	***0.04***	*0.8*	*0.1*
$CD4^+CD45RA^+CCR7^+$ (T_N) at EoI	44.4 [35.4 - 59.6]	47 [32 - 52]	32.3 [23.9 - 41.6]			
$CD4^+CD45RA^+CCR7^+$ (T_N) at EoI+4w		47.7 [39.5 - 52.1]	34.2 [23.5 - 39.9]			
p-values between timepoints (BL vs EoI)	*0.5*	*0.2*	*0.7*			
p-values between timepoints (BL vs EoI+4w)		*1.0*	*0.8*			
$CD4^+CD45RA^-CCR7^+CD27^+$ (T_{CM}) at BL	26.9 [22.3 - 31]	26 [21.2 - 31]	24.5 [22 - 34.2]	*0.8*	*1.0*	*0.9*
$CD4^+CD45RA^-CCR7^+CD27^+$ (T_{CM}) at EoI	27.9 [22.2 - 31.4]	29.2 [24.5 - 37.5]	22.2 [16.1 - 32.8]			
$CD4^+CD45RA^-CCR7^+CD27^+$ (T_{CM}) at EoI+4w		28.1 [24.2 - 28.9]	25.8 [22.8 - 30.3]			
p-values between timepoints (BL vs EoI)	*0.4*	*0.2*	*0.2*			
p-values between timepoints (BL vs EoI+4w)		*0.6*	*1.0*			

$CD4^+CD45RA^-CCR7^-CD27^+$ (T_{TM}) at BL	12.1 [9.4 - 17.7]	14.3 [10.7 - 17.1]	22.8 [14.5 - 29.3]	*0.4*	*0.5*	*0.06*
$CD4^+CD45RA^-CCR7^-CD27^+$ (T_{TM}) at EoI	12 [8.9 - 14.1]	10.3 [7.3 - 13.2]	24.1 [19.6 - 31.6]			
$CD4^+CD45RA^-CCR7^-CD27^+$ (T_{TM}) at EoI+4w		12.8 [10.6 - 13.5]	23.8 [17 - 28.9]			
p-values between timepoints (BL vs EoI)	*0.7*	*0.06*	*0.2*			
p-values between timepoints (BL vs EoI+4w)		*0.2*	*1.0*			
$CD4^+CD45RA^-CCR7^-CD27^-$ (T_{EM}) at BL	12.8 [8.2 - 16.8]	8.1 [5.7 - 10.7]	11.2 [8.6 - 14.8]	*0.2*	*0.2*	*1.0*
$CD4^+CD45RA^-CCR7^-CD27^-$ (T_{EM}) at EoI	8.5 [4.5 - 13]	8 [6.6 - 10.4]	12.1 [9.6 - 15.7]			
$CD4^+CD45RA^-CCR7^-CD27^-$ (T_{EM}) at EoI+4w		6.1 [5.5 - 11.6]	11.1 [6.9 - 15]			
p-values between timepoints (BL vs EoI)	*0.2*	*0.6*	*0.7*			
p-values between timepoints (BL vs EoI+4w)		*0.2*	*0.5*			
$CD4^+CD45RA^+CCR7^-CD27^-$ (T_{EMRA}) at BL	1.6 [0.7 - 2.8]	2.2 [1.1 - 3.2]	0.8 [0.5 - 1.3]	*0.1*	*0.3*	*0.5*
$CD4^+CD45RA^+CCR7^-CD27^-$ (T_{EMRA}) at EoI	0.4 [0.3 - 2.5]	1.6 [1 - 2.1]	1.3 [0.7 - 2.4]			
$CD4^+CD45RA^+CCR7^-CD27^-$ (T_{EMRA}) at EoI+4w		1.3 [0.9 - 1.9]	1 [0.7 - 2.7]			
p-values between timepoints (BL vs EoI)	*0.07*	*0.4*	*0.6*			
p-values between timepoints (BL vs EoI+4w)		*0.5*	*1.0*			

Table 7. Effect of obefazimod on activation of peripheral T cells throughout intervention and subsequent discontinuation. *p*-values between timepoints in each group were determined using Wilcoxon signed rank test. *p*-values between groups were determined using Mann-Whitney U test. *n*: number of participants; IQR: interquartile range; BL: baseline; EoI: end of intervention; EoI+4w: 4 weeks after end of intervention.

				p-values between groups at baseline		
	HN$^{50mg/4w}$ (*n*=12)	**HIV$^{50mg/12w}$ (*n*=13)**	**HIV$^{150mg/4w}$ (*n*=11)**	***HIV$^{50mg/12w}$ vs HIV$^{150mg/4w}$***	***HN$^{50mg/4w}$ vs HIV$^{50mg/12w}$***	***HN$^{50mg/4w}$ vs HIV$^{150mg/4w}$***
Peripheral CD4$^+$ T-cell percentages, *median [IQR]*						
CD4$^+$CD38$^+$HLA-DR$^+$ at BL	1.6 [1.5 - 2.1]	1.7 [1.3 - 2.4]	1.6 [1.4 - 2.5]	*0.9*	*1.0*	*0.8*
CD4$^+$CD38$^+$HLA-DR$^+$ at EoI	2.2 [2 - 2.5]	1.6 [1.1 - 1.8]	1.5 [1.4 - 1.8]			
CD4$^+$CD38$^+$HLA-DR$^+$ at EoI+4w		1.9 [1.2 - 2.3]	1.4 [1.1 - 1.6]			
p-values between timepoints (BL vs EoI)	*0.2*	***0.04***	*0.3*			
p-values between timepoints (BL vs EoI+4w)		*0.7*	*0.4*			
CD4$^+$PD-1$^+$ at BL	36.8 [28.9 - 42.2]	29.5 [25.1 - 35.3]	42 [33.7 - 44.1]	*0.06*	*0.1*	*0.4*
CD4$^+$PD-1$^+$ at EoI	37.2 [33.7 - 48.9]	28.6 [26.5 - 33.7]	41.7 [32.8 - 50.7]			
CD4$^+$PD-1$^+$ at EoI+4w		29.6 [22.4 - 32.8]	39 [32.4 - 41]			
p-values between timepoints (BL vs EoI)	*0.1*	*0.2*	*0.7*			
p-values between timepoints (BL vs EoI+4w)		***0.02***	*0.6*			

Peripheral CD8⁺ T-cell percentages, *median [IQR]*						
CD8⁺CD38⁺HLA-DR⁺ at BL	1.9 [1.3 - 2.3]	2.5 [1.7 - 4.8]	2.3 [1.5 - 3.1]	*0.7*	*0.1*	*0.3*
CD8⁺CD38⁺HLA-DR⁺ at EoI	2.1 [1.7 - 2.8]	2.7 [1.7 - 3.2]	1.5 [1.1 - 2.3]			
CD8⁺CD38⁺HLA-DR⁺ at EoI+4w		3.4 [1.6 - 4.6]	1.5 [1.2 - 3]			
p-values between timepoints (BL vs EoI)	*0.3*	*0.1*	*0.08*			
p-values between timepoints (BL vs EoI+4w)		*0.9*	*0.4*			
CD8⁺PD-1⁺ at BL	17.6 [13.4 - 23.8]	16 [12.5 - 27.8]	30.8 [17.4 - 40.9]	*0.06*	*1.0*	*0.08*
CD8⁺PD-1⁺ at EoI	18 [13.6 - 24.7]	14 [11.5 - 17.2]	27.9 [24.4 - 33.2]			
CD8⁺PD-1⁺ at EoI+4w		15.2 [9.8 - 20]	29.9 [27.7 - 31.5]			
p-values between timepoints (BL vs EoI)	*0.9*	***0.007***	*1.0*			
p-values between timepoints (BL vs EoI+4w)		*0.2*	*0.6*			

Table 8. Effect of obefazimod on activation of rectal T cells throughout intervention and subsequent discontinuation. *p*-values between timepoints in each group were determined using Wilcoxon signed rank test. *p*-values between groups were determined using Mann-Whitney U test. *n*: number of participants; IQR: interquartile range; BL: baseline; EoI: end of intervention; EoI+4w: 4 weeks after end of intervention.

				p-values between groups at baseline		
	HN$^{50mg/4w}$ (*n*=12)	**HIV$^{50mg/12w}$ (*n*=13)**	**HIV$^{150mg/4w}$ (*n*=11)**	***HIV$^{50mg/12w}$ vs HIV$^{150mg/4w}$***	***HN$^{50mg/4w}$ vs HIV$^{50mg/12w}$***	***HN$^{50mg/4w}$ vs HIV$^{150mg/4w}$***
Rectal CD4$^+$ T-cell percentages, *median [IQR]*						
CD4$^+$CD38$^+$HLA-DR$^+$ at BL	6 [3.7 - 6.7]	5.9 [4.5 - 7]	4.6 [3.5 - 5.2]	*0.3*	*0.8*	*0.3*
CD4$^+$CD38$^+$HLA-DR$^+$ at EoI	5 [4.1 - 6.1]	7.4 [4.3 - 8.9]	2.3 [2.1 - 3.7]			
CD4$^+$CD38$^+$HLA-DR$^+$ at EoI+4w		5.1 [3.7 - 6.3]	2.4 [1.3 - 4.9]			
p-values between timepoints (BL vs EoI)	*0.9*	*0.8*	*0.2*			
p-values between timepoints (BL vs EoI+4w)		*0.3*	***0.008***			
CD4$^+$PD-1$^+$ at BL	79.8 [72.4 - 80.6]	83 [77.1 - 86.3]	85.8 [84.3 - 88.6]	*0.1*	*0.3*	***0.04***
CD4$^+$PD-1$^+$ at EoI	84 [77.4 - 85.7]	84.1 [77.3 - 87.8]	88.8 [86.7 - 90.2]			
CD4$^+$PD-1$^+$ at EoI+4w		82.7 [80.1 - 85.7]	84.8 [83.8 - 87.2]			
p-values between timepoints (BL vs EoI)	***0.01***	*1.0*	*0.06*			
p-values between timepoints (BL vs EoI+4w)		*1.0*	*0.7*			

Rectal CD8⁺ T-cell percentages, *median [IQR]*						
CD8⁺CD38⁺HLA-DR⁺ at BL	7 [5.5 - 7.5]	6.3 [5.1 - 8]	11.4 [4.5 - 13]	*0.2*	*0.7*	*0.2*
CD8⁺CD38⁺HLA-DR⁺ at EoI	5.7 [5.1 - 7.1]	7.6 [6 - 11.2]	5.6 [4.3 - 7.8]			
CD8⁺CD38⁺HLA-DR⁺ at EoI+4w		6.4 [5.2 - 9.2]	4.7 [2.8 - 8.9]			
p-values between timepoints (BL vs EoI)	*0.6*	***0.03***	*0.1*			
p-values between timepoints (BL vs EoI+4w)		*0.8*	***0.02***			
CD8⁺PD-1⁺ at BL	31.1 [22.7 - 41.2]	34.3 [25.8 - 42.2]	33.5 [29.9 - 39.2]	*1.0*	*0.7*	*0.6*
CD8⁺PD-1⁺ at EoI	30.5 [23.8 - 40]	26.2 [23.9 - 38.2]	28.9 [27.7 - 37.2]			
CD8⁺PD-1⁺ at EoI+4w		29.8 [25 - 35.5]	27.6 [23.5 - 33]			
p-values between timepoints (BL vs EoI)	*0.5*	*0.1*	*0.5*			
p-values between timepoints (BL vs EoI+4w)		*0.5*	*0.08*			

4.2. Effect of obefazimod on inflammation

As many PWH undergoing ART exhibit a chronic pro-inflammatory state that is primarily related to the extent of GALT damage, the impact of obefazimod on inflammation was evaluated by monitoring miR-124 expression in rectal biopsies. It was decided to evaluate whether miR-124 was selectively regulated by obefazimod since the cap binding complex (CBC), which is targeted by obefazimod, is involved in its biogenesis. miR-124 was detected in all participants and relative expression data was calculated according to the $2^{-(\Delta\Delta Cp)}$ method[104] normalized with the miR-16 housekeeping gene. Basal miR-124 expression was higher in the $HIV^{150mg/4w}$ group in comparison to the $HIV^{50mg/12w}$ group (p=0.02) (Figure 31a), maybe due to the longer time living with HIV-1 and receiving ART. Longitudinal analysis confirmed a potential impact of obefazimod on chronic inflammation with a statistically significant upregulation of miR-124 in all (100%) participants from all groups ($HN^{50mg/4w}$ median fold-change=2.2, p=0.0005; $HIV^{50mg/12w}$ median fold-change=4.0, p=0.0005; $HIV^{150mg/4w}$ median fold-change=6.7, p=0.004) (Figure 31b). However, this effect was reversed after drug discontinuation. These data demonstrate that obefazimod induces selective upregulation of miR-124 in PWH on suppressive ART as well as in HIV-negative individuals.

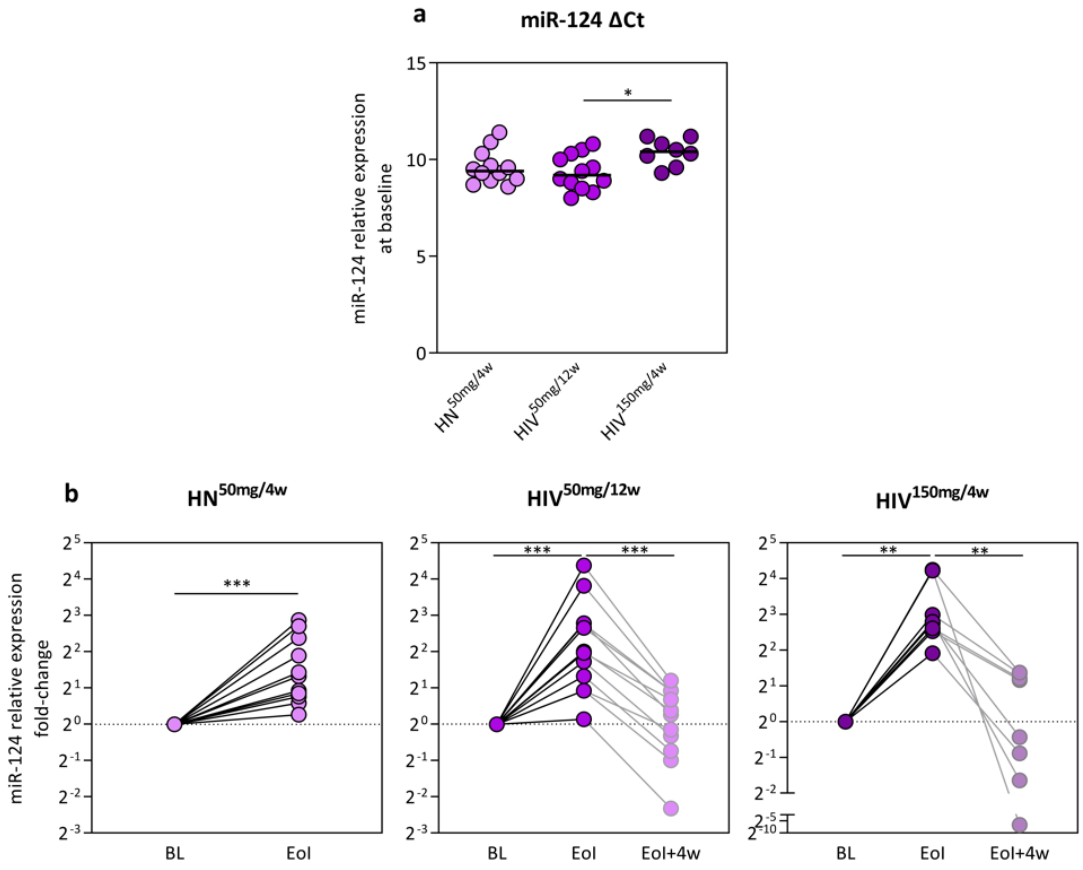

Figure 31. Effect of obefazimod on miR-124 expression throughout intervention and subsequent discontinuation. (**a**) Baseline expression of miR-124 monitored in rectal tissue in each group. (**b**) Fold-changes in miR-124 expression of each timepoint in each group. Black lines represent medians. Asterisks denote significant differences between timepoints detected using the Wilcoxon signed rank test (* p≤0.05; ** p≤0.01; *** p≤0.001). BL: baseline; EoI: end of intervention; EoI+4w: 4 weeks after end of intervention.

The impact of obefazimod on chronic inflammation was further evaluated by measuring the concentration of 26 soluble inflammation biomarkers in plasma samples. Unfortunately, data for biomarkers IL-4, IL-6, IL-8, IL-12 (p40), IL-22, and L-FABP were excluded from the analysis due to the high proportion of undetectable samples. As expected, analysis of the remaining 20 biomarkers showed significant baseline differences between PWH and HIV-negative individuals, such as the expression of G-CSF, MIP-1β (or CCL4), IL-7, MCP-1 (or CCL2), TNFα, and IL-18bp (Figure 32). This fact supports the evidence that PWH exhibit chronic inflammation, which seems to be higher in the HIV$^{150mg/4w}$ group maybe due to the longer time living with HIV-1 and undergoing ART.

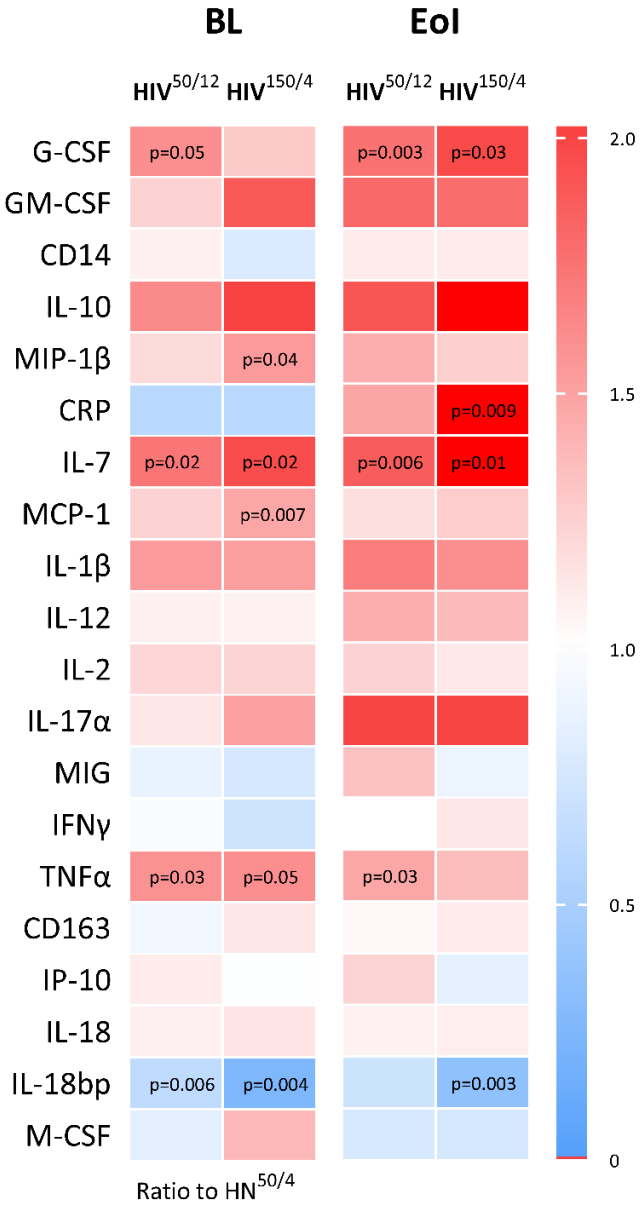

Figure 32. Differences on inflammation between PWH and HIV-negative individuals before and after obefazimod intervention. Heat-map represents median fold-changes in plasma concentration of inflammation biomarkers at baseline (BL) and at the end of obefazimod intervention (EoI) in the two groups of PWH ($HIV^{50mg/12w}$ and $HIV^{150mg/4w}$) in comparison to the group of HIV-1-negative individuals ($HN^{50mg/4w}$). Blue color represents a decrease in median fold-changes while red color represents an increase in median fold-changes. Median increase/decrease comparisons between groups were performed using the Mann-Whitney U test. *p*-values are shown. BL: baseline; EoI: end of intervention.

Longitudinal analysis reinforced the potential anti-inflammatory effect of obefazimod in both PWH and HIV-negative individuals with a statistically significant downregulation of the inflammation biomarkers G-CSF, GM-CSF, CD14, and IL-7 in the $HN^{50mg/4w}$ group (p=0.003, p=0.01, p=0.02, and p=0.05, respectively); IL-10 in

the HIV$^{50mg/12w}$ group (p=0.05); and MIP-1β (or CCL4) and MCP-1 (or CCL2) in the HIV$^{150mg/4w}$ group (p=0.01 and p=0.05, respectively) throughout obefazimod intervention (Figure 33a).

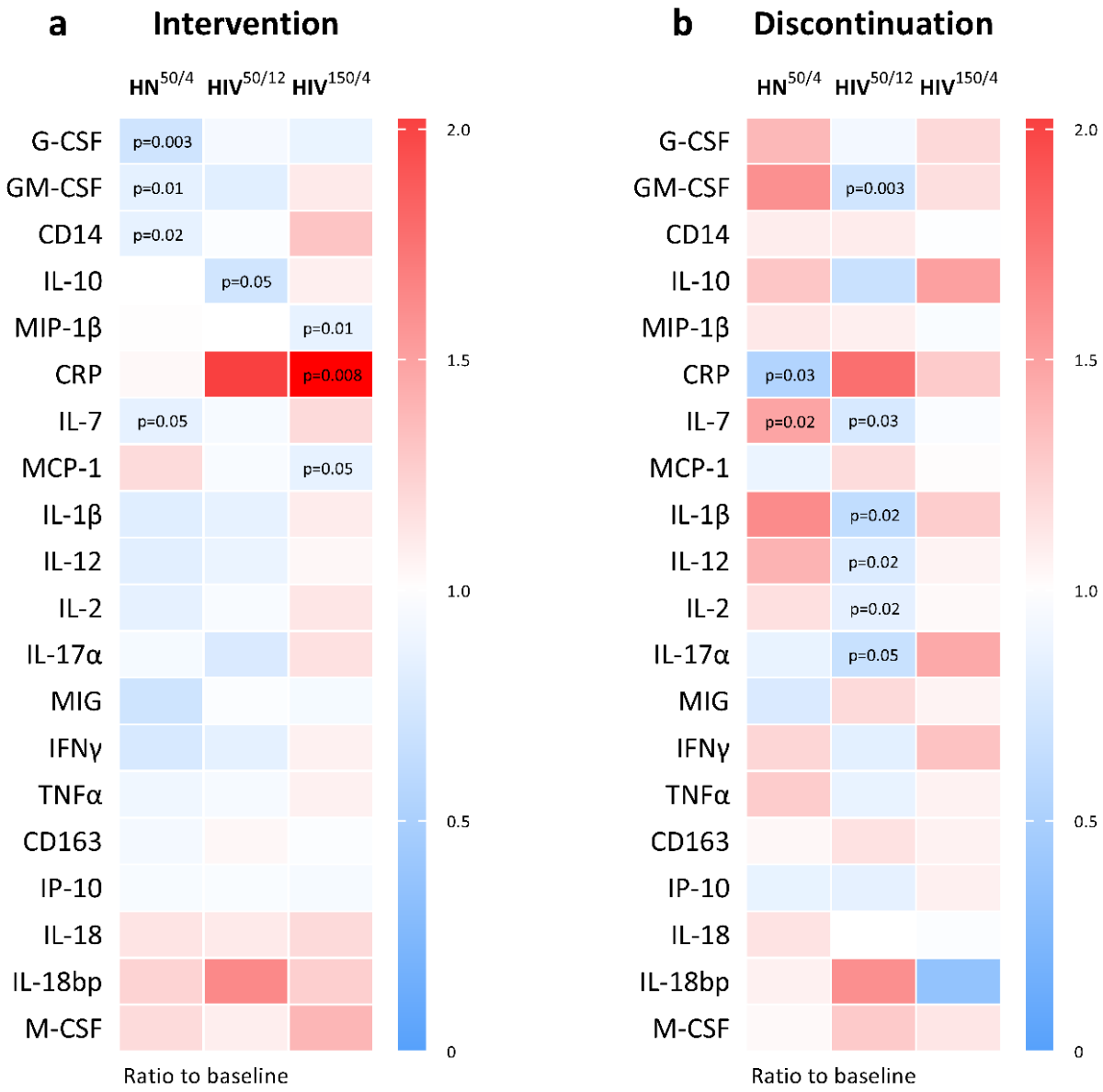

Figure 33. Effect of obefazimod on inflammation throughout intervention and subsequent discontinuation. (**a**) Left heat-map represents median fold-changes in plasma concentration of inflammation biomarkers throughout obefazimod intervention in each group. (**b**) Right heat-map represents median fold-changes in plasma concentration of inflammation biomarkers from baseline to 4 weeks after discontinuation in each group. Blue color represents a decrease in median fold-changes while red color represents an increase in median fold-changes. CRP is outside the defined range. Median increase/decrease comparisons between timepoints in each group were performed using the Wilcoxon signed rank test. p-values are shown.

Contrary to what was expected, CRP significantly increased in the HIV$^{150mg/4w}$ group after intervention (p=0.008), although mean values were always less than 10 mg/l, the upper limit of the normality range. However, CRP significantly decreased in all groups after obefazimod discontinuation (HN$^{50mg/4w}$ p=0.03; HIV$^{50mg/12w}$ p=0.03; HIV$^{150mg/4w}$ p=0.004) (Figure 34).

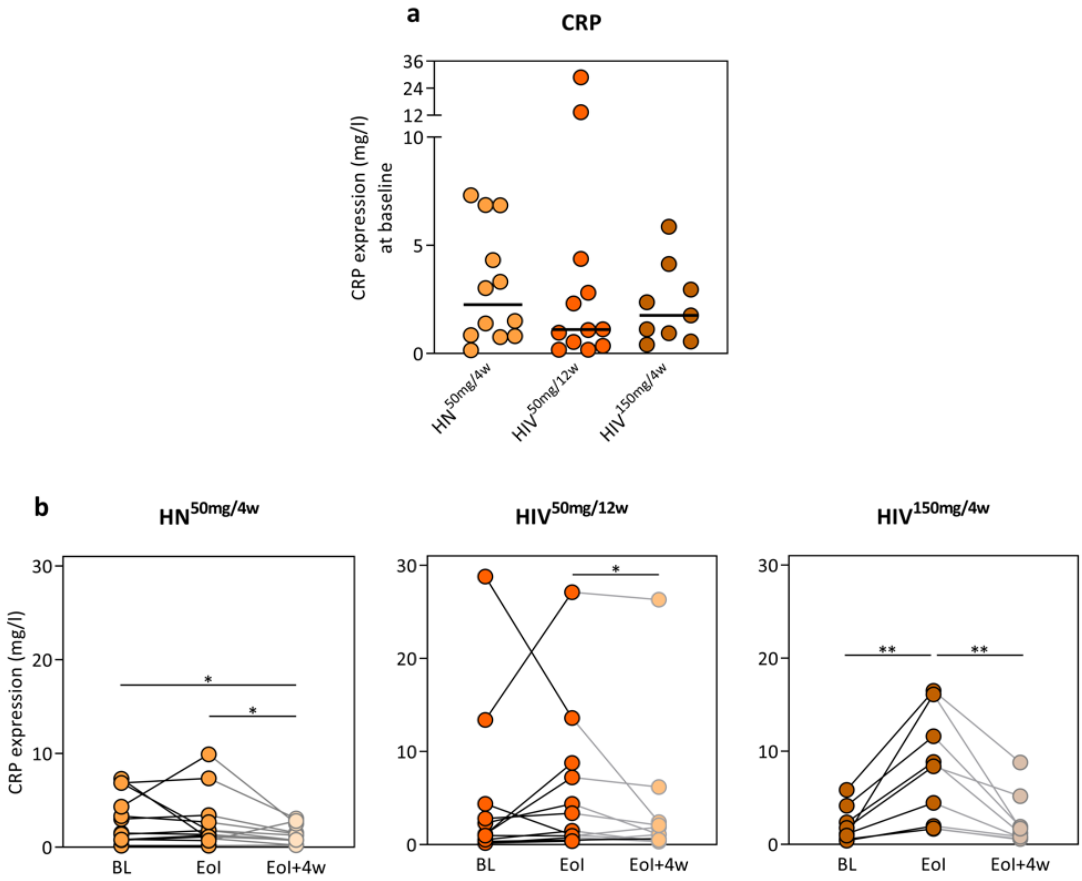

Figure 34 Effect of obefazimod on CRP expression throughout intervention and subsequent discontinuation. (**a**) Baseline expression of CRP in each group. (**b**) Changes in CRP expression of each timepoint in each group. Black lines represent medians. Asterisks denote significant differences between timepoints detected using the Wilcoxon signed rank test (* p≤0.05; ** p≤0.01). BL: baseline; EoI: end of intervention; EoI+4w: 4 weeks after end of intervention.

Nevertheless, significant differences remained present between PWH and HIV-negative individuals after obefazimod intervention, such as the expression of the inflammation biomarkers G-CSF, CRP, IL-7, TNFα, and IL-18 binding protein (Figure 32). Of note, the effect of obefazimod to reduce inflammation in PWH on ART was even greater 4 weeks after drug discontinuation, especially when

obefazimod was administered at 50 mg for 12 weeks, as it significantly downregulated the expression of GM-CSF, IL-7, IL-1β, IL-12 (p70), IL-2, and IL-17α (or CTLA-8) (p=0.003, p=0.03, p=0.02, p=0.02, p=0.02, and p=0.05, respectively) (Figure 33b). Altogether, these results suggest that obefazimod may reduce chronic inflammation in PWH on suppressive ART, and that longer duration of the intervention may enhance lasting anti-inflammatory effects.

Chapter 5. DISCUSSION

Antiretroviral therapy (ART) is highly successful in controlling viral replication, reducing viral load to undetectable levels, and reconstituting the immune system, thus improving the prognosis of HIV infection and preventing the risk of viral transmission. However, ART cannot cure HIV-1 infection because it cannot eradicate the latent viral reservoir[41]. Latent proviruses persist in many cellular and anatomical reservoirs that are hardly accessible for ART and are capable of producing viral antigens under appropriate activation conditions and contribute to chronic immune activation and inflammation[105]. Indeed, these latent proviruses are a potential source for viral rebound upon treatment interruption[42]. Hence, there remains an urgent need to investigate and implement novel therapeutic approaches that could impact the latent viral reservoir wherein it is more likely to persist and reverse the long-term clinical consequences of chronic immune activation and inflammation.

This thesis aimed at investigating a promising new therapeutical approach based on ART intensification with a novel drug, obefazimod (formerly ABX464), that might contribute to simultaneously reduce the persistence of viral reservoirs, chronic immune activation, and inflammation in long-term ART-suppressed people with HIV (PWH).

First, we evaluated the safety and tolerability of the investigational drug. Our results confirmed previous findings showing that obefazimod has a good safety and tolerability profile in PWH either alone or in combination with ART[92]. For the first time, we used obefazimod in combination with a boosted integrase inhibitor-based regimen, which was selected on the basis of absence of potential interaction with obefazimod via cytochrome P450 metabolism. Obefazimod adverse events (AEs) were mild, dose-dependent, and their nature was consistent with previous clinical trials across different indications[89–92,97–99]. The most common AEs with this treatment were neurological (headache), gastrointestinal (abdominal pain, nausea, and diarrhea), and musculoskeletal (back pain and myalgia) side effects.

Then, we evaluated the impact of obefazimod on viral persistence. Previous studies had shown a potential antiretroviral effect of obefazimod in two humanized

mouse models[79], as well as a substantial reduction of viral load and reservoir size in PWH in previous phase II clinical trials[91,92]. Our study demonstrated a reduction in the proviral reservoir size with a significant decrease in total HIV-1 DNA and a similar decreasing trend in intact HIV-1 DNA per million $CD4^+$ T cells when obefazimod was administered at 150 mg for 4 weeks in PWH on suppressive ART. This reduction could be an indirect consequence of an increase in cellular toxicity or changes in tissue distribution of $CD4^+$ T cells, especially central memory $CD4^+$ T cells, which constitute the main cellular reservoir for HIV-1[105]. However, neither we nor others[91] have observed obefazimod-related toxicity phenomena affecting $CD4^+$ T-cell counts (Figure 22), nor redistribution of the different subpopulations of memory $CD4^+$ T cells (Figure 29 and Table 6). Therefore, our results suggest that obefazimod directly impacts the proviral reservoir size in a dose-dependent manner. Previous studies in PWH have preliminary suggested a dose-dependent antiviral efficacy of the drug[91,92]. Indeed, similar trend in reducing total HIV-1 DNA per million PBMCs had previously been reported when obefazimod was also administered at 150 mg for 4 weeks but only in some participants[92]. Comparatively, we report statistically significant changes in total HIV-1 DNA, which was measured in peripheral $CD4^+$ T cells from the whole cohort, and a greater proportion of responders (88.9% *vs*. 42.9%). Moreover, our study included a higher number of participants (36 *vs*. 26), an additional obefazimod 50 mg regimen up to 12 weeks, a complementary 4-week post-treatment follow-up, and an extensive analysis of immunophenotype and inflammation biomarkers in both peripheral blood and GALT, in comparison to the previous clinical trial described by Rutsaert *et al*[92]. Furthermore, we are the first to evaluate the specific effect of obefazimod on the intact proviral reservoir and our results showed a similar decreasing trend although without reaching statistical significance[106]. Altogether these data suggest that obefazimod reduces the total proviral reservoir and may also reduce the intact proviral reservoir when it is administered in combination with ART. These results have important implications given the failure of multiple interventions to achieve a measurable reduction of the viral reservoir size in other studies. Nevertheless, the effect on HIV-1 DNA reversed after drug discontinuation, suggesting that the

changes observed during the treatment period were due to obefazimod and it should be administered for longer periods of time to achieve a more sustained effect.

Contrary to what was expected, we did not observe changes in the transcriptional activity of the viral reservoir during the intervention period using the conventional cell-associated HIV-1 RNA quantification assay. However, as this method is designed to specifically target 5' LTR and *gag* sequences resulting from unspliced viral transcripts and not further mature RNA forms, this might have impeded the detection of the impact of obefazimod in the different steps of HIV-1 RNA biogenesis. Thus, we further investigated the mechanism and the degree of inhibition of obefazimod at different stages of viral transcription. For the first time, we comprehensively characterized several cell-associated HIV-1 RNA transcripts and demonstrated that obefazimod reduces viral transcription initiation and may reduce viral transcription elongation when is administered at 150 mg for 4 weeks in PWH on suppressive ART[106]. However, while we detected a statistically significant decrease in the expression of initiated viral transcripts, and a decreasing trend in elongated and spliced viral transcripts throughout intervention, it is difficult to exclude a small effect on polyadenylated and multiple spliced transcripts due to the number of undetectable determinations. Nevertheless, as for HIV-1 DNA, these decreases reversed after drug discontinuation, suggesting that obefazimod may impact specific HIV-1 RNA transcripts but lacks lasting effect.

Furthermore, a reduction in persistent viral production was demonstrated with a substantial reduction of residual viraemia in all participants who had detectable residual viraemia at baseline when obefazimod 150 mg was administered for 4 weeks in ART-suppressed PWH. This observation is mostly consistent with other studies from our group, in which either intensification of an integrase inhibitor-based regimen with maraviroc, intensification with an integrase inhibitor of a monotherapy with boosted protease inhibitors, or switching from a protease inhibitor-based regimen to an integrase inhibitor-based regimen resulted in a decrease in residual viraemia, although without reaching statistical significance[107–109]. Nevertheless, this effect was not sustained after drug discontinuation. The very low baseline levels of residual viraemia and high proportion of undetectable samples might have interfered

to detect significant changes. However, even though these data are not statistically significant, they parallel the dynamics of HIV-1 DNA in peripheral $CD4^+$ T cells. Overall, we demonstrated that obefazimod potentially impacts viral persistence by transiently reducing viral transcription initiation and elongation, residual viraemia, and total proviral reservoir size, in a dose-dependent manner, when it is administered in combination with ART (Figure 35).

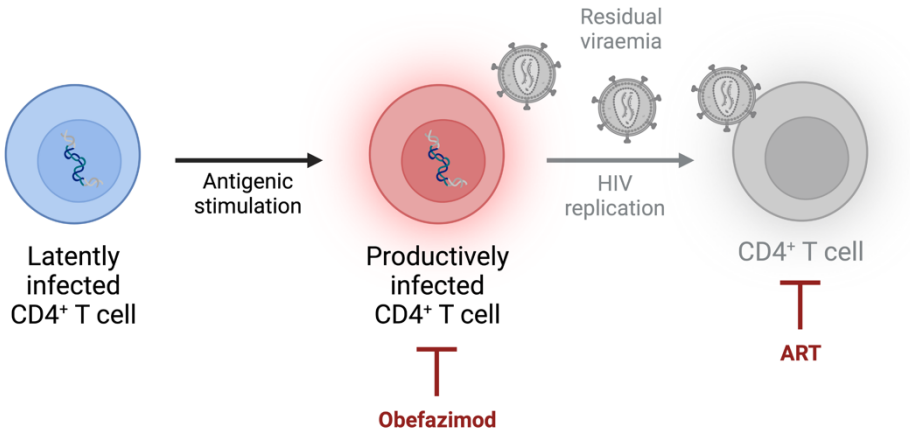

Figure 35. Inhibition of residual viraemia during ART intensification with obefazimod. Schematic representation of the suppression of viral production by adding obefazimod to ART.

Finally, we evaluated the impact of obefazimod on immune activation and inflammation. So far, no study has investigated its effect on immune activation in blood nor gut tissue from PWH. The persistent T-cell activation caused by chronic HIV-1 infection results in the overexpression of activation-induced markers (CD38 and HLA-DR) on the surface of T cells, which it is associated with a progressive loss of effector function and disease progression as well as it might be associated with the immunologic response to therapy[110,111]. Moreover, during chronic HIV-1 infection, the PD-1 marker is also overexpressed on T-cell surface, leading to immune exhaustion of HIV-1-specific T cells and inducing a resting state[112], making PD-1 a potential marker of viral persistence in long-term ART-suppressed PWH. As previously reported[113,114], our results revealed higher frequency of T-cell activation in GALT than in blood. Importantly, we demonstrated for the first time the effective and lasting effect of obefazimod at reducing immune activation in PWH on ART with a reduction in the cell surface expression of the activation-induced markers CD38,

HLA-DR, and PD-1 in $CD4^+$ and $CD8^+$ T cells from both peripheral blood and GALT. Hence, obefazimod offsets the overexpression of cell surface activation-induced markers caused by HIV-1 infection. Interestingly though, our results confirm a larger reduction of CD38 expression in comparison with that of HLA-DR when compared with other intensification strategies[115]. Nonetheless, we cannot exclude that low detectability of HLA-DR expression could prevent reliable conclusions on HLA-DR expression changes.

Consistent with previous reports[93,95,116], we confirmed the strong anti-inflammatory effect of obefazimod with the selective upregulation of miR-124 expression in PWH. miR-124 is a functionally relevant physiological miRNA associated with processes that attenuate inflammation, by promoting selective inhibition of cytokine expression, and help maintain homeostasis. Thus, obefazimod promotes a critical regulator that has the potential to reduce several inflammatory-activated pathways[117]. This upregulation of miR-124 is specific to obefazimod, as other antiretrovirals such as maraviroc, efavirenz, darunavir, and AZT did not upregulate the expression of miR-124 to a similar degree as obefazimod[93]. Indeed, an upregulated biogenesis of miR-124 has been consistently reported with obefazimod across preclinical (both *in vitro* and in humanized mouse models) and clinical studies in individuals with ulcerative colitis (UC)[97,98,118], Crohn's disease (CD), and rheumatoid arthritis (RA)[99]. Interestingly though, in our study no significant difference in miR-124 upregulation was observed between the two doses, indicating limited dose-dependent efficacy of the drug, which has also been consistently reported in the clinical studies in individuals with UC and RA[98,99]. The fact that obefazimod selectively upregulates the expression of miR-124 could have a major advantage over other therapeutical strategies, such as the simultaneous downregulation of multiple cytokines. Therefore, obefazimod might transform the treatment of multiple inflammatory diseases, including the chronic inflammation exhibited by PWH despite long-term ART suppression.

HIV infection results in a dysregulated network of HIV-inductive, HIV-suppressive, or bifunctional cytokines, together with a variety of viral and cellular factors, that contributes to the immunopathogenesis of the disease by impairing cell-

mediated immunity. HIV-inductive cytokines, such as IL-1, IL-2, IL-6, IL-7, IL-18, M-CSF, and TNF-a, induce viral replication and maintain active viral expression, whereas HIV-suppressive cytokines, such as IL-10 and MIP-1b, inhibit viral replication. Bifunctional cytokines, such as GM-CSF, IFN-γ, and IL-4, have been shown to exert both inductive and/or suppressive effects on viral replication, possibly depending on the state of differentiation of monocytes[119,120]. During HIV-1 infection, cytokine production and responsiveness differ, providing at some level protective, defective, or pathogenic responses, which play a significant role on the entire immune response to HIV and have direct effects on T cells that alter their functional properties. Hence, we aimed at further understanding this complex cytokine interactions throughout obefazimod intervention to identify useful markers of progression that could be targeted to minimize HIV-1-induced immune damage. Our results reinforced the anti-inflammatory potential of obefazimod with the simultaneous downregulation of the expression of several cytokines, such as G-CSF, GM-CSF, CD14, IL-7, IL-10, MIP-1β (or CCL4), and MCP-1 (or CCL2). Interestingly though, the greatest attenuation of soluble inflammation biomarkers was seen 4 weeks after drug discontinuation, when obefazimod was administered for a longer period, as it significantly downregulated the expression of GM-CSF, IL-1β, IL-2, IL-7, IL-12 (p70), and IL-17α (or CTLA-8). These effects on pro-inflammatory pathways are reminiscent of some, but not all, of those observed in individuals with UC treated with obefazimod, which suggest that inflammatory bowel diseases and HIV-1 infection share some inflammatory similarities[121]. Nevertheless, significant differences between PWH and HIV-negative individuals remained present either at baseline or after intervention, such as the expression of the cytokines G-CSF, IL-7, TNFα, IL-18 binding protein, MIP-1β (or CCL4), CRP, and MCP-1 (or CCL2). This fact supports the evidence that PWH exhibit elevated levels of many inflammation biomarkers than HIV-negative individuals[122], which seems to be higher in the HIV$^{150mg/4w}$ group maybe due to the longer time living with HIV-1 and receiving ART. Contrary to what was expected, obefazimod transiently increased CRP expression when it was administered at 150 mg for 4 weeks (p=0.008). CRP is an acute-phase protein synthesized by hepatocytes under inflammation stimulation[123]. However, Spearman's correlations between CRP

expression and all variables included in this study were assessed and we found no significant correlation that could explain this transient effect (data not shown). Nevertheless, the magnitude of change was within the physiological range of normally and therefore not clinically meaningful. Actually, no transient upregulation of CRP expression has been observed to date in more than 800 individuals with UC who received 50 mg of obefazimod[98]. Altogether, our results show the broad anti-inflammatory effect of obefazimod and suggest that it might be a potential therapeutic agent not only against chronic inflammation exhibited by PWH, but also against other inflammatory diseases.

Among the limitations of the study we should acknowledge the small number of participants per group, that may preclude statistical power of several results; the restricted demographics (all Caucasian men), that could hide ethnic- and gender-based differences in response to the intervention; and differences in total time of HIV infection and ART exposure between the $HIV^{50mg/12w}$ and $HIV^{150mg/4w}$ groups, that might mask differences between the 50 and 150 mg doses of treatment with obefazimod.

In conclusion, oral administration of obefazimod 50 mg for 12 weeks and 150 mg for 4 weeks, once daily, is safe and well tolerated, accelerates the decay of the proviral reservoir, and further dampens chronic immune activation and inflammation in fully suppressed PWH on conventional antiviral regimens, suggesting that obefazimod administration may have a triple effect *in vivo*. Therefore, this novel compound with its unique mode of action may have important implications for strategies aimed at sustained virological remission and immune restoration.

Based on the present results, we hypothesize that beyond the direct impact of obefazimod on the suppression of viral replication, by interfering the biogenesis of HIV RNA, and cytokine expression, by selectively upregulating miR-124, obefazimod further contributes to restore the heightened T-cell activation exhibited by PWH experiencing long-term viral suppression either directly, via suppression of viral antigen stimulation, or indirectly, via attenuation of pro-inflammatory cytokines. There could also be bidirectional effects since obefazimod-mediated reduction of T-

cell activation and inflammation might contribute to reducing T-cell viral transcriptional activity as well (Figure 36).

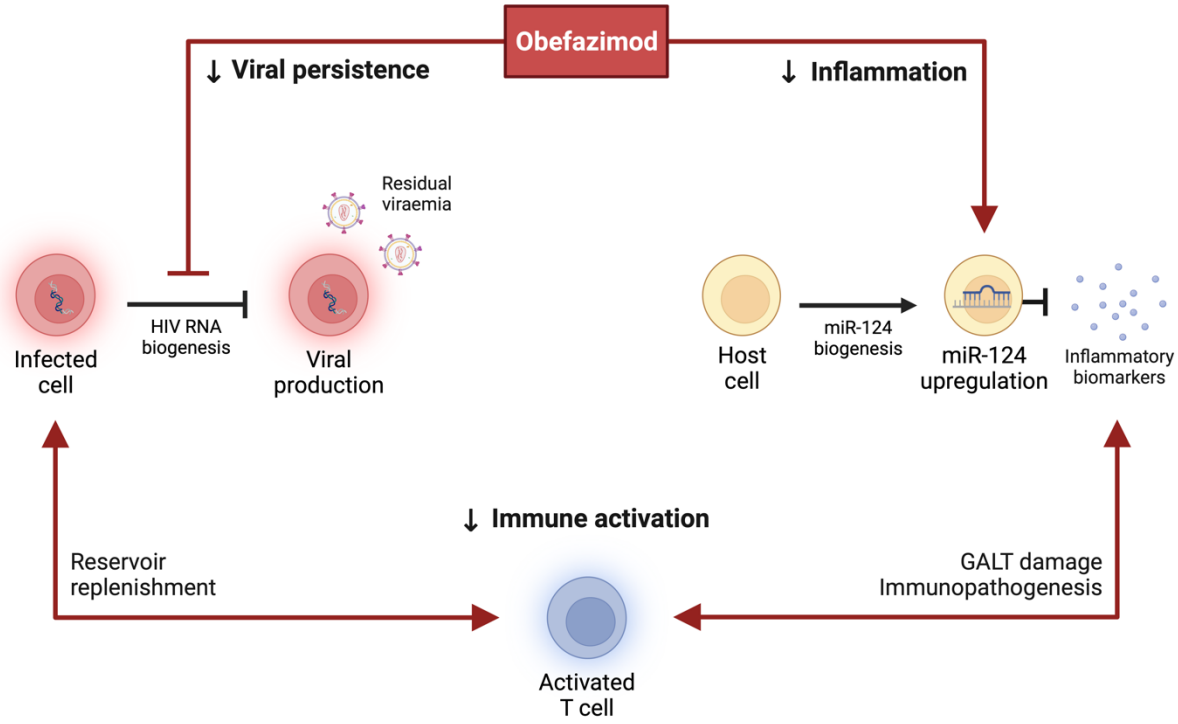

Figure 36. Effect of obefazimod on HIV-1 persistence, inflammation, and immune activation. Schematic model of obefazimod-mediated reduction of viral persistence, chronic inflammation, and immune activation in ART-suppressed PWH.

Nevertheless, these encouraging findings warrant further exploration of the drug-associated mechanisms that counteract persistent immune activation and inflammation through its specific interaction with the CBC, either by inducing specific changes in immune cells, selectively upregulating miR-124, or reducing viral antigens expression and presumably T-cell proliferation. This will be of great help to elucidate the mechanism of action of obefazimod and to further understand the involvement of the CBC under HIV-1 infection and immune cells activation. Further studies should investigate intermediate doses of obefazimod and longer treatment periods than those used in the present study as they could result in a sustained impact on viral persistence, chronic immune activation, and inflammation, while limiting drug-related AEs. Moreover, our results also support the search of alternative drugs that target viral transcription, processing, and/or maturation of viral transcripts with potential to eliminate or silence viral persistence and simultaneously suppress virus-induced immune activation and inflammation[124].

Chapter 6. CONCLUSIONS

The safety and impact of obefazimod on viral persistence, chronic immune activation, and inflammation in people with HIV (PWH) on suppressive antiretroviral therapy (ART), were evaluated in a non-randomized, open-label, phase II clinical study.

The main **conclusions** are:

1. Treatment with obefazimod, taken up to 150 mg daily for 4 weeks, is safe and well tolerated either alone or in combination with ART.
2. Obefazimod impacts viral persistence by transiently reducing viral transcription initiation and elongation, residual viraemia, and total proviral reservoir size, in a dose-dependent manner, when it is administered in combination with ART.
3. Obefazimod impacts chronic immune activation and inflammation in long-term ART-suppressed PWH, by reducing T-cell activation, selectively upregulating miR-124, and reducing the expression of multiple soluble inflammation biomarkers, and this effect is maintained up to 4 weeks after obefazimod discontinuation.

Globally, our study showed that this novel compound with its unique mode of action may have important implications for strategies aimed at sustained virological remission and immune restoration. Furthermore, our results also support the search of alternative drugs that target viral transcription, processing, and/or maturation of viral transcripts with potential to eliminate or silence viral persistence and simultaneously suppress virus-induced immune activation and inflammation.

Chapter 7. REFERENCES

1. Gottlieb, M. S. *et al.* Pneumocystis carinii Pneumonia and Mucosal Candidiasis in Previously Healthy Homosexual Men. *New England Journal of Medicine* **305**, 1425–1431 (1981).

2. Centers for Disease Control (CDC). Pneumocystis pneumonia-Los Angeles. *MMWR Morb Mortal Wkly Rep* **30**, 250–2 (1981).

3. Barré-Sinoussi, F. *et al.* Isolation of a T-Lymphotropic Retrovirus from a Patient at Risk for Acquired Immune Deficiency Syndrome (AIDS). *Science* **220**, 868–871 (1983).

4. Gallo, R. C. *et al.* Isolation of Human T-Cell Leukemia Virus in Acquired Immune Deficiency Syndrome (AIDS). *Science* **220**, 865–867 (1983).

5. Coffin, J. *et al.* Human Immunodeficiency Viruses. *Science* **232**, 697–697 (1986).

6. Clavel, F. *et al.* Isolation of a New Human Retrovirus from West African Patients with AIDS. *Science* **233**, 343–346 (1986).

7. Chakrabarti, L. *et al.* Sequence of simian immunodeficiency virus from macaque and its relationship to other human and simian retroviruses. *Nature* **328**, 543–547 (1987).

8. Huet, T. *et al.* Genetic organization of a chimpanzee lentivirus related to HIV-1. *Nature* **345**, 356–359 (1990).

9. Hirsch, V. M. *et al.* An African primate lentivirus (SIVsm closely related to HIV-2. *Nature* **339**, 389–392 (1989).

10. Sharp, P. M. & Hahn, B. H. Origins of HIV and the AIDS Pandemic. *Cold Spring Harb Perspect Med* **1**, a006841–a006841 (2011).

11. Faria, N. R. *et al.* The early spread and epidemic ignition of HIV-1 in human populations. *Science* **346**, 56–61 (2014).

12. UNAIDS. GLOBAL HIV & AIDS statistics. 2022 fact sheet. (2022).

13. King, A. *et al.* International Committee on Taxonomy of Viruses. Virus Taxonomy: Classification and nomenclature of viruses. The Ninth Report of the International Committee on Taxonomy of Viruses. (*Elsevier*, 2011).

14. Reeves, J. D. & Doms, R. W. Human immunodeficiency virus type 2. *Journal of General Virology* **83**, 1253–1265 (2002).

15. Sharp, P. M. & Hahn, B. H. Origins of HIV and the AIDS Pandemic. *Cold Spring Harb Perspect Med* **1**, a006841–a006841 (2011).

16. Gelderblom, H. R. Assembly and morphology of HIV: potential effect of structure on viral function. *AIDS* **5**, 617–37 (1991).

17. Seitz, R. Human Immunodeficiency Virus (HIV). *Transfusion Medicine and Hemotherapy* **43**, 203–222 (2016).

18. Muesing, M. A. *et al.* Nucleic acid structure and expression of the human AIDS/lymphadenopathy retrovirus. *Nature* **313**, 450–458 (1985).

19. Yu, X. F. *et al.* The vpx gene of simian immunodeficiency virus facilitates efficient viral replication in fresh lymphocytes and macrophage. *J Virol* **65**, 5088–5091 (1991).

20. Kwong, P. D. *et al.* Structure of an HIV gp120 envelope glycoprotein in complex with the CD4 receptor and a neutralizing human antibody. *Nature* **393**, 648–59 (1998).

21. Rizzuto, C. D. *et al.* A conserved HIV gp120 glycoprotein structure involved in chemokine receptor binding. *Science* **280**, 1949–53 (1998).

22. Selyutina, A. *et al.* Nuclear Import of the HIV-1 Core Precedes Reverse Transcription and Uncoating. *Cell Rep* **32**, 108201 (2020).

23. Zila, V. *et al.* Cone-shaped HIV-1 capsids are transported through intact nuclear pores. *Cell* **184**, 1032-1046.e18 (2021).

24. Craigie, R. & Bushman, F. D. HIV DNA Integration. *Cold Spring Harb Perspect Med* **2**, a006890–a006890 (2012).

25. Gonatopoulos-Pournatzis, T. & Cowling, V. H. Cap-binding complex (CBC). *Biochemical Journal* **457**, 231–242 (2014).

26. Caputi, M. The Regulation of HIV-1 mRNA Biogenesis. in *RNA Processing* (*Intech*, 2011). doi:10.5772/20899.

27. Proudfoot, N. J. *et al.* Integrating mRNA Processing with Transcription. *Cell* **108**, 501–512 (2002).

28. Sundquist, W. I. & Krausslich, H.-G. HIV-1 Assembly, Budding, and Maturation. *Cold Spring Harb Perspect Med* **2**, a006924–a006924 (2012).

29. Chen, Q. *et al.* Different transmission routes and the risk of advanced HIV disease: A systematic review and network meta-analysis of observational studies. *EClinicalMedicine* **16**, 121–128 (2019).

30. Dandekar, S. Pathogenesis of HIV in the gastrointestinal tract. *Curr HIV/AIDS Rep* **4**, 10–15 (2007).

31. Pantaleo, G. & Fauci, A. S. Immunopathogenesis of HIV infection. *Annu Rev Microbiol* **50**, 825–854 (1996).

32. McMichael, A. J. *et al.* The immune response during acute HIV-1 infection: clues for vaccine development. *Nat Rev Immunol* **10**, 11–23 (2010).

33. Veazey, R. S. *et al.* Gastrointestinal Tract as a Major Site of CD4+ T Cell Depletion and Viral Replication in SIV Infection. *Science* **280**, 427–431 (1998).

34. Babiker, A. *et al.* Time from HIV-1 seroconversion to AIDS and death before widespread use of highly-active antiretroviral therapy: a collaborative re-analysis. *The Lancet* **355**, 1131–1137 (2000).

35. Furman, P. A. & Barry, D. W. Spectrum of antiviral activity and mechanism of action of zidovudine. An overview. *Am J Med* **85**, 176–81 (1988).

36. Staszewski, S. *et al.* Virological and immunological analysis of a triple combination pilot study with loviride, lamivudine and zidovudine in HIV-1-infected patients. *AIDS* **10**, F1–F7 (1996).

37. U.S. Food and Drug Administration, U.S. Department of Health and Human Services. HIV/AIDS Treatment - HIV Treatment Information for adults. *https://www.fda.gov/drugs/hiv-treatment/hiv-treatment-information-adults*.

38. Johnson, V. A. Combination Therapy: More Effective Control of HIV Type 1? *AIDS Res Hum Retroviruses* **10**, 907–912 (1994).

39. Arts, E. J. & Hazuda, D. J. HIV-1 antiretroviral drug therapy. *Cold Spring Harb Perspect Med* **2**, a007161 (2012).

40. Maartens, G. *et al.* HIV infection: epidemiology, pathogenesis, treatment, and prevention. *The Lancet* **384**, 258–271 (2014).

41. Chun, T.-W. *et al.* In vivo fate of HIV-1-infected T cells: Quantitative analysis of the transition to stable latency. *Nat Med* **1**, 1284–1290 (1995).

42. Chun, T.-W. *et al.* Re-emergence of HIV after stopping therapy. *Nature* **401**, 874–875 (1999).

43. Deeks, S. G. *et al.* The end of AIDS: HIV infection as a chronic disease. *The Lancet* **382**, 1525–1533 (2013).

44. Siliciano, J. D. *et al.* Long-term follow-up studies confirm the stability of the latent reservoir for HIV-1 in resting CD4+ T cells. *Nat Med* **9**, 727–728 (2003).

45. Chomont, N. *et al.* HIV reservoir size and persistence are driven by T cell survival and homeostatic proliferation. *Nat Med* **15**, 893–900 (2009).

46. Kulpa, D. A. & Chomont, N. HIV persistence in the setting of antiretroviral therapy: when, where and how does HIV hide? *J Virus Erad* **1**, 59–66 (2015).

47. Buzon, M. J. *et al.* HIV-1 persistence in CD4+ T cells with stem cell-like properties. *Nat Med* **20**, 139–142 (2014).

48. Barton, K. *et al.* HIV-1 Reservoirs During Suppressive Therapy. *Trends Microbiol* **24**, 345–355 (2016).

49. Ananworanich, J. *et al.* HIV DNA Set Point is Rapidly Established in Acute HIV Infection and Dramatically Reduced by Early ART. *EBioMedicine* **11**, 68–72 (2016).

50. Henrich, T. J. *et al.* HIV-1 persistence following extremely early initiation of antiretroviral therapy (ART) during acute HIV-1 infection: An observational study. *PLoS Med* **14**, e1002417 (2017).

51. Colby, D. J. *et al.* Rapid HIV RNA rebound after antiretroviral treatment interruption in persons durably suppressed in Fiebig I acute HIV infection. *Nat Med* **24**, 923–926 (2018).

52. Chavez, L. *et al.* HIV Latency Is Established Directly and Early in Both Resting and Activated Primary CD4 T Cells. *PLoS Pathog* **11**, e1004955 (2015).

53. Vandergeeten, C. *et al.* Interleukin-7 promotes HIV persistence during antiretroviral therapy. *Blood* **121**, 4321–4329 (2013).

54. Wong, J. K. & Yukl, S. A. Tissue reservoirs of HIV. *Curr Opin HIV AIDS* **11**, 362–370 (2016).

55. Westermann, J. & Pabst, R. Distribution of lymphocyte subsets and natural killer cells in the human body. *Clin Investig* **70**, (1992).

56. Wong, J. K. & Yukl, S. A. Tissue reservoirs of HIV. *Curr Opin HIV AIDS* **11**, 362–370 (2016).

57. Chun, T. *et al.* Persistence of HIV in Gut-Associated Lymphoid Tissue despite Long-Term Antiretroviral Therapy. *J Infect Dis* **197**, 714–720 (2008).

58. Martinez-Picado, J. & Deeks, S. G. Persistent HIV-1 replication during antiretroviral therapy. *Curr Opin HIV AIDS* **11**, 417–423 (2016).

59. Lorenzo-Redondo, R. *et al.* Persistent HIV-1 replication maintains the tissue reservoir during therapy. *Nature* **530**, 51–56 (2016).

60. Ho, H. N. *et al.* Circulating HIV-specific CD8+ cytotoxic T cells express CD38 and HLA-DR antigens. *J Immunol* **150**, 3070–9 (1993).

61. Day, C. L. *et al.* PD-1 expression on HIV-specific T cells is associated with T-cell exhaustion and disease progression. *Nature* **443**, 350–354 (2006).

62. Deeks, S. G. *et al.* Immune activation set point during early HIV infection predicts subsequent CD4+ T-cell changes independent of viral load. *Blood* **104**, 942–947 (2004).

63. Baxter, A. E. *et al.* Beyond the replication-competent HIV reservoir: transcription and translation-competent reservoirs. *Retrovirology* **15**, 18 (2018).

64. Chomont, N. *et al.* HIV reservoir size and persistence are driven by T cell survival and homeostatic proliferation. *Nat Med* **15**, 893–900 (2009).

65. Lackner, A. A. *et al.* HIV Pathogenesis: The Host. *Cold Spring Harb Perspect Med* **2**, a007005–a007005 (2012).

66. Brenchley, J. M. *et al.* Microbial translocation is a cause of systemic immune activation in chronic HIV infection. *Nat Med* **12**, 1365–1371 (2006).

67. Doisne, J.-M. *et al.* CD8+ T Cells Specific for EBV, Cytomegalovirus, and Influenza Virus Are Activated during Primary HIV Infection. *The Journal of Immunology* **173**, 2410–2418 (2004).

68. Appay, V. & Sauce, D. Immune activation and inflammation in HIV-1 infection: causes and consequences. *J Pathol* **214**, 231–241 (2008).

69. Yeh, Y.-H. J. & Ho, Y.-C. Shock-and-kill versus block-and-lock: Targeting the fluctuating and heterogeneous HIV-1 gene expression. *Proceedings of the National Academy of Sciences* **118**, (2021).

70. Hütter, G. *et al.* Long-Term Control of HIV by CCR5 Δ32/Δ32 Stem-Cell Transplantation. *New England Journal of Medicine* **360**, 692–698 (2009).

71. Henrich, T. J. *et al.* Long-Term Reduction in Peripheral Blood HIV Type 1 Reservoirs Following Reduced-Intensity Conditioning Allogeneic Stem Cell Transplantation. *Journal of Infectious Diseases* **207**, 1694–1702 (2013).

72. Gupta, R. K. *et al.* HIV-1 remission following CCR5Δ32/Δ32 haematopoietic stem-cell transplantation. *Nature* **568**, 244–248 (2019).

73. Gupta, R. K. *et al.* Evidence for HIV-1 cure after CCR5Δ32/Δ32 allogeneic haemopoietic stem-cell transplantation 30 months post analytical treatment interruption: a case report. *Lancet HIV* **7**, e340–e347 (2020).

74. Jenson B-EO *et al.* CCR5-Δ32 SCT HIV remission-traces of HIV DNA but fading immunoreactivity. *Conference on retroviruses and Opportunistic Infections (CROI)* (2020).

75. Deborah Persaud & Yvonne Bryson. HIV-1 remission with CCR5Δ32/Δ32 haplo-cord transplant in a U.S. woman: IMPAACT P1107. *Conference on Retroviruses and Opportunistic Infections (CROI)* (2022).

76. Massanella, M. *et al.* Dynamics of CD8 T-Cell Activation After Discontinuation of HIV Treatment Intensification. *JAIDS Journal of Acquired Immune Deficiency Syndromes* **63**, 152–160 (2013).

77. Towards an HIV cure: a global scientific strategy. *Nat Rev Immunol* **12**, 607–614 (2012).

78. Bernal, S. *et al.* Impact of Obefazimod on Viral Persistence, Inflammation, and Immune Activation in People With Human Immunodeficiency Virus on Suppressive Antiretroviral Therapy. *J Infect Dis* (2023) doi:10.1093/infdis/jiad251.

79. Campos, N. *et al.* Long lasting control of viral rebound with a new drug ABX464 targeting Rev-mediated viral RNA biogenesis. *Retrovirology* **12**, 30 (2015).

80. Ratmeyer, L. *et al.* Inhibition of HIV-1 Rev−RRE Interaction by Diphenylfuran Derivatives. *Biochemistry* **35**, 13689–13696 (1996).

81. Heguy, A. Inhibition of the HIV Rev transactivator A new target for therapeutic intervention. *Frontiers in Bioscience* **2**, A191 (1997).

82. Nakaya, T. *et al.* Inhibition of HIV-1 replication by targeting the Rev protein. *Leukemia* **11 Suppl 3**, 134–7 (1997).

83. DeJong, E. S. *et al.* Proflavine Acts as a Rev Inhibitor by Targeting the High-Affinity Rev Binding Site of the Rev Responsive Element of HIV-1. *Biochemistry* **42**, 8035–8046 (2003).

84. Shuck-Lee, D. *et al.* Heterocyclic Compounds That Inhibit Rev-RRE Function and Human Immunodeficiency Virus Type 1 Replication. *Antimicrob Agents Chemother* **52**, 3169–3179 (2008).

85. Prado, S. *et al.* Bioavailable inhibitors of HIV-1 RNA biogenesis identified through a Rev-based screen. *Biochem Pharmacol* **107**, 14–28 (2016).

86. Prado, S. *et al.* A small-molecule inhibitor of HIV-1 Rev function detected by a diversity screen based on RRE-Rev interference. *Biochem Pharmacol* **156**, 68–77 (2018).

87. González-Bulnes, L. *et al.* Structure-based design of an RNA-binding p-terphenylene scaffold that inhibits HIV-1 Rev protein function. *Angewandte Chemie - International Edition* **52**, 13405–13409 (2013).

88. Medina-Trillo, C. *et al.* Nucleic acid recognition and antiviral activity of 1,4-substituted terphenyl compounds mimicking all faces of the HIV-1 Rev protein positively-charged α-helix. *Sci Rep* **10**, 7190 (2020).

89. Scherrer, D. *et al.* Pharmacokinetics and tolerability of ABX464, a novel first-in-class compound to treat HIV infection, in healthy HIV-uninfected subjects. *J Antimicrob Chemother* **72**, 820–828 (2017).

90. Scherrer, D. *et al.* Randomized trial of food effect on pharmacokinetic parameters of ABX464 administered orally to healthy male subjects. *Antimicrob Agents Chemother* **61**, 1–10 (2017).

91. Steens, J.-M. *et al.* Safety, Pharmacokinetics, and Antiviral Activity of a Novel HIV Antiviral, ABX464, in Treatment-Naive HIV-Infected Subjects in a Phase 2 Randomized, Controlled Study. *Antimicrob Agents Chemother* **61**, (2017).

92. Rutsaert, S. *et al.* Safety, tolerability and impact on viral reservoirs of the addition to antiretroviral therapy of ABX464, an investigational antiviral drug, in individuals living with HIV-1: A Phase IIa randomised controlled study. *J Virus Erad* **5**, 10–22 (2019).

93. Vautrin, A. *et al.* Both anti-inflammatory and antiviral properties of novel drug candidate ABX464 are mediated by modulation of RNA splicing. *Sci Rep* **9**, 1–15 (2019).

94. Qin, Z., Wang, P.-Y., Su, D.-F. & Liu, X. miRNA-124 in Immune System and Immune Disorders. *Front Immunol* **7**, (2016).

95. Chebli, K. *et al.* The Anti-HIV Candidate Abx464 Dampens Intestinal Inflammation by Triggering IL-22 Production in Activated Macrophages. *Sci Rep* **7**, 1–11 (2017).

96. Begon-Pescia, C. *et al.* THU0199 ABX464, a novel drug in the field of inflammation, increases miR-124 and modulates macrophages and T-cell functions. *Ann Rheum Dis* **79**, 321–322 (2020).

97. Vermeire, S. *et al.* Induction and Long-term Follow-up With ABX464 for Moderate-to-severe Ulcerative Colitis: Results of Phase IIa Trial. *Gastroenterology* **160**, 2595-2598.e3 (2021).

98. Vermeire, S. *et al.* ABX464 (obefazimod) for moderate-to-severe, active ulcerative colitis: a phase 2b, double-blind, randomised, placebo-controlled induction trial and 48 week, open-label extension. *Lancet Gastroenterol Hepatol* **7**, 1024–1035 (2022).

99. Daien, C. *et al.* Safety and efficacy of the miR-124 upregulator ABX464 (obefazimod, 50 and 100 mg per day) in patients with active rheumatoid arthritis and inadequate response to methotrexate and/or anti-TNFα therapy: a placebo-controlled phase II study. *Ann Rheum Dis* **81**, 1076–1084 (2022).

100. Morón-López, S. *et al.* Sensitive quantification of the HIV-1 reservoir in gut-associated lymphoid tissue. *PLoS One* **12**, 1–10 (2017).

101. Bruner, K. M. *et al.* A quantitative approach for measuring the reservoir of latent HIV-1 proviruses. *Nature* **566**, 120–125 (2019).

102. Yukl, S. A. *et al.* HIV latency in isolated patient CD4+T cells may be due to blocks in HIV transcriptional elongation, completion, and splicing. *Sci Transl Med* **10**, 1–16 (2018).

103. Martínez-Bonet, M. *et al.* Establishment and Replenishment of the Viral Reservoir in Perinatally HIV-1-infected Children Initiating Very Early Antiretroviral Therapy. *Clinical Infectious Diseases* **61**, 1169–1178 (2015).

104. Livak, K. J. & Schmittgen, T. D. Analysis of Relative Gene Expression Data Using Real-Time Quantitative PCR and the 2−ΔΔCT Method. *Methods* **25**, 402–408 (2001).

105. Chomont, N. *et al.* HIV reservoir size and persistence are driven by T cell survival and homeostatic proliferation. *Nat Med* **15**, 893–900 (2009).

106. Moron-Lopez, S. *et al.* ABX464 Decreases the Total Human Immunodeficiency Virus (HIV) Reservoir and HIV Transcription Initiation in CD4+ T Cells From Antiretroviral Therapy–Suppressed Individuals Living With HIV. *Clinical Infectious Diseases* 1–4 (2021) doi:10.1093/cid/ciab733.

107. Puertas, M. C. *et al.* Intensification of a raltegravir-based regimen with maraviroc in early HIV-1 infection. *AIDS* **28**, 325–334 (2014).

108. Puertas, M. C. *et al.* Impact of intensification with raltegravir on HIV-1-infected individuals receiving monotherapy with boosted PIs. *Journal of Antimicrobial Chemotherapy* **73**, 1940–1948 (2018).

109. Morón-López, S. *et al.* Switching from a Protease Inhibitor–based Regimen to a Dolutegravir-based Regimen: A Randomized Clinical Trial to Determine the Effect on

Peripheral Blood and Ileum Biopsies From Antiretroviral Therapy-suppressed Human Immunodeficiency Virus-infected Individuals. *Clinical Infectious Diseases* **69**, 1320–1328 (2019).

110. Hunt, P. W. *et al.* T cell activation is associated with lower CD4+ T cell gains in human immunodeficiency virus-infected patients with sustained viral suppression during antiretroviral therapy. *Journal of Infectious Diseases* **187**, 1534–1543 (2003).

111. Day, C. L. *et al.* PD-1 expression on HIV-specific T cells is associated with T-cell exhaustion and disease progression. *Nature* **443**, 350–354 (2006).

112. D'Souza, M. *et al.* Programmed Death 1 Expression on HIV-Specific CD4+ T Cells Is Driven by Viral Replication and Associated with T Cell Dysfunction. *The Journal of Immunology* **179**, 1979–1987 (2007).

113. Khoury, G. *et al.* Human immunodeficiency virus persistence and T-cell activation in blood, rectal, and lymph node tissue in human immunodeficiency virus-infected individuals receiving suppressive antiretroviral therapy. *Journal of Infectious Diseases* **215**, 911–919 (2017).

114. Yukl, S. A. *et al.* Differences in HIV burden and immune activation within the gut of HIV-positive patients receiving suppressive antiretroviral therapy. *J Infect Dis* **202**, 1553–61 (2010).

115. Massanella, M. *et al.* Raltegravir intensification shows differing effects on CD8 and CD4 T cells in HIV-infected HAART-suppressed individuals with poor CD4 T-cell recovery. *AIDS* **26**, 2285–2293 (2012).

116. Tazi, J. *et al.* Specific and selective induction of miR-124 in immune cells by the quinoline ABX464: a transformative therapy for inflammatory diseases. *Drug Discov Today* **26**, 1030–1039 (2021).

117. Ghafouri-Fard, S. *et al.* An update on the role of miR-124 in the pathogenesis of human disorders. *Biomedicine & Pharmacotherapy* **135**, 111198 (2021).

118. Vermeire, S. *et al.* OP21 ABX464 is safe and efficacious in a proof-of-concept study in ulcerative colitis patients. *J Crohns Colitis* **13**, S014–S015 (2019).

119. Kedzierska, K. & Crowe, S. M. Cytokines and HIV-1: Interactions and Clinical Implications. *Antivir Chem Chemother* **12**, 133–150 (2001).

120. Reuter, M. A. *et al.* Cytokine production and dysregulation in HIV pathogenesis: Lessons for development of therapeutics and vaccines. *Cytokine Growth Factor Rev* **23**, 181–191 (2012).

121. Alzahrani, J. *et al.* Inflammatory and immunometabolic consequences of gut dysfunction in HIV: Parallels with IBD and implications for reservoir persistence and non-AIDS comorbidities. *EBioMedicine* **46**, 522–531 (2019).

122. Catalfamo, M. *et al.* The role of cytokines in the pathogenesis and treatment of HIV infection. *Cytokine Growth Factor Rev* **23**, 207–214 (2012).

123. Pepys, M. B. & Hirschfield, G. M. C-reactive protein: a critical update. *Journal of Clinical Investigation* **112**, 299–299 (2003).

124. Pasternak, A. O. & Berkhout, B. The splice of life: Does RNA processing have a role in HIV-1 persistence? *Viruses* **13**, 1–10 (2021).

Chapter 8. PUBLICATIONS

1. Silvia Bernal, Maria C. Puertas, Sara Morón-López, Ross D. Cranston, Víctor Urrea, Judith Dalmau, María Salgado, Cristina Gálvez, Itziar Erkizia, Ian McGowan, Didier Scherrer, Boris Revollo, Guillem Sirera, José Ramón Santos, Bonaventura Clotet, Roger Paredes, Javier Martinez-Picado. **Impact of obefazimod on viral persistence, inflammation, and immune activation in people with HIV on suppressive antiretroviral therapy**. *Journal of Infectious Diseases*. 2023.

2. Sara Morón-López*, Silvia Bernal*, Joseph K. Wong, Javier Martinez-Picado, Steven A. Yukl. **ABX464 decreases the total human immunodeficiency virus (HIV) reservoir and HIV transcription initiation in CD4$^+$ T cells from antiretroviral therapy-suppressed individuals living with HIV**. *Clinical Infectious Diseases*. 2022.

3. Sergi Chumillas, Saurabh Loharch, Manuela Beltran, Mateusz Piotr Szewczyk, Silvia Bernal, Maria C. Puertas, Javier Martinez-Picado, José Alcamí, Luis Miguel Bedoya, Vicente Marchán, Jose Gallego. **Exploring the HIV-1 RRE-Rev inhibitory capacity and antiretroviral action of benfluron analogs**. *Molecules*. 2023

4. Cristina Gálvez, Víctor Urrea, Maria C. Garcia-Guerrero, Silvia Bernal, Susana Benet, Beatriz Mothe, Lucía Bailón, Judith Dalmau, Andrea Martinez, Aroa Nieto, Lorna Leal, Felipe García, Bonaventura Clotet, Javier Martinez-Picado, Maria Salgado. **Altered T-cell subset distribution in the viral reservoir in HIV-1-infected individuals with extremely low proviral DNA (LoViReTs)**. *Journal of Internal Medicine*. 2022.

Chapter 9. ACKNOWLEDGEMENTS

En primer lloc, em vull donar les gràcies a mi mateixa per haver arribat fins aquí; per l'esforç, la dedicació, la constància i la perseverança; per complir el somni de la meva nena petita; i per tot el que he sacrificat pel camí.

En segon lloc, vull agrair als meus incondicionals, la meva mare, el meu pare i la meva germana. Gràcies per ser l'energia que emprèn el meu motor; per animar-me a ser la millor versió de mi; per confiar en mi plenament; per recolzar-me en totes les decisions; per estar sempre al meu costat, en els bons moments, per celebrar-los, i en els dolents, per donar-me l'empenta que necessito per seguir endavant; per no deixar-me baixar la guàrdia; i per estar sempre tant orgullosos de mi. Gràcies per fer-ho tot tant fàcil.

En tercer lloc a tota la gent d'IrsiCaixa que ha fet possible que pugui ser doctora. Ventura, gràcies per crear una institució i promoure uns valors tant macos, n'has fet una petita família; i per donar-me l'oportunitat de poder fer el doctorat aprenent de tant bons professionals. Admiro profundament tot el que has aconseguit, la teva noblesa, proximitat, senzillesa, elegància, humilitat i el teu *savoir faire*. Si al món hi haguessin més persones com tu, seria molt millor. Javier, gràcies per ensenyar ciència amb tanta il·lusió; per cuidar i mimar l'equip; per la teva humanitat, assertivitat i paciència; per la teva capacitat de resolució; i per transmetre'ns valors i aconsellar-nos amb tant de carinyo. Ets un gran professional i he après molt de tu durant aquests anys. Mari Carmen, gràcies per guiar-me en aquesta etapa. Ets la persona més resolutiva, més didàctica, més perfeccionista i més totes-les-coses-que-es-puguin-ser que he conegut mai. Sense dubte no hagués pogut tenir millor mentora que tu. Sara, gràcies per compartir els teus coneixements, per deixar fàcil el camí darrere teu i per la súper experiència de San Francisco. Ets una gran promesa. Itziar, eres la mejor compañera de cabina y de grupo que se puede tener. Gracias por siempre estar dispuesta a escuchar, enseñar y ayudar. Y sobre todo gracias por tener siempre una sonrisa dibujada en la cara. Cuesta encontrar esencias tan puras como la tuya. María, la *viejoven* (cómo tú dices) más *cool* del grupo, ha sido genial trabajar cerca de un espíritu tan vivo, alegre y risueño como el tuyo. Admiro mucho tu seguridad e independencia. Pat, moltes gràcies pels teus consells, tant en el terreny científic com en el personal, durant tot el temps que vam

ser companyes d'oficina. M'agrada envoltar-me de gent que trepitja fort, és vàlida i decidida. Víctor, gràcies per donar valor estadísticament significatiu a aquesta tesi. A la resta de GRECs, ha estat un plaer compartir amb vosaltres tants moments. Gràcies per estar sempre disposats a parlar, compartir i ajudar. El clima de treball ha estat immillorable. Susana, la paraula amiga per mi és molt gran i a tu et queda petita. Gràcies per estar sempre que ho he necessitat, per escoltar-me, aconsellar-me, recolzar-me i animar-me. M'emporto un tresor. Bueno i de regal dos petits tresors que em tenen el cor robat. Eli, si tuviera que escoger a una deuteragonista para mi tesis, sin duda serías tú. Gracias por estar desde el principio hasta el final. Ruth, gràcies per endolcir la meva estada. Sou un trio genial. Miguel, gracias por tantos momentos y experiencias mágicas, desde pasar una Navidad en Miami a besar los pies a Dua Lipa. Es lo que tiene tener luna en Aries y 100% de compatibilidad astral. Óscar, Anna, Amaya y Raquel, sois el mejor equipo para disfrutar de un buen *afterwork*. Penélope i Arnau, gràcies per la bona energia i per fer de qualsevol moment, un bon moment per amenitzar la rutina i riure. A la resta de persones d'IrsiCaixa, gràcies per tants bons moments al laboratori, als mòduls, a l'*office*, a la cafeteria, als passadissos, també als congressos, als sopars de Nadal i a les activitats extra-acadèmiques. Em sento molt afortunada d'haver gaudit d'aquesta experiència amb totes vosaltres. També vull agrair el tracte tant meravellós amb totes les persones de la Fundació Lluita contra les Infeccions que han participat en aquest estudi i als pacients. Sense totes i cadascuna de vosaltres, aquesta tesi no hagués estat possible.

Finalment, a la meva família i amigues, que encara que no s'assabentin gaire de què va la tesi, sempre estan al meu costat. Gràcies per tots els ànims, recolzament i moments de desconnexió i diversió, tant necessaris per tirar endavant. I per últim, i no menys important, gràcies a la meva família de peluts, a la Tinky i al Winky, per ajudar-me a *lqeiwufhjkfnewqiyuqfbiue* escriure part de la tesi i per obligar-me a parar quan consideraven que portava massa temps davant de l'ordinador, i al Marley, per la seva companyia i amor incondicionals, que han fet que el procés d'escriptura sigui molt més fàcil.

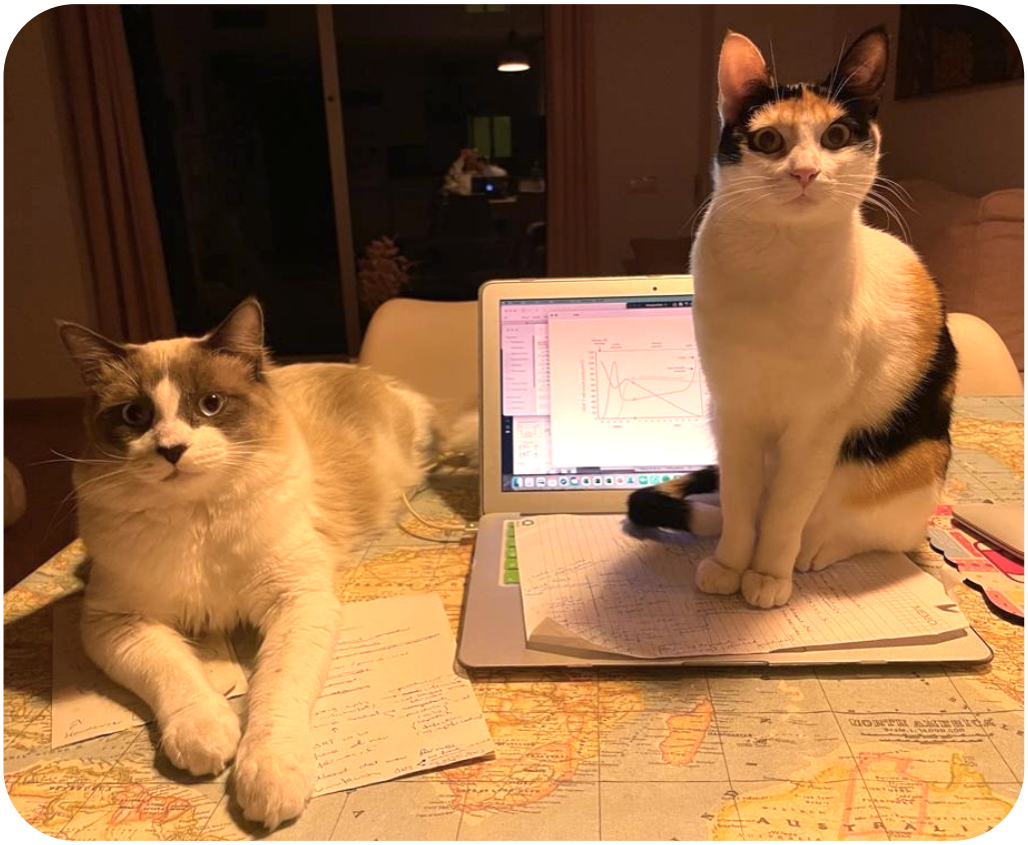

Gràcies per tant.

Us estimo.